69-18,367

DeACETIS, Louis Anthony, 1940-

KIRCHHOFF THEORY AND KELLER'S GEOMETRICAL THEORY APPLIED TO EXPERIMENTAL DIFFRACTION BY TWO LONG, THIN, CONDUCTING STRIPS.

The City University of New York, Ph.D., 1969
Physics, electronics and electricity
University Microfilms, Inc., Ann Arbor, Michigan

KIRCHHOFF THEORY AND KELLER'S GEOMETRICAL THEORY APPLIED TO EXPERIMENTAL DIFFRACTION BY TWO LONG, THIN, CONDUCTING STRIPS

by

Louis A. DeAcetis

A dissertation submitted to the Graduate Faculty in Physics in partial fulfillment of the requirements for the degree of Doctor of Philosophy, The City University of New York.

1969

This manuscript has been read and accepted for the Graduate Faculty in Physics in satisfaction of the dissertation requirement for the degree of Doctor of Philosophy.

May 7, 1969
date

Irving Lerch
Chairman of Examining Committee

May 7 1969
date

Henry Linstone
Executive Officer

Leo Diesendruck

Leopold Felsen

Benjamin Roth

Edward Thorndike
Supervisory Committee

The City University of New York

ABSTRACT

Fraunhofer diffraction of electromagnetic radiation by two long, thin, parallel, conducting strips is investigated for the case where the radiation incident upon the strips is polarized with the electric field vector parallel to the strip axes. Experimental results, obtained in terms of the intensity of radiation diffracted into different directions, are compared with theoretical diffraction patterns predicted by scalar Kirchhoff theory and Keller's "geometrical theory of diffraction."

An indoor microwave facility, capable of investigating electromagnetic diffraction in the millimeter wavelength range under both Fresnel and Fraunhofer conditions, was constructed and is described. Experimental results obtained using this facility with radiation of approximately 5 mm wavelength are presented for three different strip widths (from two to three wavelengths in size), for various strip separations (between three and eight wavelengths), and several orientations of the strip surfaces with respect to each other and the incident radiation.

Theoretical results based upon the geometrical theory of diffraction are carried out to second-order in an attempt to account for some interactions between the strips in the form of "doubly-diffracted" radiation. An examination of

the significant second-order terms is made and an estimate of the error involved in the use of these terms is given.

A comparison between theory and experiment indicates that even to first-order, Keller's geometrical theory is better able to describe the results obtained experimentally. Moreover, second-order Keller theory is found to improve the agreement between theory and experiment in most cases, as long as the strip separation is not too small (closest edges less than approximately one wavelength).

Finally, a comparison between Kirchhoff theory, Keller's geometrical theory, and an exact solution of Maxwell's equations for the case of single strip diffraction is given. The limiting cases of small glancing angle and small strip width are considered. It is found that the geometrical theory is in better agreement with exact solution, especially in the limiting cases.

PREFACE

Since J. C. Maxwell's Treatise on Electricity and Magnetism appeared in 1837, the description of electromagnetic radiation has been a main interest of both physicist and mathematician. Problems of propagation of electromagnetic radiation through media and interactions in general between such radiation and matter are of fundamental concern to the physicist. The mathematician finds interest in seeking solutions to the complex equations that arise. The result to date has been a large number of articles, in both physical and mathematical journals, which deal with electromagnetic wave propagation and diffraction.

A survey of previous work in the area of diffraction reveals that most publications are theoretical in nature. One reason for this was the lack of sources of continuous electromagnetic radiation with wavelengths in the centimeter to millimeter range, before the mid 1930's. Also, these early sources of "microwaves" generated the relatively long wavelengths which often necessitated the use of outdoor test ranges.[+] Work in the visible part of the spectrum is still limited by the small size of the individual diffracting elements required. Lengthy theoretical calculations on modern computers were often easier to do than the actual work in the laboratory.

[+]See, for example, Moseley.

Within recent years, however, sources of sufficient energy in the centimeter, millimeter (and now sub-millimeter) ranges have become readily available (hence the current interest in "microwave optics"*). These sources are of significance to the experimentalist because they permit studies with diffracting obstacles which can easily be made to satisfy a variety of diffraction conditions within the confines of a laboratory. Also, and of equal importance, the wavelength of the radiation in the millimeter region is not too long to preclude the use of lenses and/or mirrors which are large enough (but not of unwieldy physical size) to allow the use of ray optics in focusing the radiation. Thus, recent developments in microwave generation enable one to move electromagnetic diffraction studies from an outdoor test range into the laboratory where more systematic investigations can take place. It is the purpose of this discourse to describe such an investigation.

---

*See the October 1965 issue of Appl. Opt. (Vol. 4, 1213ff).

ACKNOWLEDGEMENTS

There are many who have in some way influenced the work described in this dissertation. Any attempt to name all of them in the space provided here would of necessity be unsuccessful because of omissions. I can only indicate here those who have directly affected the course of this research and without whom the venture would not have been possible to complete, but I owe gratitude to many more than it is possible to name below.

I am most indebted to Dr. Irving Lazar, who served not only as mentor but also as the closest of friends. Without his direction, assistance, and encouragement, this project could not have been started, let alone completed. I also wish to thank Dr. Leopold Felsen for the many hours of discussions and his indispensable suggestions concerning the theoretical aspects of the work. The considerable help of Mr. Donald Veit in the construction of the spectrometer arm, strip frame and various other equipment built at Queens College must also be acknowledged. I also wish to thank the members of my thesis committee, including Profs. Edward Thorndike, Leo Diesendruck, and Benjamin Roth, for their guidance and suggestions on ways to improve this dissertation. Finally, I wish to thank my wife -- not for direction, guidance, or helpful discussions concerning the work, but for her encouragement and her forbearance.

TABLE OF CONTENTS

Appendices

LIST OF TABLES (IN APPENDICES)

LIST OF FIGURES

1. Introduction

A survey of the large number of articles dealing with the problem of electromagnetic diffraction[1] reveals that:

a) the vast majority of the publications are theoretical in nature and

b) most experimental work deals with diffraction by single obstacles, or many obstacles (gratings).[2]

These findings can be attributed to the theoretical as well as experimental difficulties inherent in diffraction studies. In principle, theoretical electromagnetic diffraction problems are an exercise in the application of Maxwell's equations with appropriate boundary conditions. In practice, however, very few configurations are capable of exact solution because, in general, the equations are not separable. The transverse nature of the radiation involves vector solutions and therefore compounds the difficulties. Thus, one is forced to seek approximate solutions to most diffraction problems.[3] Gratings, or random distributions of "diffractors" may offer less difficulty than several

---

[1] See, for example, Tremblay and Boivin; Felsen and Weston.

[2] Adey; Adonina and Shestopalov; Bousquet; Erma; Kodis; Labrum; Macrakis; Meecham and Peters; Palmer and Phelps; Provalov, et. al.; Siegel, et. al.; Tang; Watson and Horton; Wiles and McLay.

[3] Adey; Karczewski and Wolf; Keller I; Keller II; Meecham; Morse; Stratton and Chu; Yeh III; Yu and Rudduck.

diffracting elements in proximity because superposition, and/or statistical averaging techniques can be used to obtain approximate solutions.[4] In relatively few cases has the problem of two or three diffracting elements (e.g., two infinite cylinders or strips) been considered because of the difficulties in the theoretical considerations (interactions between elements must generally be included).[5] There is, therefore, an apparent need for theoretical and experimental investigations in this latter area.

We shall here consider the case of Fraunhofer diffraction by two long, thin, parallel conducting strips whose faces are at various angles with respect to each other and the incident radiation, and at various separations. The incident radiation, polarized with the electric field vector parallel to the axes of the strips, has a wavelength which is of the order of the strip width. Experimental results for the intensity of radiation diffracted into different directions will be compared with theoretical patterns obtained from scalar Kirchhoff theory and the Keller "geometrical theory of diffraction."

Previous experimental work with strips includes work done by Lazar at New York University. He considered in detail the case of single strip diffraction for various

---

[4] Beard, et. al.; Mathur and Yeh.

[5] Andrews II; Germey; Lazar; Row; Twersky I, II; Zitron and Karp.

strip widths and incident angles and polarizations both parallel and perpendicular to the strip axis. His work also included a preliminary investigation of the effects of strip thickness, conductivity, and the nature of the surface on the diffraction patterns. A description of the diffracted energy from a small number of identical strips whose faces were parallel was also given. No systematic investigation, however, was made of the effects upon the pattern when strip width, separation, and orientation are varied.

2. Experimental Apparatus

A. Description of Spectrometer and Chamber

Since we will be considering diffraction under Fraunhofer conditions, an experimental set-up is required which will both generate and detect plane radiation. One method of approximately realizing these conditions is to place both source (assumed to be a point) and detector at large distances from the diffracting elements. This method, however, has the disadvantage of low intensity levels both for incident and diffracted radiation, especially when the size of the diffracting obstacles is of the same order as the wavelength of the radiation. It was therefore decided to collimate the radiation by placing the mouth of the source waveguide at the focal point of a parabolic mirror. The mirror chosen was a large government surplus searchlight mirror with an aperture of approximately 36 inches and a quoted focal length of 14 5/16 inches. Measurements were taken to test the quality of the paraboloidal shape of the mirror and also to verify its focal length. The details and results of the procedure used to accomplish these objectives are indicated in Appendix I. The focal length of the parabola as measured there was found to be $14.25 \pm .16$ inches.

Once the quality of the mirror was established, the next concern was the degree of accuracy required in locating the source of microwave radiation (which was to be open-

ended waveguide) at the focal point. A survey of optics texts and the literature did not supply a satisfactory answer to this question, nor did they indicate the degree of aberration in the radiation emerging from the mirror if the source is off the focal point. A Fermat's Principle analysis was made to determine the distortion in the emerging radiation from a parabolic mirror if the source is not at the focal point.[6] The conclusion from this analysis, later confirmed experimentally, was that it is important to place the source on the axis of the mirror since the most distortion, both in phase and amplitude, occurs for off-axis locations.

For radiation, microwaves whose wavelength was approximately 5 mm was selected. An OKI 55V11 klystron tube with frequency (wavelength) output of 50 - 60 ghz (6 - 5 mm) was chosen as the source. The rated output of this tube is approximately 100 milliwatts into a matched load. The klystron was immersed in an oil bath using a TRG klystron tube mount (model #946A). An FXR universal klystron power supply (model #Z815B) served as the power source for the tube. The reflector voltage of the tube was modulated with a 1000 hz square wave. The frequency of the modulation required external triggering because it was

---

[6]Lazar and DeAcetis, I; DeAcetis.

discovered that the internal frequency generator of the Z815B power supply was subject to drift. The output of the tube was fed through waveguide (type RG(98)/U) to the large collimating parabola, where the waveguide terminated at the focal point. The klystron and its associated electronics, plus the collimating mirror, constitute what will be called the "source system."

At the receiving end, a small paraboloidal mirror of 12 inch diameter and 5 3/4 inch focal length gathered the parallel radiation emenating from the diffracting obstacles and focused it into a horn (Microwave Components model #531) placed at the focal point of the mirror. A short section of waveguide carried this detected radiation through a frequency meter (Narda model #M807) to a crystal (type 1N53C) in a tunable mount (TRG model #V970) where the crystal acted as a square-law detector. A Hewlett-Packard SWR meter (model #415D), tuned to detect a 1000 hz signal, served as the amplifier for the crystal. The small paraboloid, horn receiver, frequency meter, crystal detector in mount and amplifier constitute what will be called the "detection system."

The receiving mirror and associated detecting apparatus were mounted at the end of a long U-beam spectrometer arm constructed at Queens College (Fig. 1). The spectrometer has the capability of a full 360° rotation. The measurement

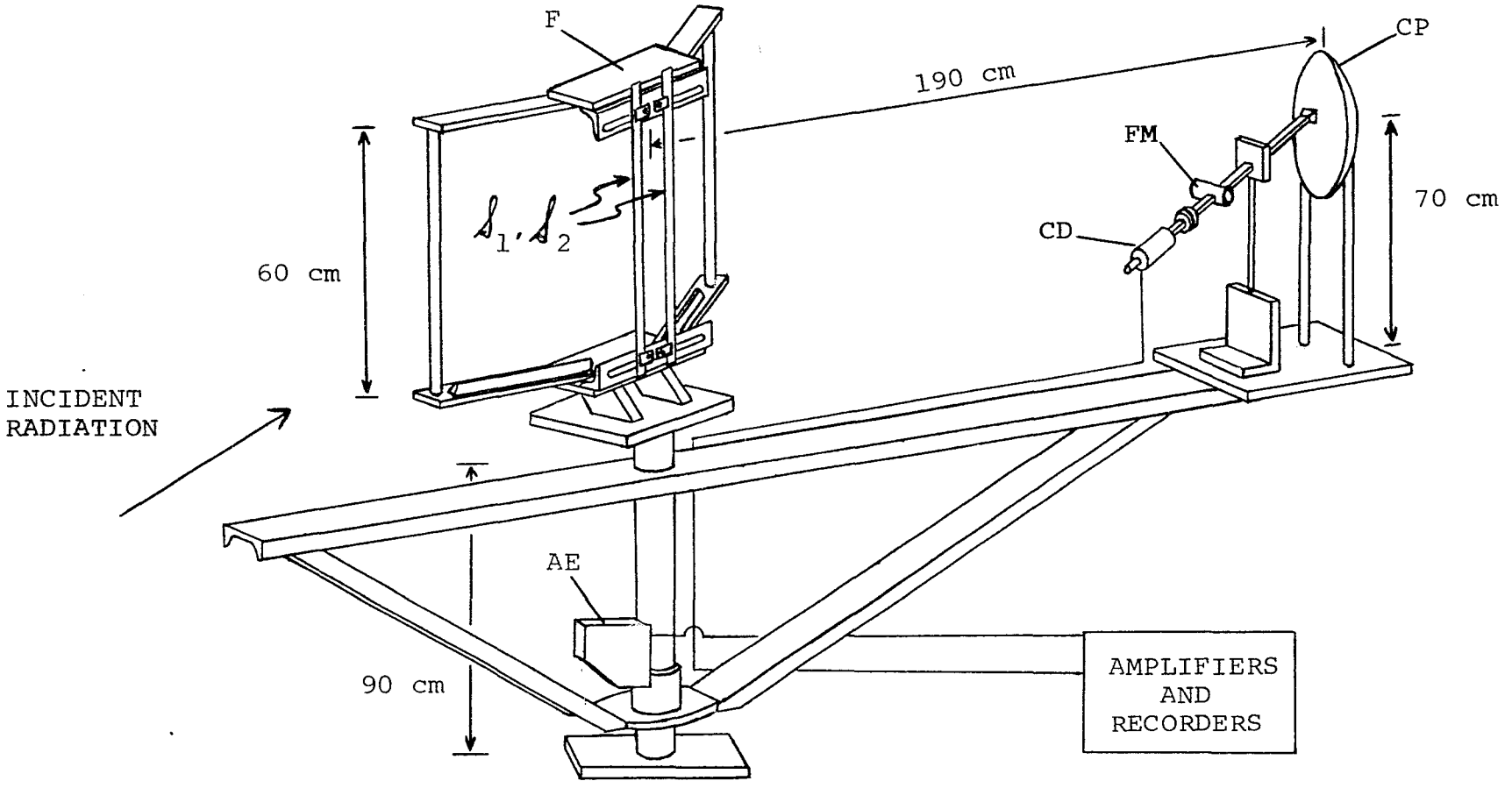

Fig. 1. Schematic sketch of the spectrometer: AE--angle encoder, CD--crystal detector in mount, CP--parabolic mirror to collect diffracted radiation, F--supporting frame for strips, FM--frequency meter, and δ_1, δ_2--diffracting strips.

of angular position was accomplished by using an electro-mechanical angular position display system supplied by Theta Instruments. The principle part of this system is the angle encoder which was held fixed at the base of the spectrometer shaft. Gears, custom manufactured by Pic Gears, East Rockaway, New York, were used to transfer the rotational motion of the spectrometer arm to the encoder, which in conjunction with its supporting electronics, visually displayed the angular position. The combination of gears and encoder allowed angular determinations accurate to within 0.1^{o}.

The diffracting elements used were strips of aluminum or steel gauge stock with lengths of approximately 65 cm and .051 cm (.020 in.) thickness. The aluminum strips were either 1.220 cm or 1.475 cm in width while the steel strips had a width of 1.270 cm (.500 in.). The strips were supported in a frame under tension in order to ensure the planarity of their individual faces over their usable length of approximately 50 cm. The tension was obtained by stretching the strips between a plate placed in the ceiling, and the bottom of the frame which was mounted on the spectrometer shaft. Wedges, machined with various wedge angles, were clamped to the faces of the frame and the strips were held against these wedges, thus placing the planes of the strips at various angles with respect to each

other. Rotation of the frame with respect to the incident radiation allowed further variation of the angles of incidence with respect to the individual strips.

Since the experiment was to be conducted indoors, a chamber was required which would contain the spectrometer, diffracting strips in frame, and other necessary equipment. In order to minimize unwanted reflections as much as possible, the walls and ceiling of the chamber were covered with microwave absorbing material (Eccorsorb type CH445). Various parts of the frame and detection system were also covered with flexible absorber (Eccosorb type AN72). It was at first thought necessary to cover the floor as well, but this proved unnecessary.

B. Alignment Procedures

The procedures followed in aligning the system were found to be most important as the experimental work progressed. The two critical adjustments were the positioning of the source waveguide and receiver horn at the focal points of their respective mirrors. These two procedures are discussed in detail below together with the general alignment method.

The first alignment step was the mounting of the receiver paraboloid on the spectrometer arm so that the axis of the mirror is parallel to both the length of the arm and the ground. The axis of the mirror when so mounted will be referred to as the "z-axis." Once this was accomplished, a beam of parallel visible light was directed along the z-axis. The receiver horn, on the end of a short segment of waveguide which connected it to the frequency meter and crystal detector, was then positioned. Only half of the receiver mirror was used. The horn was therefore directed toward the center of the upper half. A piece of masking tape was placed over the horn mouth to allow the focused radiation to be clearly visible. The horn was positioned so that the visible light was brought to focus

at the plane of the horn opening.[7]

The large searchlight mirror used as a collimator was mounted with its axis vertical. This orientation was chosen because of the large size and weight of the mirror which would make other mounting orientations difficult. To turn the direction of the radiation emerging from the mirror from vertical to horizontal, a front-surfaced plane mirror, 2 ft x 3 ft, was suspended above the large paraboloid at an angle of 45^{o} with the horizontal. The orientation of this plane mirror was somewhat adjustable so that the radiation could be directed toward the axis of rotation of the spectrometer where the diffracting strips were located (Fig. 2). Here, again, only half of the mirror was used.[8] Thus the source was directed toward the center of that part of the mirror. The source used was open end waveguide whose face sides were beveled back to eliminate as much as possible reflections from the waveguide. The

---

[7] This focus position was chosen experimentally. Other positions were tried, including the focusing of the light at a point half-way down the horn and at a point at the base of the horn. It was found for these latter positions that, for single strip patterns used as test patterns, the relative heights of the test pattern maxima did not have the proper intensities relative to each other, and the curves were not smooth. See also King, p. 281.

[8] This is done to eliminate non-uniformities at the beam center due to diffraction by the source waveguide.

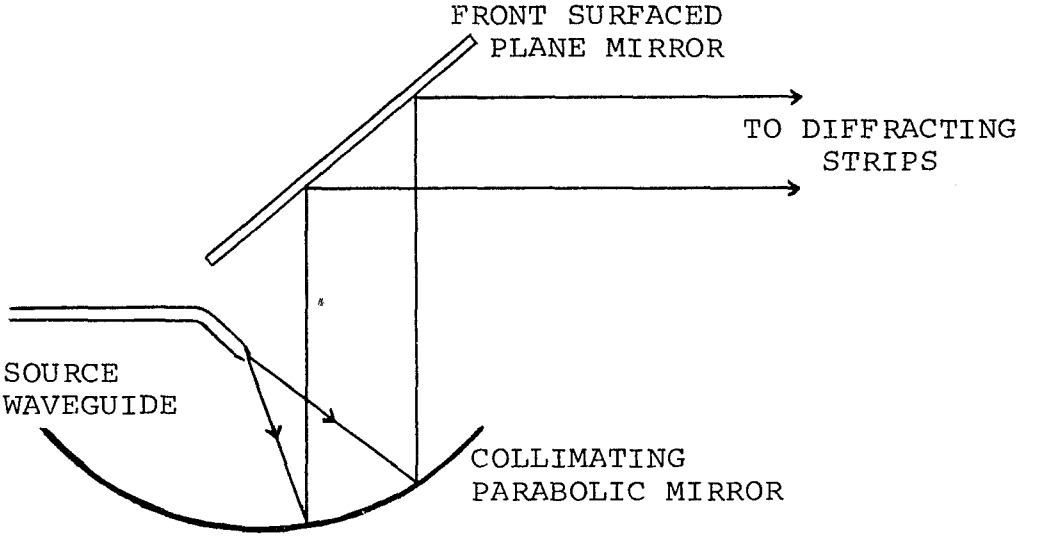

Fig. 2. That part of the source system used to produce the plane radiation incident upon the strips.

z-axis of the arm was set to coincide with the direction of the radiation from the collimator. At first, the source waveguide was positioned by eye. It was then moved along three perpendicular axes until the intensity detected by the receiving mirror was a maximum. The assumption used here is that the received radiation is a maximum when the incident radiation is plane since the detector was set to receive plane radiation. Inspection of the position of the end of the source waveguide revealed that it was slightly high above the focal point and slightly off-axis. This indicates that the effective position of the "point source" of the microwaves coming from the open ended waveguide is slightly outside the open end of the waveguide.[9]

The final alignment procedure was the orientation of the frame and its reference faces relative to the direction of the incident radiation. This was accomplished by clamping a 6" X 24" X ¼" plane mirror to the frame faces. If the faces are to be at angle U with the incident beam direction, then specular reflection by the mirror will occur at angle 2U. The spectrometer arm was rotated to the 2U position and the frame was rotated and oriented so that the detected radiation reflected by the mirror was a maximum. Since the mirror on the frame is wide compared to the

---

[9]This confirms results obtained by Lazar.

wavelength (approximately 30 wavelengths), it was assumed that the maximum reflected intensity is at the angle of specular reflection. This completed the major parts of the alignment procedure.

C. Alignment Tests

The above alignment procedures were followed in the spring of 1967 and the summer of 1968. Once aligned properly, the system was used to take many sets of readings over the course of several months, with periodic checks on the state of the alignment. The basic test of the incident beam and system as a whole was comparison between single strip results obtained experimentally, and theoretical results predicted by either exact theory (when available) or first-order Keller theory applied to a single strip.[10] Most experimental results involved strips of widths 1.220, 1.270, and 1.475 cm, and these strips were most often used in the test runs. Typical incident angles (measured relative to a normal to the strip) were 36°, 46° or 56°. The features checked were the smoothness of the patterns, the relative heights of maxima, and the angular positions of maxima and minima. Typical single strip patterns are given in Figs. 3, 4, 5, along with the pattern predicted by Keller theory. Similar patterns were taken at various positions in the incident beam.

---

[10] The use here of Keller theory applied to single strip diffraction is justified in Appendix II where a comparison is made between results predicted by Keller theory and results obtained from an exact solution of Maxwell's equations. For cases involving strip widths and incident angles comparable to those used in the experiment, the agreement between Keller theory and exact solution is excellent.

To compare phases at different parts of the beam, some of the first multiple strip patterns taken were for strips in a plane.[11] (Examples are included below with other results). The good agreement between theory and experiment with respect to location of maxima and minima, the relative heights of the maxima and the near zero values of the minima in these latter patterns are all indications that the phase across the used part of the beam was good.

---

[11] Lazar and DeAcetis, II, III; DeAcetis and Lazar.

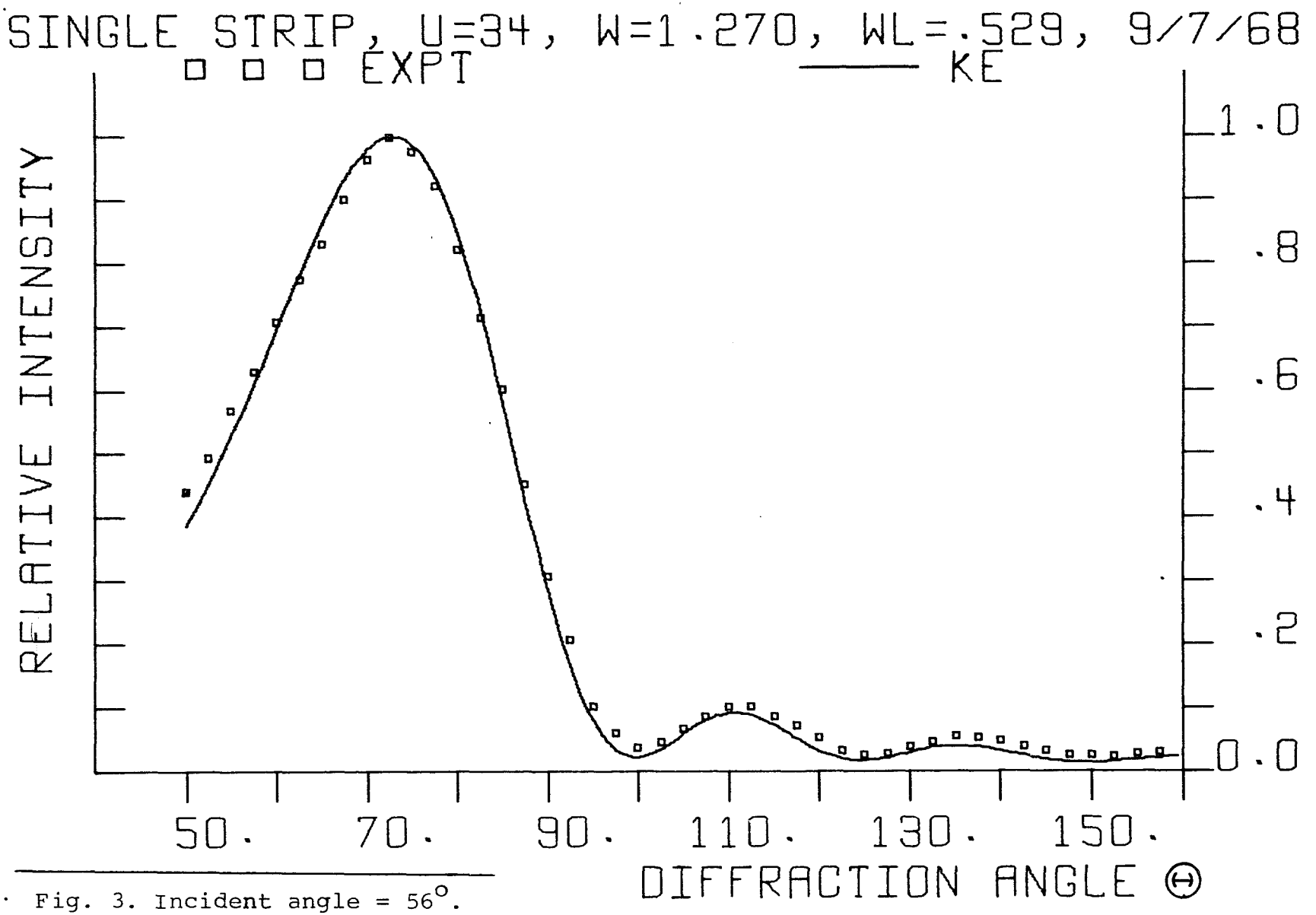

Fig. 3. Incident angle = 56°.

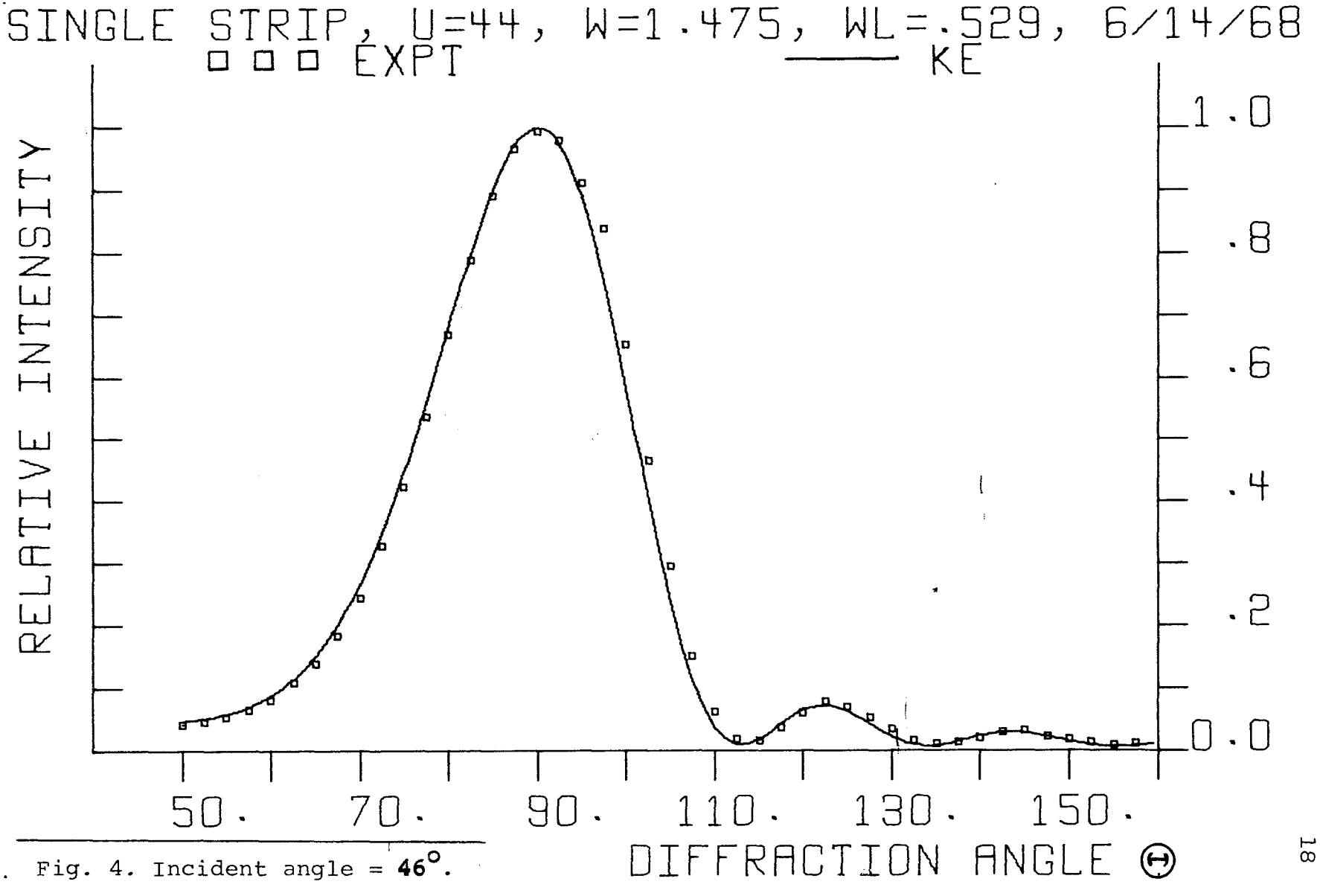

Fig. 4. Incident angle = **46°**.

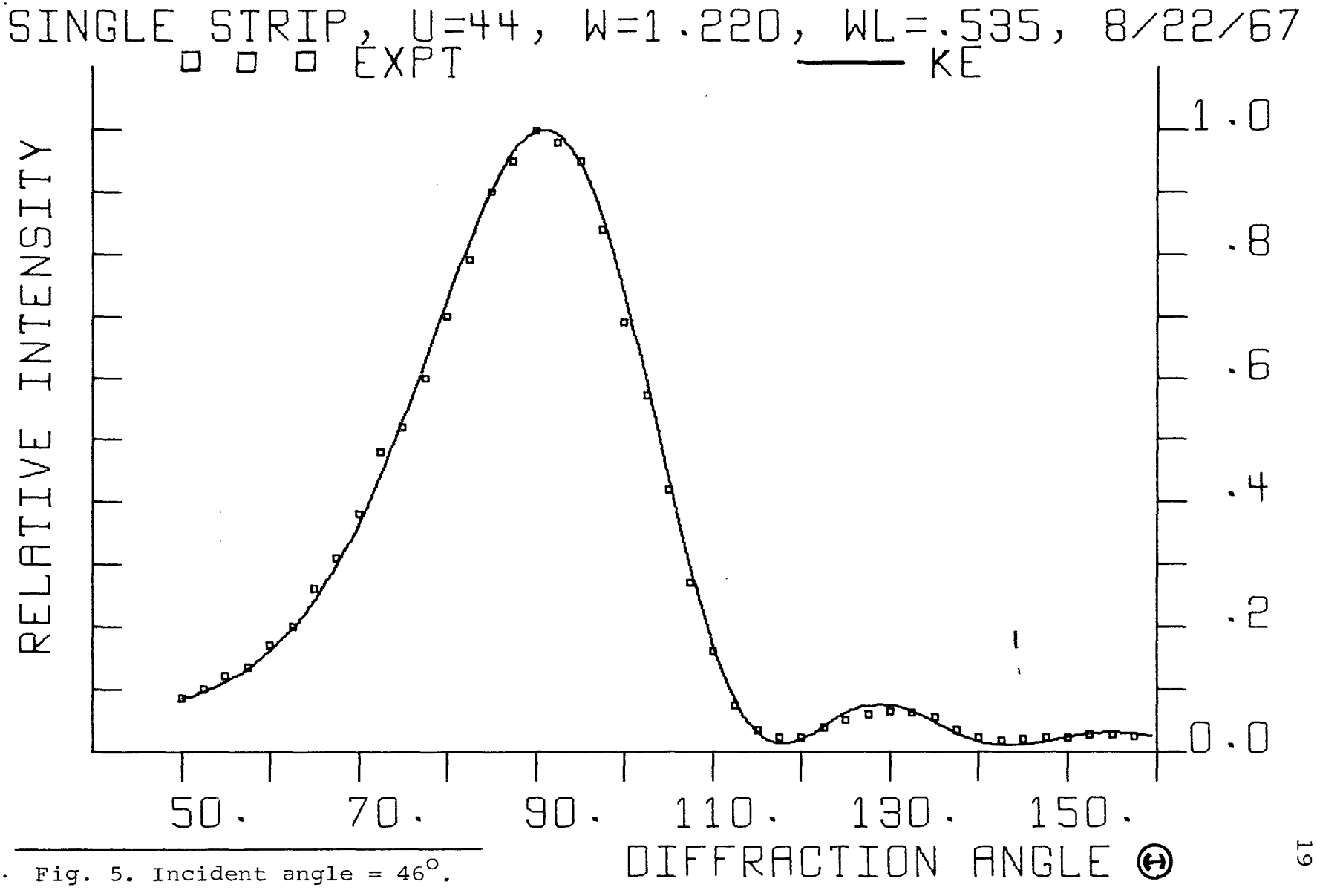

Fig. 5. Incident angle = 46°.

3. Comparison of Theories

The results obtained experimentally are compared with scalar Kirchhoff theory and Keller's geometrical theory of edge diffraction. The Kirchhoff theory is a scalar theory which makes no distinction between polarizations, while the Keller theory takes into account the boundary conditions on the diffracting elements and therefore does distinguish between polarizations.

A. Kirchhoff Theory

The well known Kirchhoff integral solution to the Helmholz equation, based upon Green's theorem, can be written[12]

$$\psi = \frac{1}{4\pi} \oint_{\Sigma} \left[\frac{\partial \psi}{\partial n} \frac{e^{ikr}}{r} - \psi \frac{\partial}{\partial n} \left(\frac{e^{ikr}}{r} \right) \right] d\sigma \qquad (1)$$

where ψ, the amplitude of the disturbance within a volume enclosed by a surface Σ, is expressed in terms of the value it and its normal derivative, $\partial\psi/\partial n$, have on the surface. The disturbance has wave number k, and r is the distance from a surface element $d\sigma$ to the observation point (harmonic time dependence has been suppressed).

Applying Eq. 1 to the case of two long, flat, thin, conducting strips, we assume that the field and its normal

---

[12] Stratton, p. 460.

derivative are everywhere zero except on the strips (s_1, s_2) where the values are the same as those of the incident radiation. Under these conditions, and assuming the incident waves are from a point source with unit amplitude, Eq. 1 reduces to

$$\psi = \frac{ik}{4\pi} \int_{s_1, s_2} e^{ik(r+r_o)} \frac{\cos\theta_i' + \cos\theta'}{r_o r} \, d\sigma \qquad (2)$$

where r_o and r are the distances from the area element $d\sigma$ on a strip, to the source and observation points respectively (Fig. 6). The angles θ_i' and θ' are respectively the angles of incidence and diffraction measured relative to a normal to the strip. If we assume strips of infinite length, then Eq. 2 reduces to a one-dimensional integral over each strip. Consider two strips of width w located as shown in Fig. 7, where the axes of the strips are parallel to each other and perpendicular to the page. A coordinate system is chosen with its origin at the intersection of extensions of the strips such that both strips form angle $\beta/2$ with respect to the y-axis as shown. The distance between strip centers is D. In the Fraunhofer limit, the source and observation points are at large distances from the strips. The incident radiation is then essentially parallel and makes an angle θ_i with the x-axis as shown, and is diffracted into angle θ, also measured relative to the x-axis. All phases will

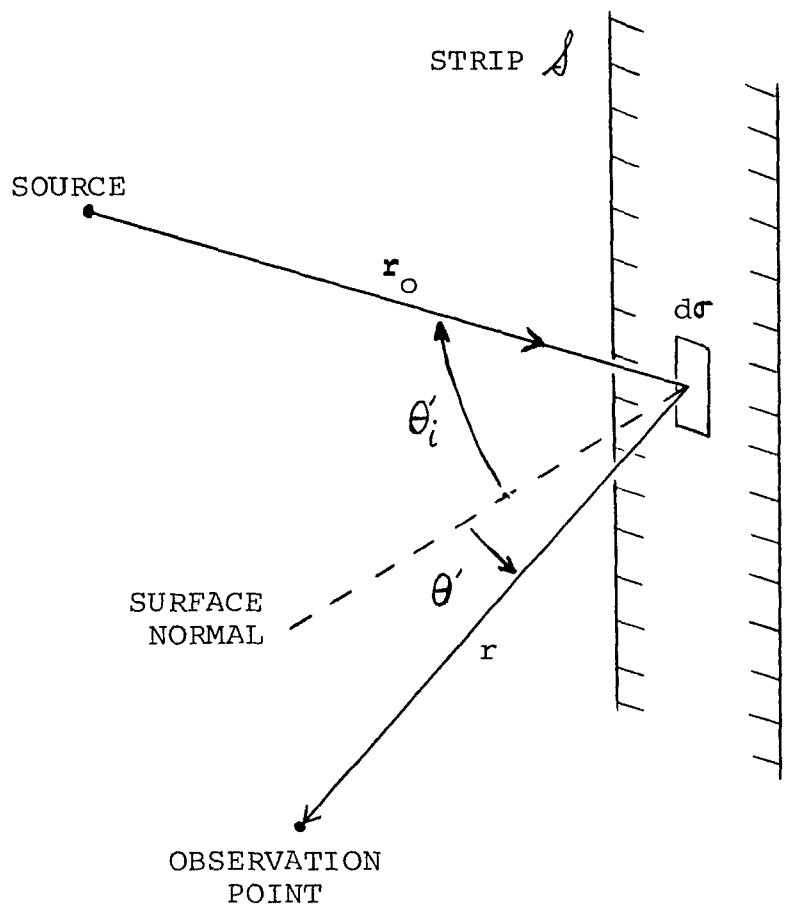

Fig. 6. Kirchhoff theory geometry. Only one strip is shown. Radiation from a point source is incident upon a surface element $d\sigma$ at angle θ'_i and is diffracted into angle θ' to the observation point. The strips are part of a closed surface Σ, which consists of the planes in which the strips lie and part of a sphere at infinity.

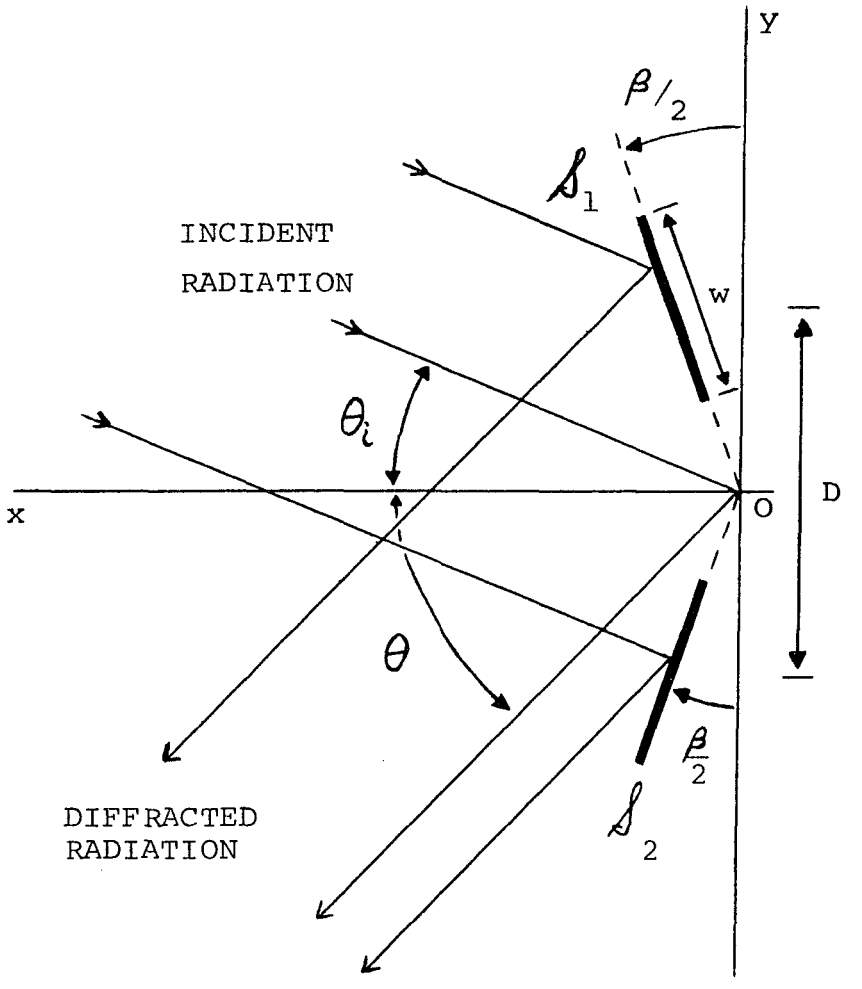

Fig. 7. Geometry for Kirchhoff diffraction by two infinitely long, parallel strips ($\mathcal{S}_1, \mathcal{S}_2$) in the Fraunhofer limit.

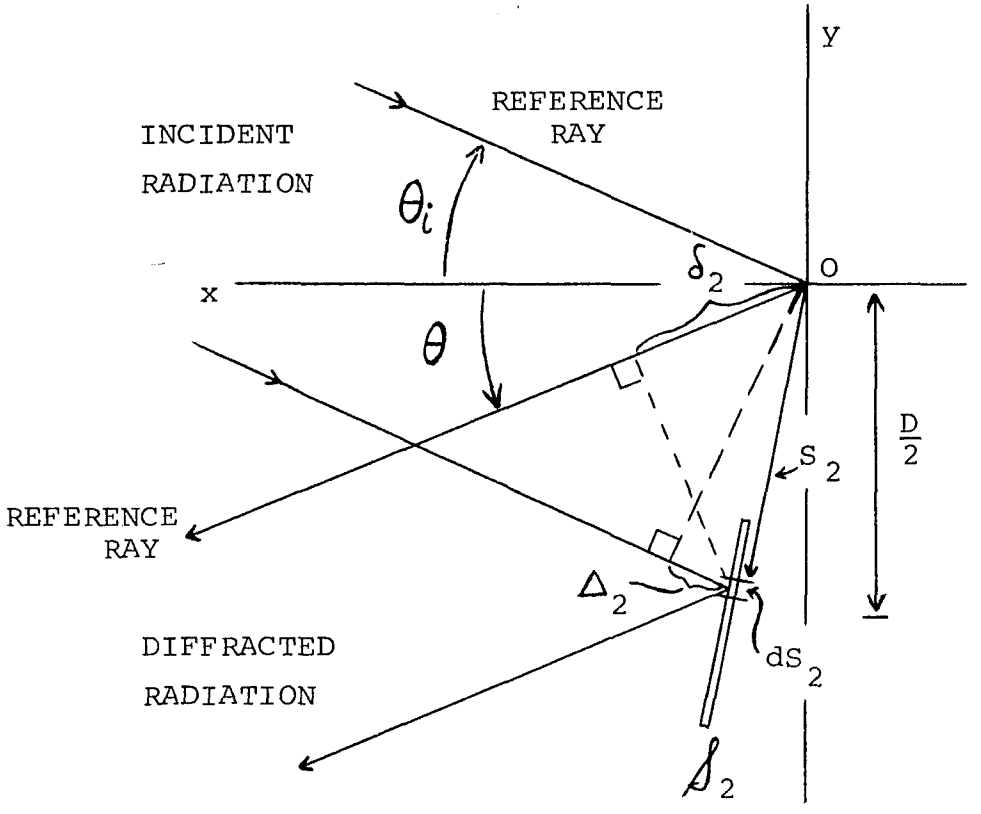

Fig. 8. Detail of the integration variables used in the Kirchhoff theory as applied to one of the strips ($\mathcal{S}_2$).

be measured with respect to that of an incident ray travelling through the origin, and a "diffracted" ray emerging from the origin. Consider strip s_2 (Fig. 8). The differential form of the Kirchhoff integral applied to the radiation diffracted by a one-dimensional differential segment of the strip dS_2 yields

$$d\psi_2 = A_2'\left[\cos\left(\theta_i - \frac{\beta}{2}\right) + \cos\left(\theta + \frac{\beta}{2}\right)\right] e^{ik(\Delta_2 + \delta_2)}\, dS_2 \qquad (3)$$

where $d\psi_2$ is the diffracted field from dS_2, A_2' is independent of direction, and $k(\Delta_2 + \delta_2)$ is the phase difference between the incident and diffracted rays for dS_2 and the reference rays through the origin. From the geometry, it is easily seen that

$$\begin{aligned} \Delta_2 &= S_2 \sin\left(\theta_i - \frac{\beta}{2}\right) \\ \delta_2 &= -S_2 \sin\left(\theta + \frac{\beta}{2}\right) \end{aligned} \qquad (4)$$

where S_2 is the distance from the origin to dS_2 measured along the strip (Fig. 8). Thus,

$$d\psi_2 = dS_2\, A_2'\left[\cos\left(\theta_i - \frac{\beta}{2}\right) + \cos\left(\theta + \frac{\beta}{2}\right)\right] e^{ikS_2\left[\sin\left(\theta_i - \frac{\beta}{2}\right) - \sin\left(\theta + \frac{\beta}{2}\right)\right]} \qquad (5)$$

Similarly, the radiation diffracted from a differential segment dS_1 of strip s_1 yields the differential field

$$d\psi_1 = A_1' \, dS_1 \left[\cos(\theta_i + \beta/2) + \cos(\theta - \beta/2)\right] e^{ik(\Delta_1 + \delta_1)} \tag{6}$$

where $\Delta_1 + \delta_1 = S_1 \left[- \sin(\theta_i + \beta/2) + \sin(\theta - \beta/2)\right]$ and A'_1 is independent of direction.[13] The total field diffracted into angle θ is then

$$\psi = \int d\psi = \int_{S_1, S_2} (d\psi_1 + d\psi_2) \tag{7}$$

$$= A_1 \int_{S_1} e^{i\gamma S_1} \, dS_1 + A_2 \int_{S_2} e^{i\alpha S_2} \, dS_2 \tag{8}$$

where

$$\begin{aligned} A_2 &= A_2' \left[\cos(\theta_i - \beta/2) + \cos(\theta + \beta/2)\right] \\ A_1 &= A_1' \left[\cos(\theta_i + \beta/2) + \cos(\theta - \beta/2)\right] \\ \alpha &= k \left[+ \sin(\theta_i - \beta/2) - \sin(\theta + \beta/2)\right] \\ \gamma &= k \left[- \sin(\theta_i + \beta/2) + \sin(\theta - \beta/2)\right] \end{aligned} \tag{9}$$

Let d equal the distance from the origin to the center of either strip. The limits of integration are then from $S_{1,2} = d - w/2$ to $S_{1,2} = d + w/2$ for each strip. Evaluation

---

[13] If the incident radiation has the same amplitude on each strip, $A_1' = A_2'$; we have allowed here for the possibility of unequal amplitudes due to non-uniform incident radiation.

of Eq. 8 yields

$$\psi = A_1 w e^{i\gamma d} \frac{\sin\left(\frac{\gamma w}{2}\right)}{\gamma \frac{w}{2}} + A_2 w e^{i\alpha d} \frac{\sin\left(\alpha \frac{w}{2}\right)}{\alpha \frac{w}{2}} \qquad (10)$$

The intensity I is proportional to the square magnitude of ψ. Hence

$$\begin{aligned} I &= \psi^2 = \psi\psi^* \\ &= A_1^2 w^2 \frac{\sin^2(\gamma w/2)}{(\gamma w/2)^2} + A_2^2 w^2 \frac{\sin^2(\alpha w/2)}{(\alpha w/2)^2} + \\ &\qquad 2A_1 A_2 w^2 \frac{\sin(\gamma w/2)}{(\gamma w/2)} \frac{\sin(\alpha w/2)}{(\alpha w/2)} \cos \frac{D(\gamma - \alpha)}{2\cos(\beta/2)} \end{aligned} \qquad (11)$$

where we have used the fact that d is related to the distance D between strip centers by $d = D/(2\cos(\beta/2))$.

B. Keller's Geometrical Theory of Diffraction

The "geometrical theory of diffraction" as developed by Keller[14] (and referred to as "Keller theory" below) describes diffraction in terms of interactions between incident radiation and boundaries. Incident radiation, represented by rays which travel in straight line paths when in a homogeneous medium, gives rise to "diffracted rays" when incident upon a boundary. If the boundary is an edge of a thin screen with radiation incident normal to the edge at an angle α' (measured with respect to a surface perpendicular to the screen), and diffracted at angle θ' to an observer at point P (Fig. 9), then the diffracted field at P is given by Keller theory as

$$u = -\frac{v\, e^{i\left(\frac{\pi}{4}+kr\right)}}{2(2\pi kr)^{\frac{1}{2}}}\left[\sec\left(\frac{\theta'-\alpha'}{2}\right) \pm \csc\left(\frac{\theta'+\alpha'}{2}\right)\right] \qquad (12)$$

where r is the distance from the edge to P, and v is the field incident upon the edge. The upper sign applies when the boundary condition on the screen is u = 0, and the lower sign is used when the normal derivative of u is zero on the screen.

For the case of two long, parallel strips, there are four edges effective in diffraction and the total first-

---

[14] Keller I; Keller III.

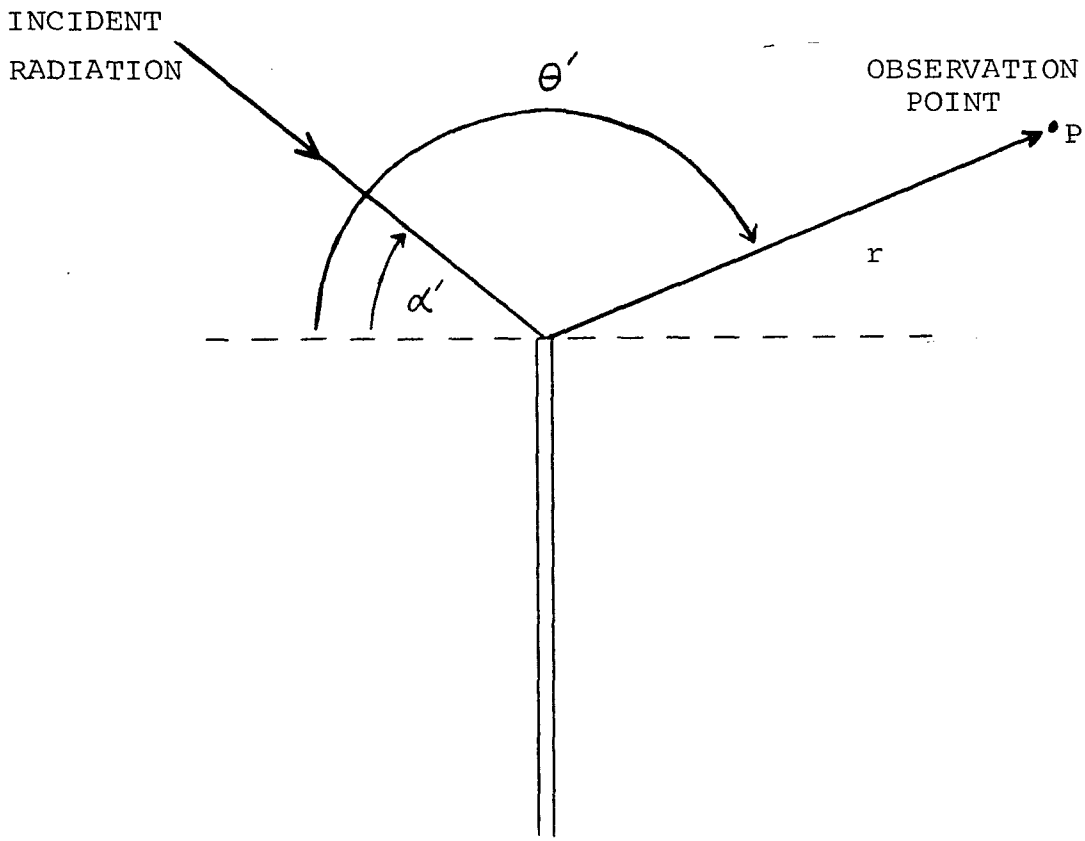

Fig. 9. Geometry for the Keller geometrical theory of edge diffraction. A thin screen, perpendicular to the page, has radiation incident upon it at angle α'. This gives rise to diffracted rays, one of which emerges at angle θ' and passes through observation point P. Both α' and θ' are measured relative to a plane that is perpendicular to both the edge and the page.

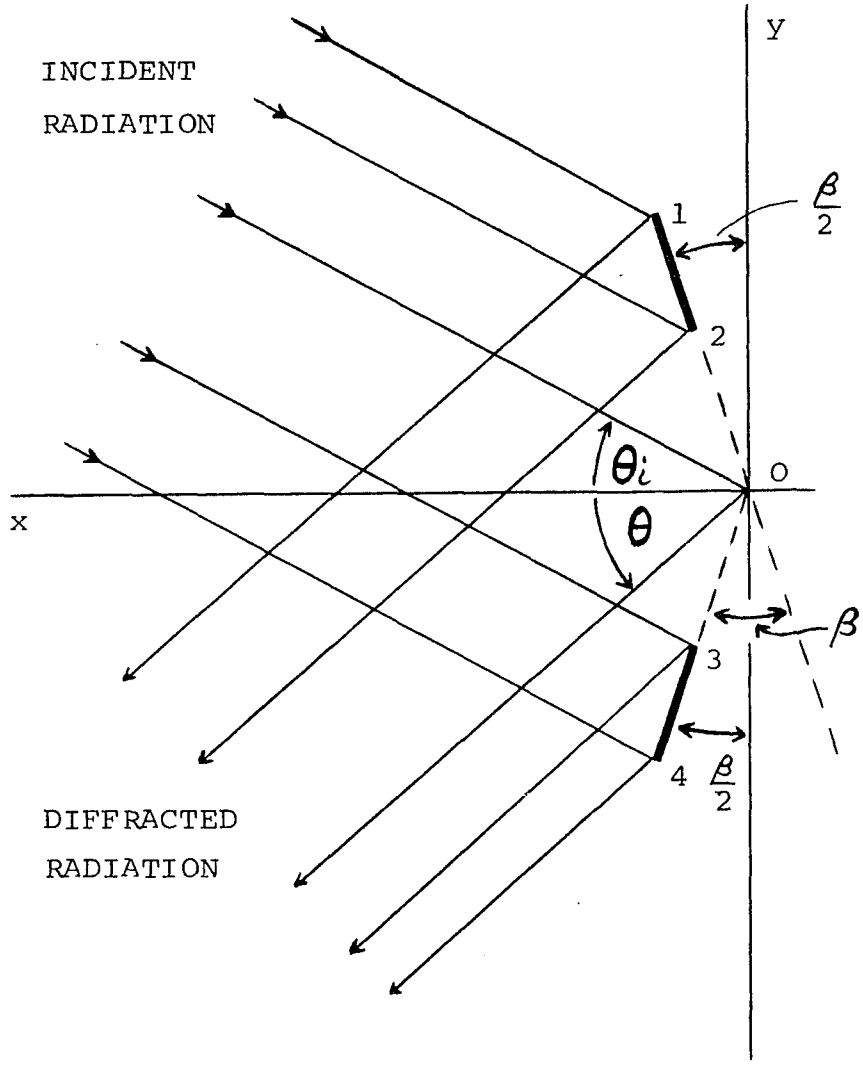

Fig. 10. Keller's geometrical theory of edge diffraction (first-order) applied to Fraunhofer diffraction by two long, parallel strips. Four diffracted rays add to yield the total field in a given direction. The center rays which travel through the origin O are reference rays.

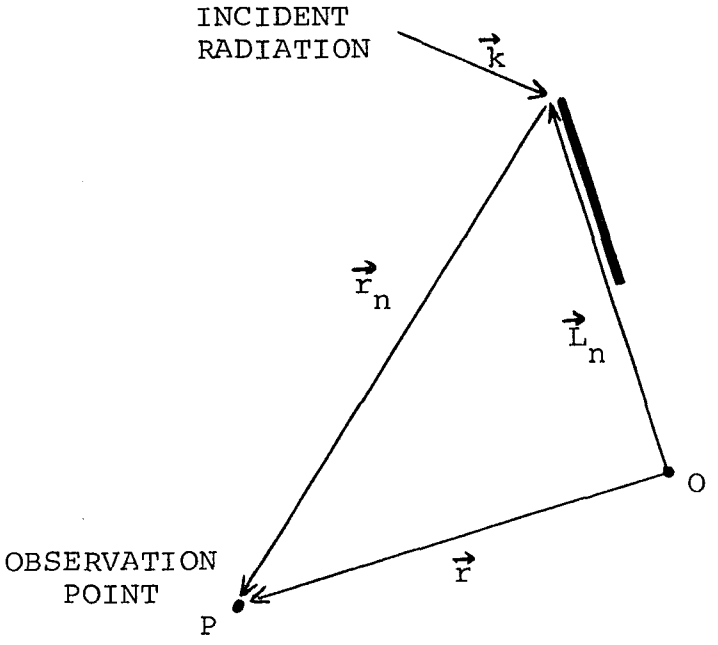

Fig. 11. Definition of vectors used in the geometrical theory equations.

order field, $u^{(1)}$, at an observation point is the sum of the contributions of each of these edges.[15] Consider two such strips whose planesmake angle β with respect to each other (Fig. 10). Let the strips be positioned in a coordinate system such that the plane of each makes angle $\beta/2$ with the y-axis. Since the strips are considered infinite in length, the diffraction problem is a two-dimensional one in the plane perpendicular to the strip axes. As before, the strips are of width w, and D is the distance between strip centers. Let $\vec{L}_n$ be a vector from the origin to the n^{th} edge (n = 1, 2, 3, 4) where the edges are numbered as shown in Fig. 10. Plane radiation, wave vector $\vec{k}$, is incident upon the strips at angle θ_i and diffracted into angle θ, where both angles are measured with respect to the x-axis as shown. All phases will be measured relative to the value, ϕ_o, at the origin. The field incident upon edge n is then of the form (unit amplitude):

$$v_n = e^{i(\vec{k}\cdot\vec{L}_n + \phi_o)} \tag{13}$$

Let $\vec{r}_n$ be the displacement from edge n to the observation

---

[15] Rays incident upon the faces of the strips are considered to be specularly reflected. Under Fraunhofer conditions, the effects of these rays cancel.

point P, and r be the displacement of P with respect to the origin (Fig. 11). If α_n and θ_n represent the values of α' and θ' (defined in Fig. 9) for edge n, and choosing the phase at the origin as zero, then equation (12) yields

$$u_n = -\frac{e^{i\vec{k}\cdot\vec{L}_n + i\left(\frac{\pi}{4}+\vec{k}\cdot\vec{r}_n\right)}}{2(2\pi k r_n)^{\frac{1}{2}}}\left[\sec\left(\frac{\theta_n-\alpha_n}{2}\right)+\csc\left(\frac{\theta_n+\alpha_n}{2}\right)\right] \quad (14)$$

where the upper sign is chosen for polarization parallel to the strip axes. In the Fraunhofer limit of distant observation point, the magnitude of $\vec{r}_n = \vec{r} - \vec{L}_n$ approaches the value of $r - \vec{L}_n \cdot \hat{r}$ where $\hat{r}$ is a unit vector in the $\vec{r}$ direction. Now, $k\hat{r}$ is the wave number of the radiation diffracted into angle θ. Let $\vec{k}' = k\hat{r}$ and denote the value of u_n in the Fraunhofer limit by u_{nn}. Then,

$$u_{nn} = -\left\{\frac{e^{i\left(\frac{\pi}{4}+kr\right)}}{2(2\pi kr)^{\frac{1}{2}}}\, e^{i\vec{L}_n\cdot(\vec{k}-\vec{k}')}\left[\sec\left(\frac{\theta_n-\alpha_n}{2}\right)+\csc\left(\frac{\theta_n+\alpha_n}{2}\right)\right]\right\} \quad (15)$$

In terms of the geometry of Fig. 10, the contributions of each of the edges to the Fraunhofer pattern is

$$u_{11} = -A e^{ikL_1\left[\sin\left(\theta-\frac{\beta}{2}\right)-\sin\left(\theta_i+\frac{\beta}{2}\right)\right]}\left[\sec\left(\frac{\theta+\theta_i}{2}\right)+\csc\left(\frac{\theta_i-\theta+\beta}{2}\right)\right] \quad (16a)$$

$$u_{22} = -A e^{ikL_2\left[\sin\left(\theta-\frac{\beta}{2}\right)-\sin\left(\theta_i+\frac{\beta}{2}\right)\right]}\left[\sec\left(\frac{\theta+\theta_i}{2}\right)+\csc\left(\frac{\theta-\theta_i-\beta}{2}\right)\right] \quad (16b)$$

$$u_{33} = -A e^{-ikL_3\left[\sin\left(\theta+\frac{\beta}{2}\right)-\sin\left(\theta_i-\frac{\beta}{2}\right)\right]} \left[\sec\left(\frac{\theta+\theta_i}{2}\right)+\csc\left(\frac{\theta_i-\theta-\beta}{2}\right)\right] \quad (16c)$$

$$u_{44} = -A e^{-ikL_4\left[\sin\left(\theta+\frac{\beta}{2}\right)-\sin\left(\theta_i-\frac{\beta}{2}\right)\right]} \left[\sec\left(\frac{\theta+\theta_i}{2}\right)+\csc\left(\frac{\theta-\theta_i+\beta}{2}\right)\right] \quad (16d)$$

where A is independent of direction and equal to

$$\frac{e^{i\left(\frac{\pi}{4}+kr\right)}}{2(2\pi kr)^{\frac{1}{2}}}$$

The total first-order diffracted field is then the sum of the contributions of each of the edges:

$$u^{(1)} = \sum_{n=1}^{4} u_{nn} \quad (17)$$

Second-order effects arise when diffracted rays are incident upon an edge and are diffracted again to produce "doubly diffracted rays." If a diffracted ray is incident upon edge m after having been previously diffracted from edge n, then Eq. (12) is applied at edge m. The value of v is set equal to u_n (Eq. 14) with appropriate values for r_n and θ_n. Let u_{mn} denote the second-order field from edge m in the Fraunhofer limit. We have

$$u_{mn} = -u_n A e^{i\vec{k}\cdot\vec{r}_m}\left[\sec\left(\frac{\theta_m - \alpha_{mn}}{2}\right) + \csc\left(\frac{\theta_m + \alpha_{mn}}{2}\right)\right] \qquad (18)$$

where α_{mn} is the appropriate value of α' (defined in Fig. 9) at edge m for a ray coming from edge n. As an example, consider the evaluation of u_{13} (Fig. 12). Evaluation of Eq. (18) yields

$$u_{13} = \frac{A}{2(2\pi k r_{13})^{\frac{1}{2}}} e^{i\left[\frac{\pi}{4} + kr_{13} - \vec{k}\cdot\vec{r}_1 + \vec{k}\cdot\vec{r}_3\right]} \times$$

$$\left[\sec\left(\frac{-90+\eta+\theta_i}{2}\right) + \csc\left(\frac{\theta_i+90-\eta-\beta}{2}\right)\right]\left[\sec\left(\frac{\theta_1-\alpha_{13}}{2}\right) + \csc\left(\frac{\theta_1+\alpha_{13}}{2}\right)\right] \qquad (19)$$

with

$$\theta_1 = -\theta + \frac{\beta}{2}$$

$$\alpha_{13} = -90^\circ + \frac{\beta}{2} - \eta$$

$$r_{13} = |\vec{r}_1 - \vec{r}_3| = D/\cos\eta$$

and

$$\eta = \tan^{-1}\left(\frac{w\sin(\beta/2)}{D}\right)$$

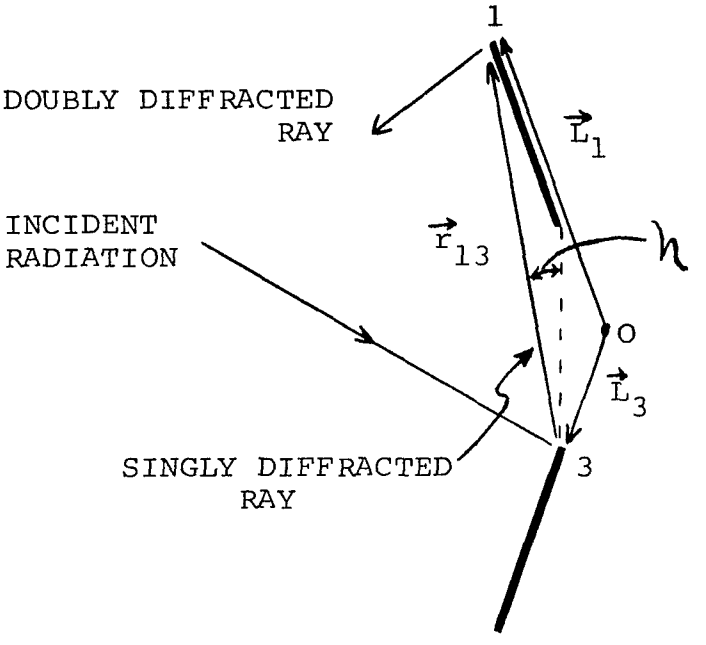

Fig. 12. Evaluation of the doubly diffracted ray u_{13}.

L_1 and L_3 can be expressed in terms of D, w, and $\beta/2$, and evaluation of the scalar products in the exponential then yields

$$\vec{k}' \cdot \vec{L}_1 = -k\left(\frac{D}{2\cos(\beta/2)} + \frac{w}{2}\right)\sin\left(\theta - \frac{\beta}{2}\right)$$

(20)

$$\vec{k} \cdot \vec{L}_3 = k\left(\frac{D}{2\cos(\beta/2)} - \frac{w}{2}\right)\sin\left(\theta_i - \beta/2\right)$$

The total diffracted field, $u^{(2)}$, including both first- and second-order effects is then given by

$$u^{(2)} = u^{(1)} + \sum_{m=1}^{2}\sum_{n=3}^{4}\left(u_{mn} + u_{nm}\right) \qquad (21)$$

Intensity patterns are obtained from Eqs. 17 and 21 by evaluating the square magnitudes of the fields $u^{(1)}$ and $u^{(2)}$.

The intensity diffraction patterns predicted by Kirchhoff theory (Eq. 11) and by first- and second-order Keller theory (Eqs. 16, 17, 18 and 21) were evaluated on IBM 1620 computers located at Queens College and Bronx Community College. Results obtained experimentally were punched onto cards and both experimental points and theoretical curves were plotted by the IBM 1627 plotter located at Queens College.

4. Comparison Between Experiment and Theory

A. Normalization Procedures and Notation

The experimental results presented below were obtained for the most part during the spring and summer of 1967 and the summer of 1968. The theoretical investigations were carried out at interim times. Theoretical points were calculated at 0.5° intervals in order to yield smooth curves when plotted by the IBM 1627 plotter. Experimental readings were taken at various increments, with most of the results presented here at intervals of 2.0° or 2.5°. Unless otherwise stated, experimental points are plotted at the center of small boxes or circles, first-order Keller theory is represented by a dashed line while second order is a solid line; Kirchhoff results are represented by "x's."

The angular position in the diffraction pattern recorded experimentally was measured relative to the incident beam direction. It will be denoted by Θ, and, in terms of the quantities defined in Figures 7 and 10, is given by $\Theta = 180^{\circ} - (\theta_i + \theta)$. Also, the "glancing angle of incidence," u, will be used in the following discussions; it is defined by $u = 90^{\circ} - \theta_i$ (Fig. 13).

With the exception of Fig. 14, the theoretical intensity curves are compared on a relative scale using the value of a single strip pattern maximum as a standard basis of comparison. Unless otherwise indicated, the

standard used was the maximum value of the intensity of the single strip pattern for incident angle $\theta_i = 36^o$ ($u = 54^o$). The maximum of the second-order Keller pattern was then set equal to unity (except in several cases, viz., Figs. 30, 35, 36 and 37 where the first-order Keller maximum was used) and all other theoretical values adjusted accordingly.

The experimental results are compared with theory in two ways. For those cases where experimental results are represented by boxes, the maximum of the experimental pattern was set equal to unity. For those cases where experimental points are represented by zeros, a single strip maximum for $u = 54^o$ was recorded experimentally at the time that the double strip pattern was obtained. The double strip values were then compared with the single strip reading to obtain relative intensity in the same way as was done for the theoretical points. These values were then adjusted relative to the second-order Keller theory maximum (chosen as unity).[16]

---

[16] These normalization procedures will be considered again in the Discussion, Section 5.

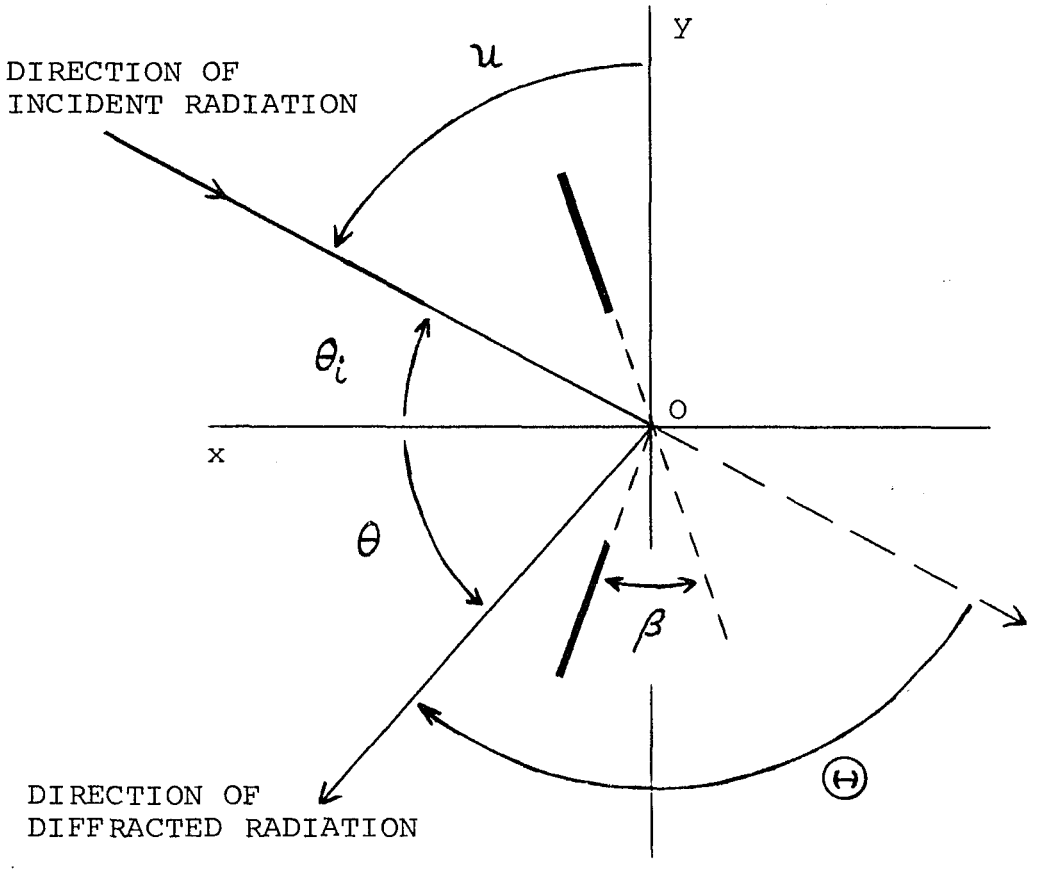

Fig. 13. Relationship between the angles used in the theoretical derivations, and the angles recorded experimentally.

NOTATION

The following notation and designations will be used in the discussion below. All lengths are expressed in centimeters and all angles in degrees.

w	- strip width
D	- separation between strip centers
θ_i	- angle of incidence
u	- glancing angle ($= 90^\circ - \theta_i$)
β	- acute angle between the planes of the strips
$u(\pm \beta/2, \mp \beta/2)$	- denotes the orientation of the strips relative to the glancing angle u; the upper signs are used for strips whose active faces meet at an angle greater than 180°, while the lower signs are for strips with an angle between active faces which is less than 180°.
WL, λ	- wavelength
KI	- Kirchhoff theory
KE-1	- first-order Keller theory
KE-2	- second-order Keller theory

B. Strips in a Plane

As indicated earlier, some of the first patterns taken were for strips in a plane at various separations. These patterns were to serve as a sampling of the phase and amplitude distribution across the incident beam. Phase aberrations would lead to misplaced maxima and minima, while amplitude aberrations, if large, would result in errors in the relative heights of maxima and the depths of the minima.

Fig. 14 presents the experimental and theoretical results for the case of two strips (w = 1.220 cm) with radiation incident at glancing angle u = 54^{o} (54(0,0) case). This is theoretically equivalent to the case of a single strip element of width w = 2.440 cm. On this graph, both theoretical patterns (KI and KE-1) and the experimental points were normalized relative to their maximum intensity. Since the equivalent strip width is approximately 4.6 wavelengths wide (a rather "wide" strip), the good agreement between Kirchhoff and first-order Keller theory is not surprising, and experiment agrees well with either, confirming that the two strips act as one.

Fig. 15 compares Kirchhoff theory with both first- and second-order Keller theory for the same strips as in Fig. 14 (w = 1.220 cm) but with a separation of approximately 3λ (D = 1.629 cm) between strip centers. Note that the Kirchhoff

values (KI) and the corresponding first-order Keller theory (KE-1) agree well with each other over the entire pattern but that the KI heights to the right of the principal maximum are consistently slightly lower than those of KE-1. The two closest edges of the strips are here approximately 0.8λ apart and relatively large higher order effects between these edges[17] can be expected under these circumstances. However, since the gap between the strips is less than a wavelength, the validity of the geometrical theory is in question. Indeed, over much of the experimental pattern, there is better agreement with KE-1 than with KE-2. Only at the far right, where the slightly higher values predicted by KE-2 are found experimentally, is there better agreement with the higher order. Fig. 16 considers the case of planar strips with approximately the same separation (D = 1.559 cm) but of greater width (w = 1.475 cm). Under these circumstances, the distance between the closest edges is approximately 0.2λ. Here the disparity between first- and second-order Keller and experiment is even greater, with first-order clearly in better agreement with experiment -- the pattern is approaching that of a single strip where the

---

[17] Second-order effects occur only between the closest edges in the geometrical theory for this case since the formulation assumes that no radiation travels across the strips.

multiple order effects vanish. In this region where the two closest edges are very close ($< \lambda$), it seems evident from Figs. 15 and 16 that further investigation is needed with regard to the influence of higher order effects.

Figs. 17 to 22 represent results obtained as the separation between strip centers was varied from approximately 4λ to 8λ for strips of widths 1.220 cm or 1.475 cm. As would be expected, second-order effects diminish as the strip separation is increased, and, therefore, only the second-order Keller is indicated on most of the graphs. As the distance between the strips is changed, the number of peaks and their relative heights change mainly because of interference effects. Fig. 18 compares first- and second-order Keller theory for a glancing angle of $u = 54^{o}$ and we see one of the anomalies of the second-order Keller theory, viz., the presence of singularities in certain regions. In this case, a singularity appears in the second-order as one approaches the plane of the strips. One could argue that this is "out of the region of interest," (at $\Theta = 54^{o}$ we are in the plane of the strips), but it is interesting to note that the first-order theory has the proper behavior in this region.[18]

---

[18] More of these singularities and discontinuities will appear later when the case of angled strips will be considered. The locations of the singularities and a general discussion of second-order effects as predicted by Keller theory can be found in Appendix III.

In general, a comparison between the Kirchhoff and Keller solutions for the planar strip cases seems to indicate close agreement between them and experiment, with the Keller solution in slightly better agreement with experiment, especially to the right of the principal maximum where the Kirchhoff solution is consistently too low. Also, in the regions where second-order effects are detectable, the Keller second-order corrections are able to improve the agreement between theory and experiment as long as the gap between the strips is not too small. Finally, the good general agreement between either theory and experiment verifies that the phase was uniform across that part of the incident radiation beam that was used.

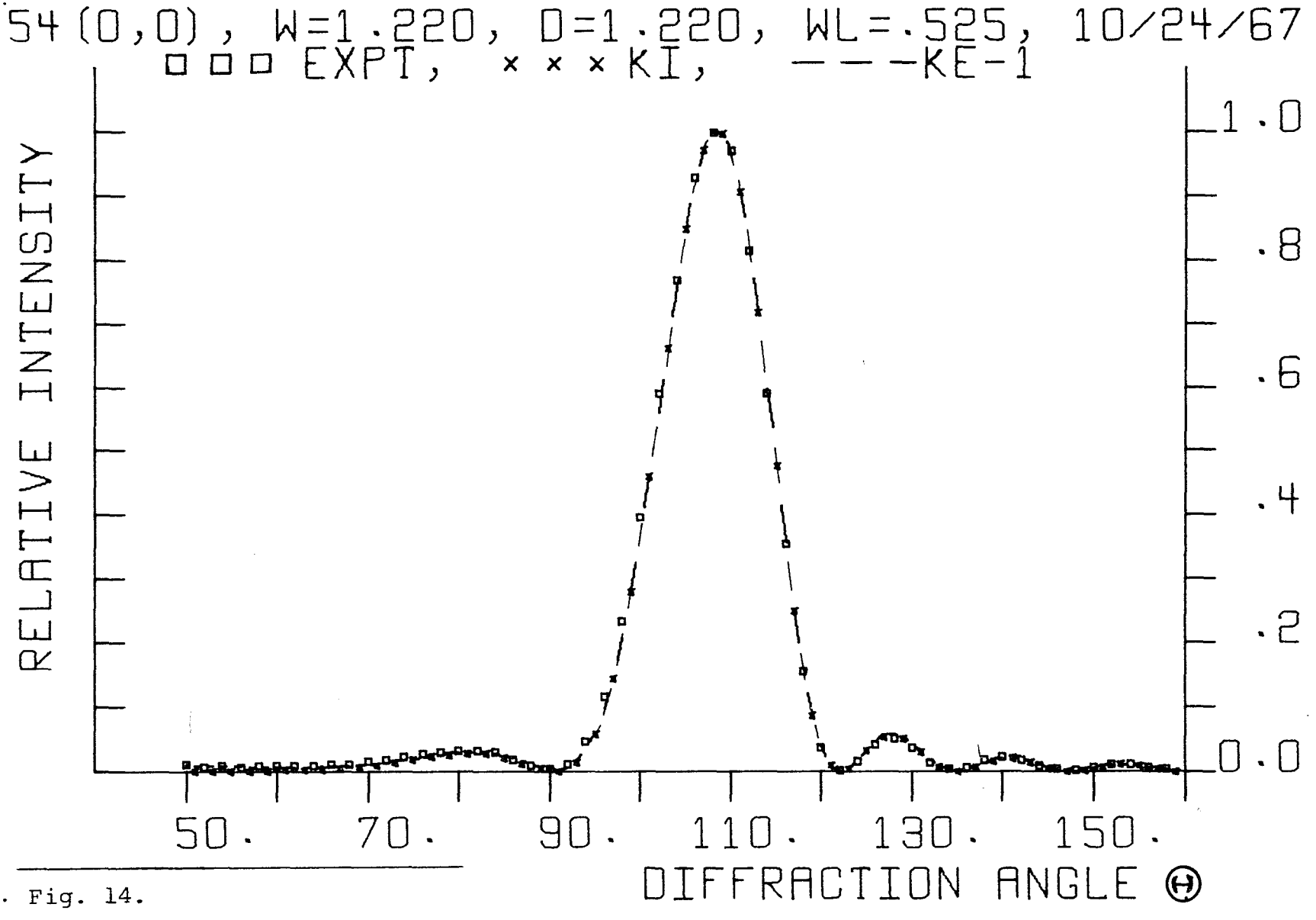
54 (0,0), W=1.220, D=1.220, WL=.525, 10/24/67
□ □ □ EXPT, × × × KI, — — —KE-1
RELATIVE INTENSITY
1.0
.8
.6
.4
.2
0.0
50.
70.
90.
110.
130.
150.
DIFFRACTION ANGLE Θ

Fig. 14.

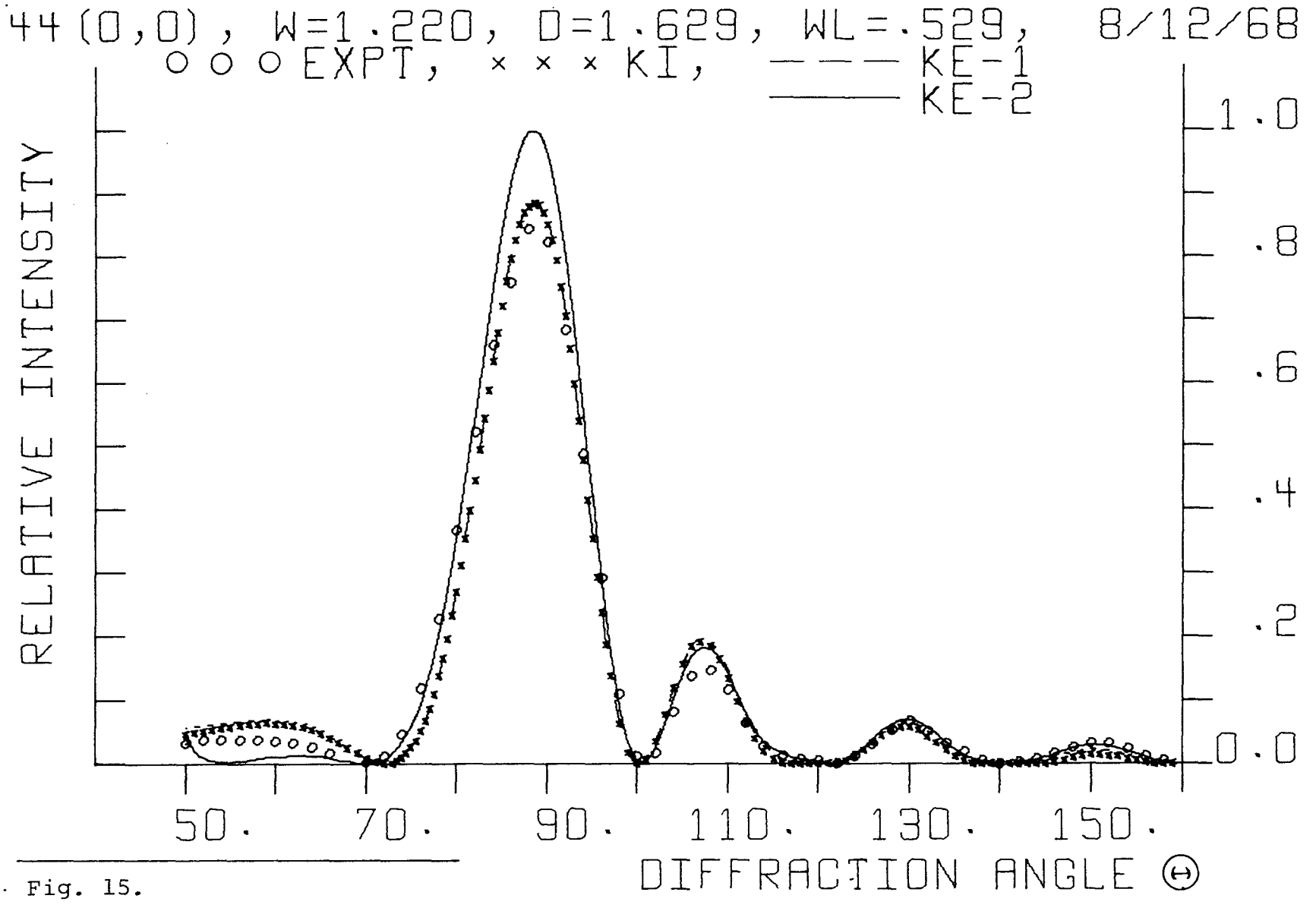
44 (0,0), W=1.220, D=1.629, WL=.529, 8/12/68
○ ○ ○ EXPT, × × × KI, — — — KE-1
——— KE-2
RELATIVE INTENSITY
1.0
.8
.6
.4
.2
0.0
50.
70.
90.
110.
130.
150.
DIFFRACTION ANGLE (2θ)

Fig. 15.

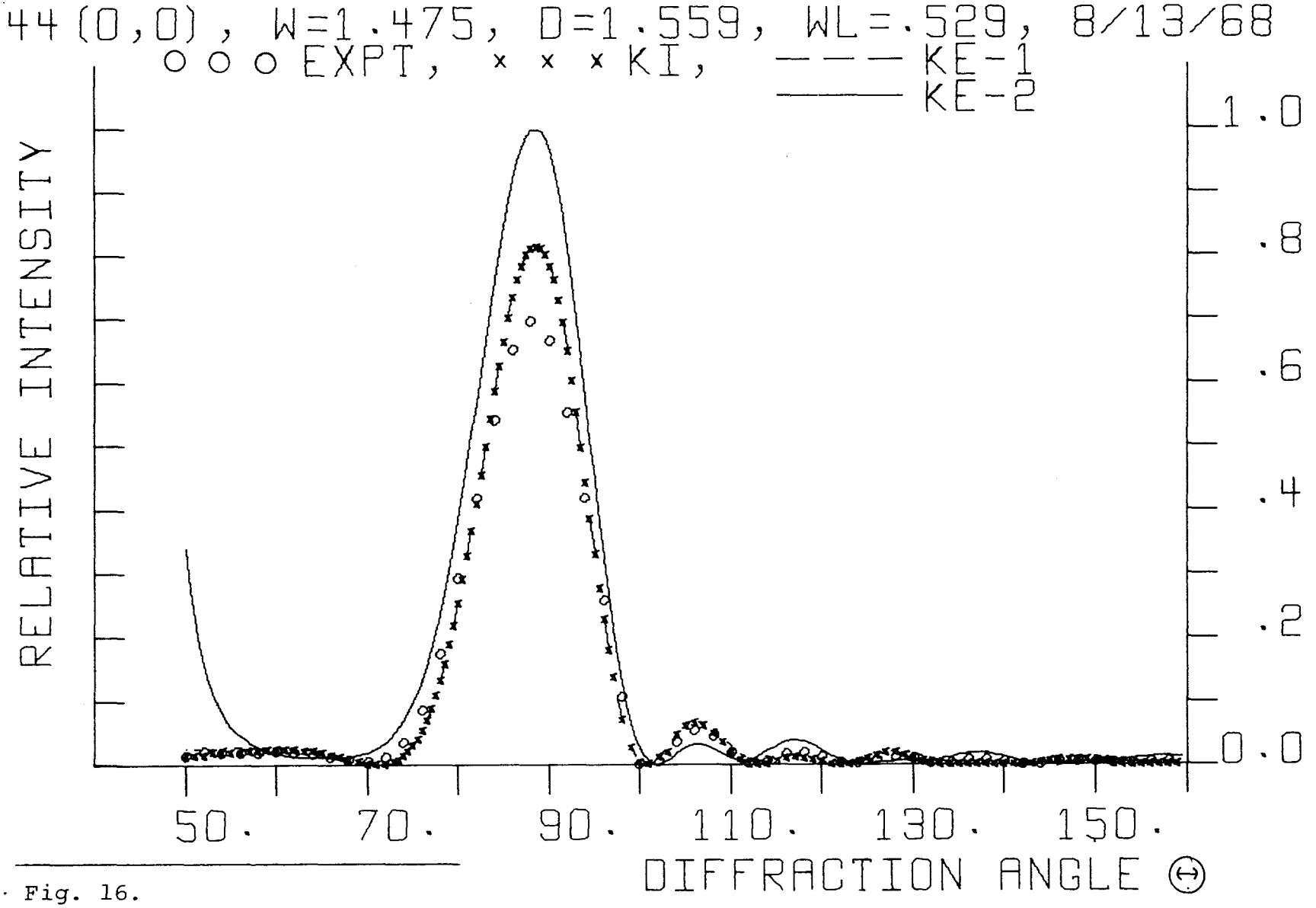
44 (0,0), W=1.475, D=1.559, WL=.529, 8/13/68
o o o EXPT, x x x KI, — — — KE-1 ——— KE-2
RELATIVE INTENSITY
1.0
.8
.6
.4
.2
0.0
50.
70.
90.
110.
130.
150.
DIFFRACTION ANGLE Θ

Fig. 16.

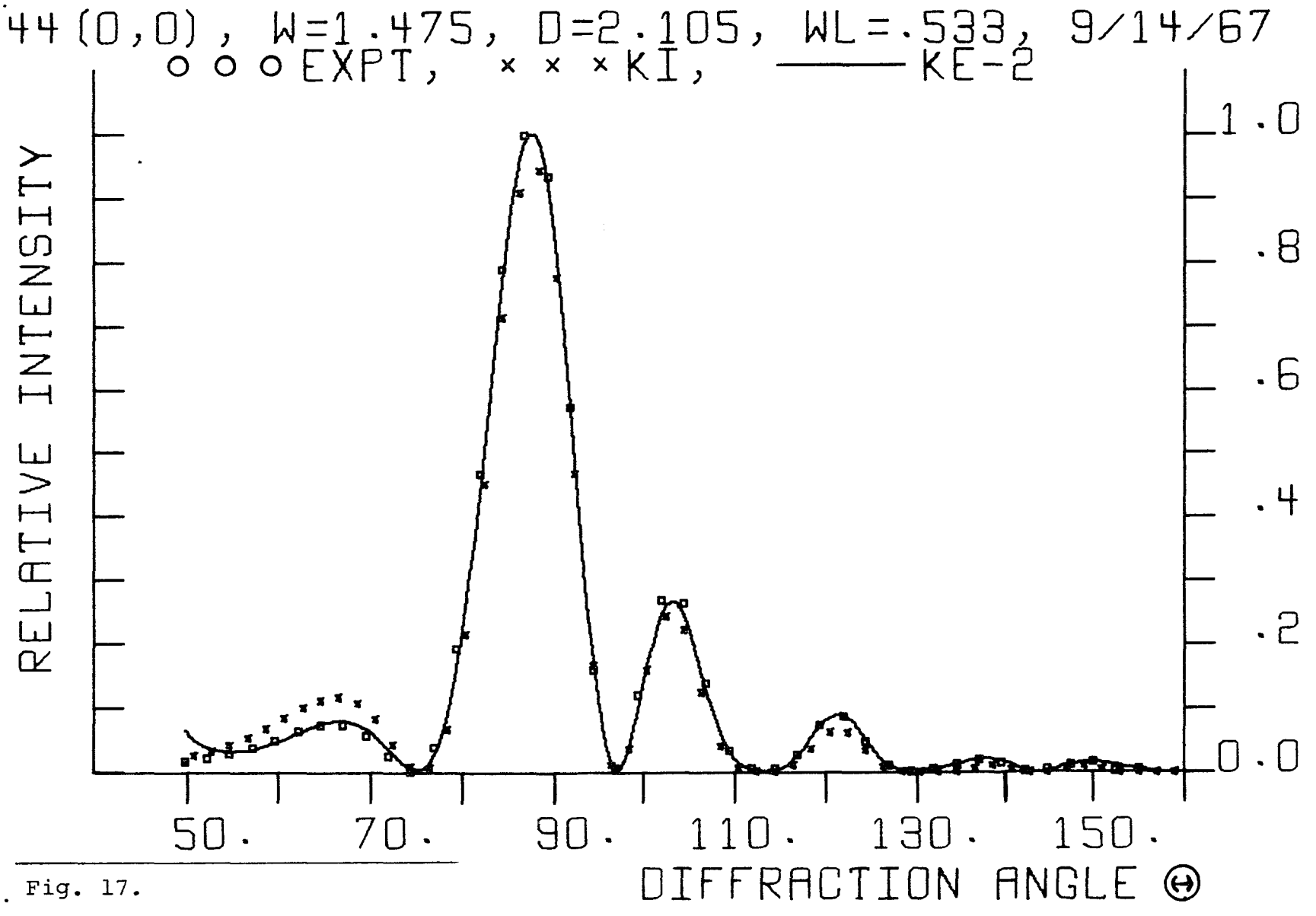
44 (0,0), W=1.475, D=2.105, WL=.533, 9/14/67
o o o EXPT, x x x KI, ——— KE-2
RELATIVE INTENSITY
1.0
.8
.6
.4
.2
0.0
50.
70.
90.
110.
130.
150.
DIFFRACTION ANGLE Θ

Fig. 17.

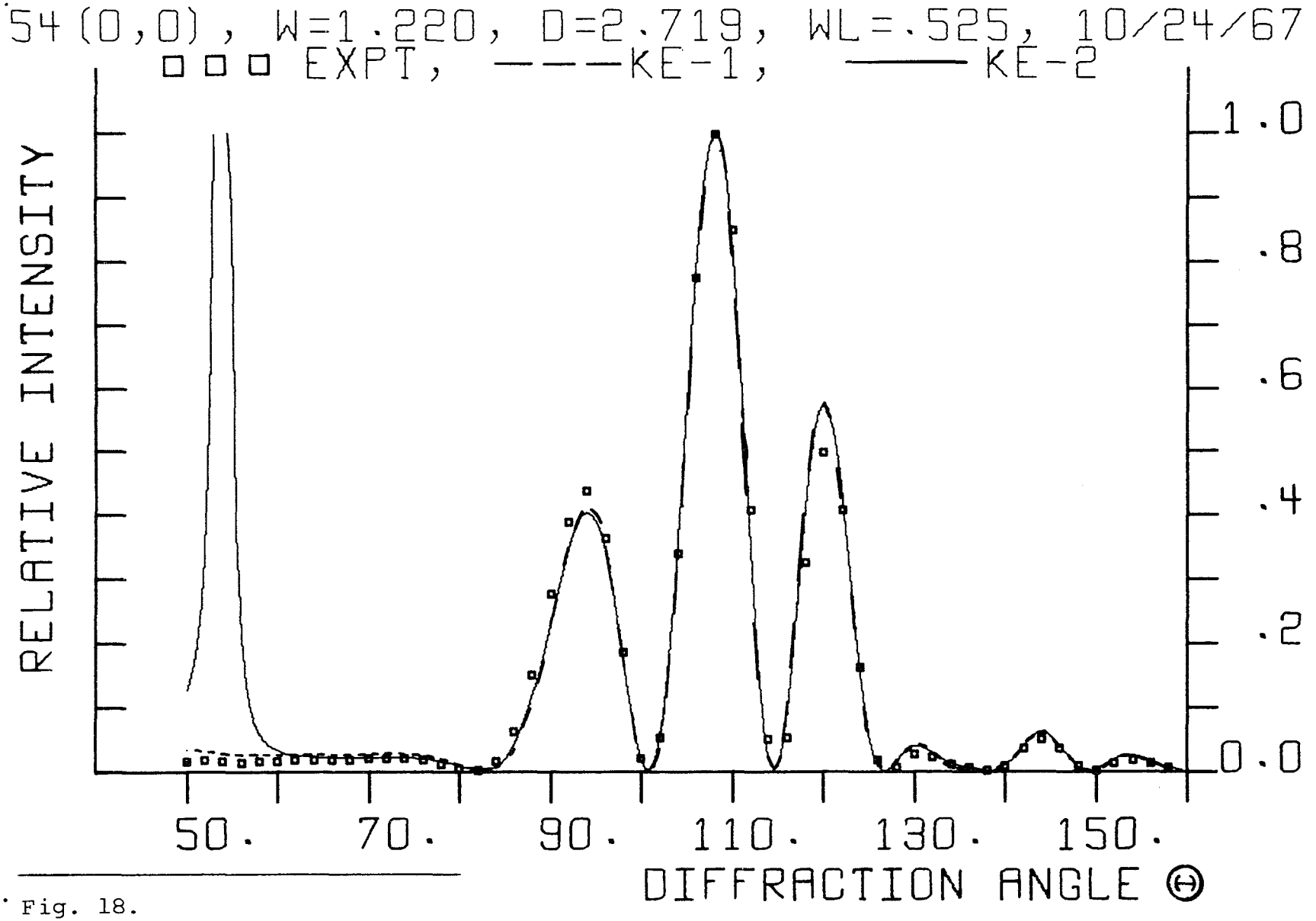
54 (0,0), W=1.220, D=2.719, WL=.525, 10/24/67
□ □ □ EXPT, ———KE-1, ——— KE-2
RELATIVE INTENSITY
1.0
.8
.6
.4
.2
0.0
50.
70.
90.
110.
130.
150.
DIFFRACTION ANGLE Θ

Fig. 18.

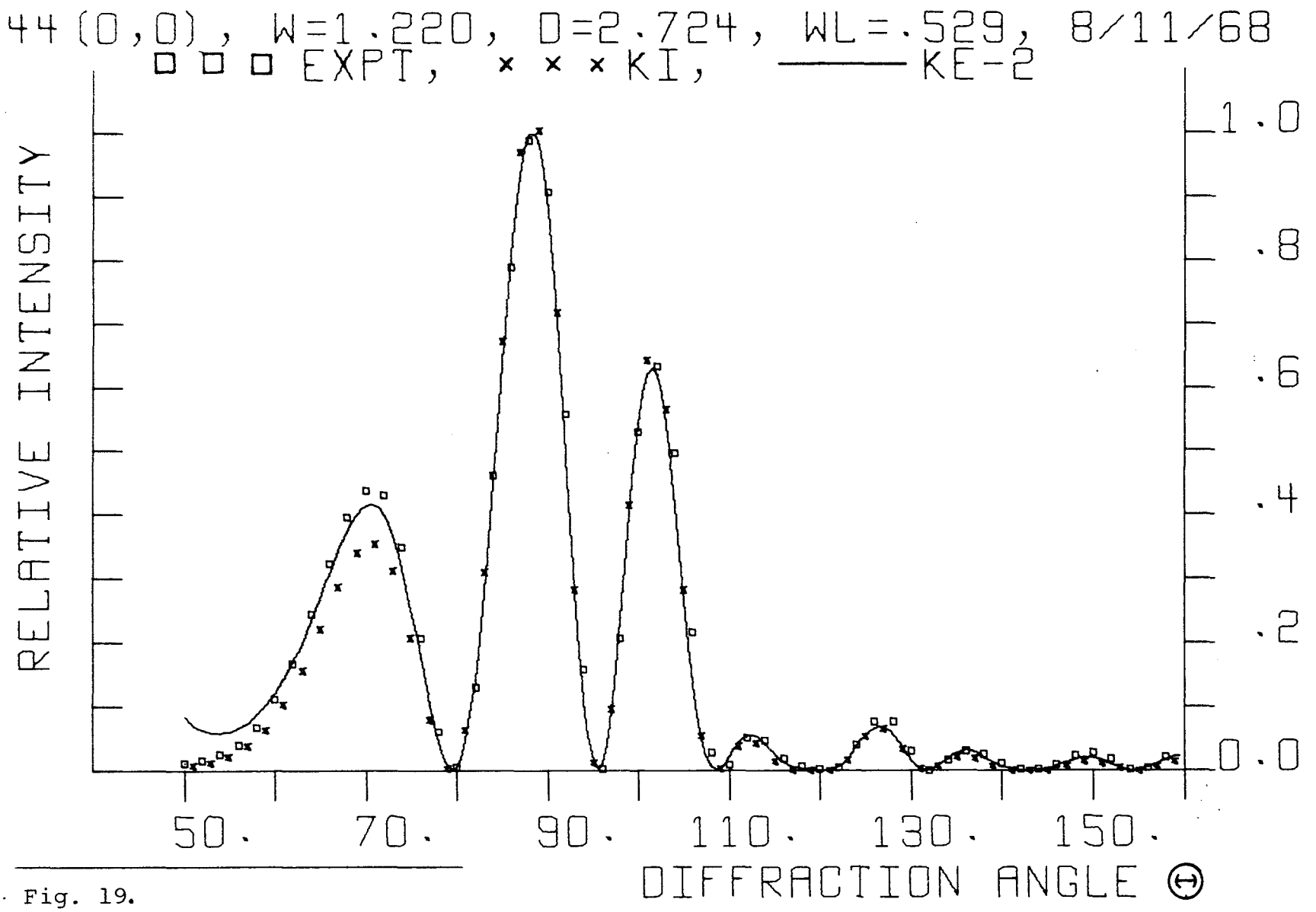
44 (0,0), W=1.220, D=2.724, WL=.529, 8/11/68
□ □ □ EXPT, × × × KI, ——— KE-2
RELATIVE INTENSITY
1.0
.8
.6
.4
.2
0.0
50.
70.
90.
110.
130.
150.
DIFFRACTION ANGLE Θ

Fig. 19.

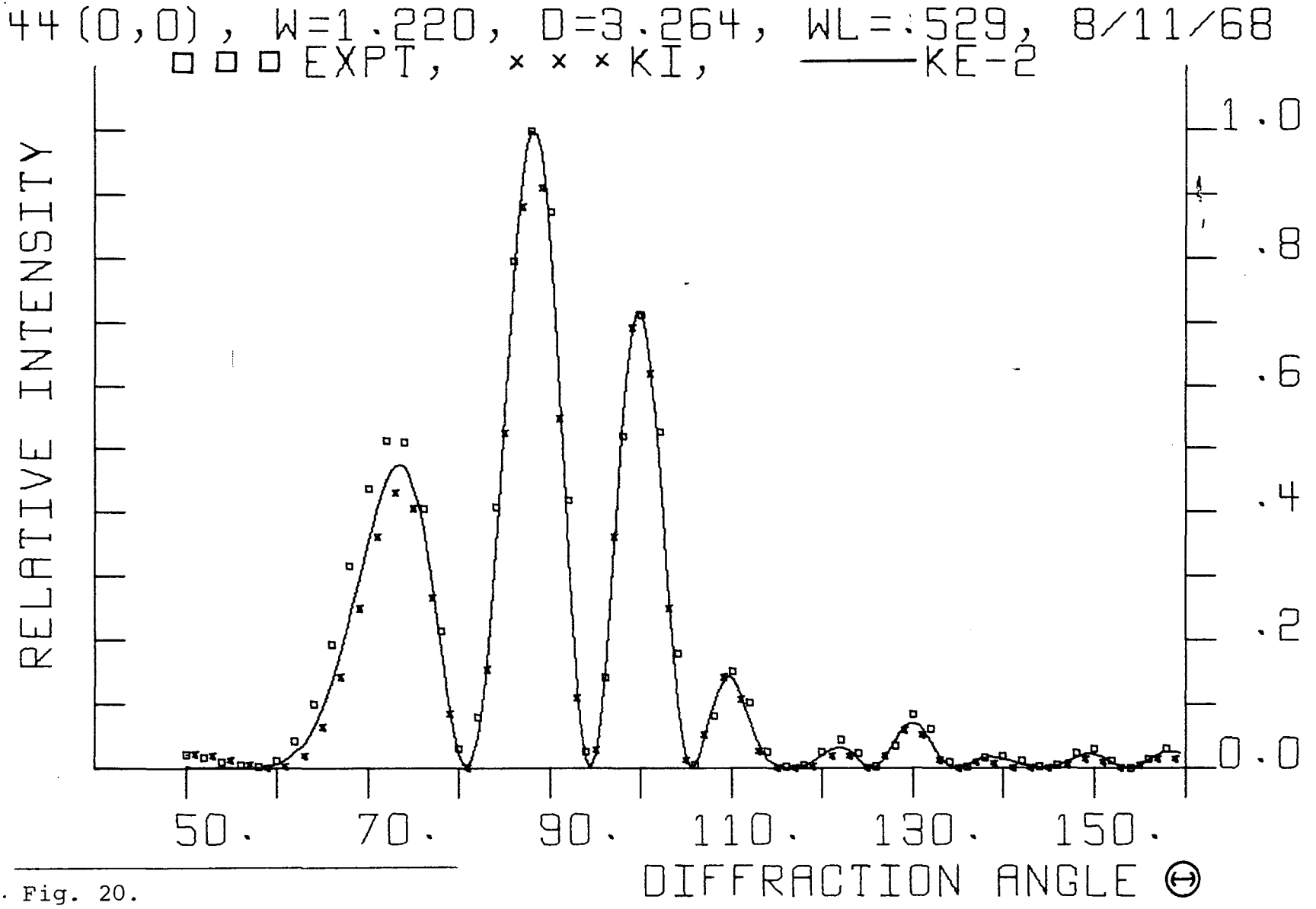
44 (0,0), W=1.220, D=3.264, WL=.529, 8/11/68
□ □ □ EXPT, × × × KI, ——— KE-2
RELATIVE INTENSITY
1.0
.8
.6
.4
.2
0.0
50.
70.
90.
110.
130.
150.
DIFFRACTION ANGLE ⊖

Fig. 20.

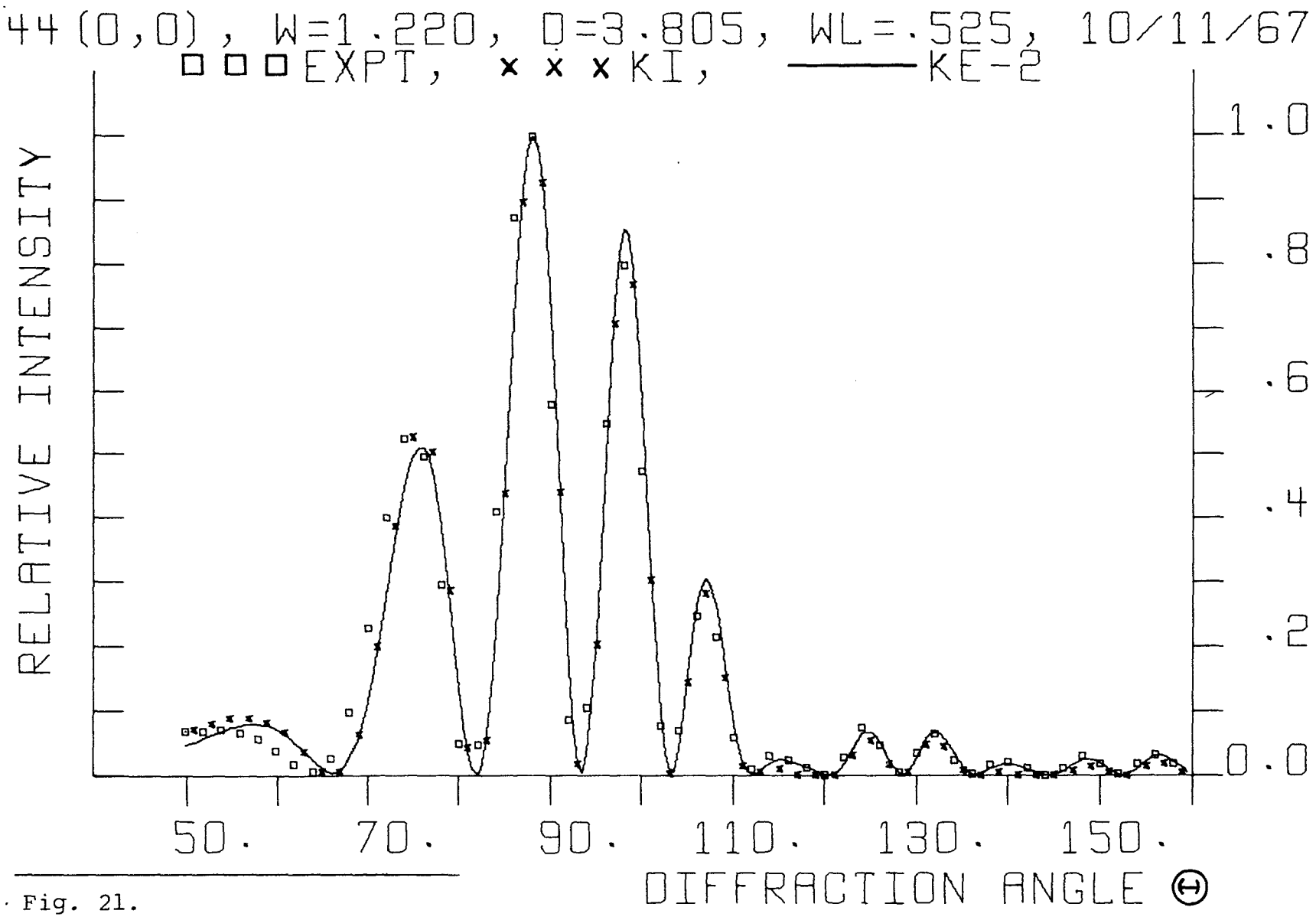
44 (0,0), W=1.220, D=3.805, WL=.525, 10/11/67
□ □ □ EXPT, × × × KI, ——— KE-2
RELATIVE INTENSITY
1.0
.8
.6
.4
.2
0.0
50.
70.
90.
110.
130.
150.
DIFFRACTION ANGLE Θ

Fig. 21.

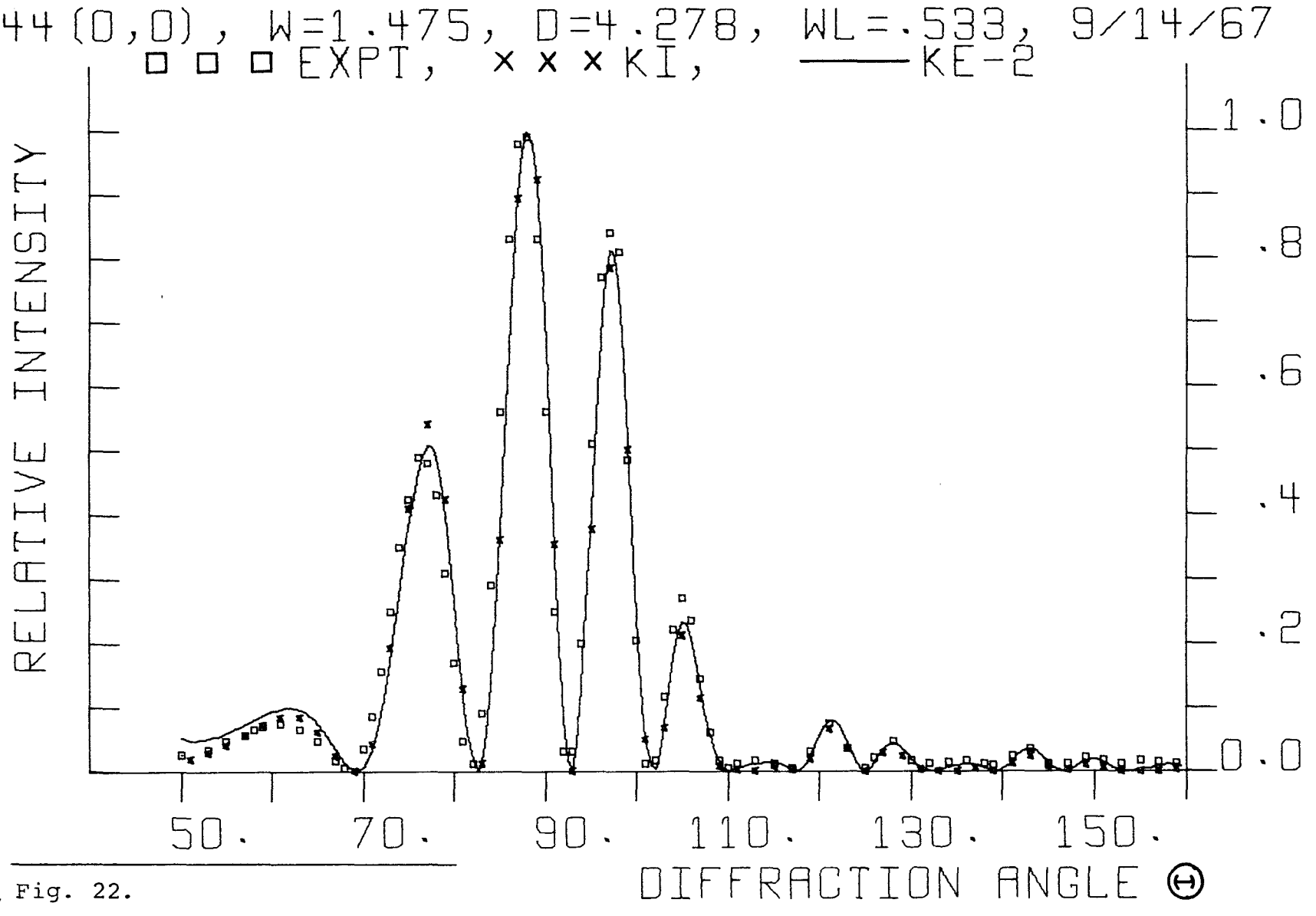
44 (0,0), W=1.475, D=4.278, WL=.533, 9/14/67
□ □ □ EXPT, x x x KI, —— KE-2
RELATIVE INTENSITY
1.0
.8
.6
.4
.2
0.0
50.
70.
90.
110.
130.
150.
DIFFRACTION ANGLE Θ

Fig. 22.

C. Inclined Strips - Small Angle

In order to further investigate strip interactions and compare Kirchhoff and Keller theories, a series of experiments was undertaken involving strips whose faces were at an angle with respect to each other and with the incident radiation. The angle between the faces (or β, the angle between the planes in which the strips lie) could be used to influence the degree of interaction. The results in this section are for strips whose planes make a "small" angle of 20° with respect to each other while the next section considers the case where $\beta = 60^{\circ}$.

Fig. 23 presents the case of strips (w = 1.270 cm) whose faces are inclined away from each other (44(10,-10) case) with a separation of approximately 3λ (D = 1.660 cm). Since the closest edges here are only approximately 0.8λ apart, we are again considering a case where the validity of the geometrical theory is in question. A comparison, however, between first-order Keller theory and Kirchhoff theory reveals that KE-1 is more accurate in predicting the experimental results. The comparison between first- and second-order Keller (where second-order now consists of eight terms) reveals rather large corrections because of the proximity of the strips. These corrections however significantly improve the agreement between theory and experiment.

In Fig. 24 we consider the same strip separation as in Fig. 23 but with the strip faces inclined toward each other (the angle between the planes of the strips is again 20°). In this instance, the Kirchhoff predictions are precisely the same as for the preceding case, i.e., the Kirchhoff formulation does not distinguish between the cases of strips inclined toward or away from each other. Keller theory, on the other hand, does predict different results for the different orientations. To first-order, the Keller theory is slightly better than Kirchhoff, especially in the region $110^{\circ} < \theta < 160^{\circ}$ where it predicts more of the general character of the curve observed. The second-order Keller suffers severely from singularities for $50^{\circ} < \theta < 80^{\circ}$ and some of the effects of this anomalous behavior extend to the subsidiary maximum at $\theta = 88^{\circ}$. If we restrict ourselves to consideration of the region $100^{\circ} < \theta < 160^{\circ}$, it appears that over most of this part of the pattern, the second-order terms are taking into account some interactions between the strips (see Appendix III for further discussion).

As the strip separation is increased, the second-order effects again diminish in importance, especially for strips whose faces are inclined away from each other. Theoretically, comparison between first- and second-order Keller shows small contributions due to second-order effects when

the distance D is approximately 4λ [19] or larger. Figs. 25 to 27 compare second-order Keller to Kirchhoff for separations of approximately 4λ, 6λ, 8λ (D = 2.208, 3.294, 4.363 cm). The results show good agreement with Keller theory and fair to poor agreement with Kirchhoff theory.

When the strips are inclined toward each other, one might expect second-order effects to be important for greater strip separations than for the cases discussed above. Fig. 28 compares first- and second-order Keller theory for strips (w = 1.270 cm) inclined toward each other (44(-10,10) case) with a separation of approximately 5λ (D = 2.755 cm). To the left of the principal maximum, the second-order effects are large. Ignoring the region about the singularities, which can extend to values of Θ up to 90° (as discussed in Appendix III), the second-order results are in closer agreement with experiment than either Kirchhoff or first-order Keller.[20] Comparison between KI and KE-1 indicates that both are in general agreement with experiment at the far right of the pattern.

Fig. 29 considers the above strips (w = 1.270 cm, 44(-10,10) case) at wider separation (D = 3.841 cm, approximately 7λ) where first-order and second-order are

---

[19] The corresponding distance between the closest edges is approximately 1.8λ.

[20] It is interesting to note that in the region of singularities, the first-order has the general shape of the experimental points if not the same relative intensities.

in close agreement (except for singular regions). This plot compares first-order Keller with Kirchhoff and experiment. Again, it appears that the Keller is able to predict more of the detail observed experimentally at the far right of the pattern.

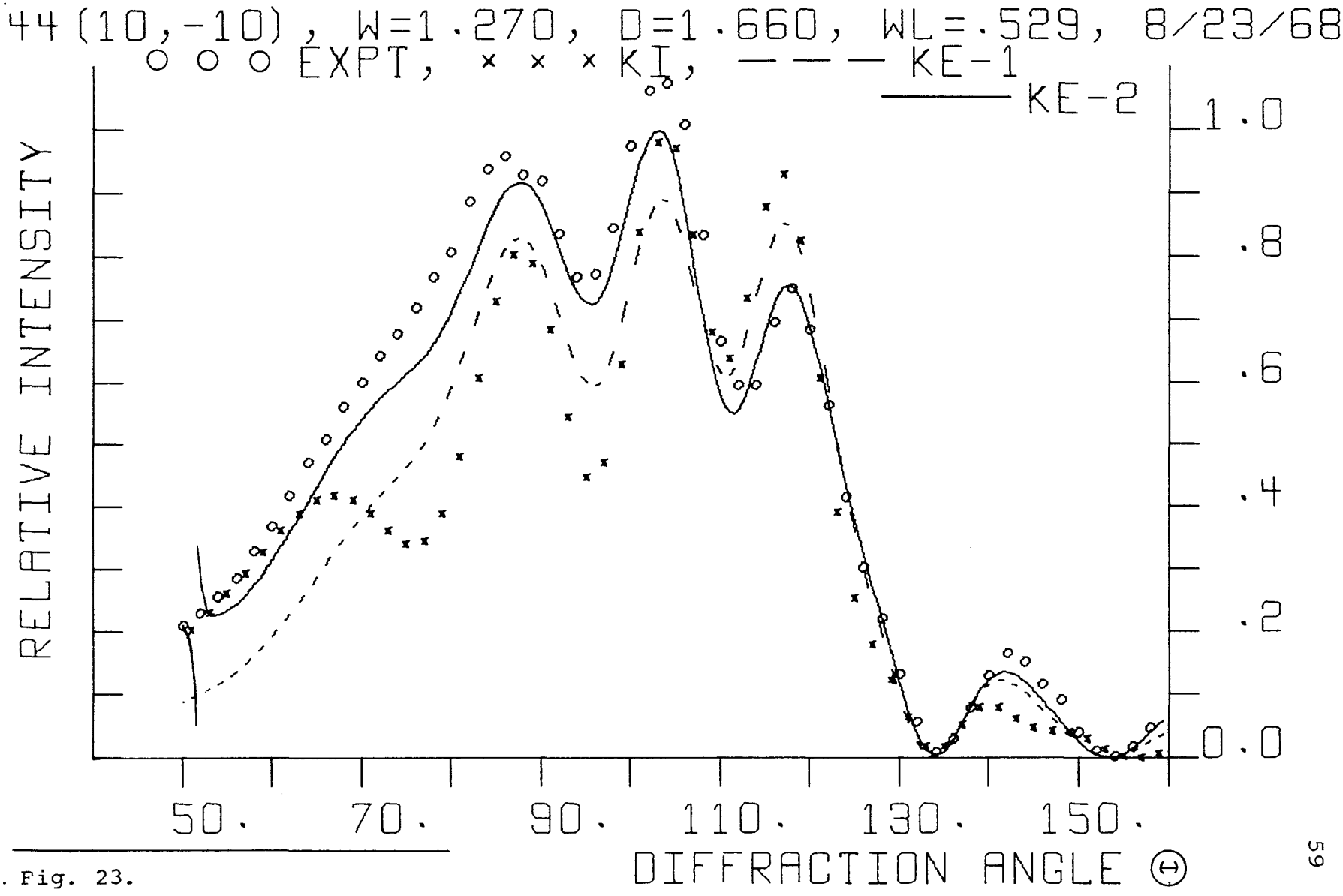
44 (10,-10), W=1.270, D=1.660, WL=.529, 8/23/68
○ ○ ○ EXPT, × × × KI, — — — KE-1
KE-2
RELATIVE INTENSITY
1.0
.8
.6
.4
.2
0.0
50.
70.
90.
110.
130.
150.
DIFFRACTION ANGLE Θ

Fig. 23.

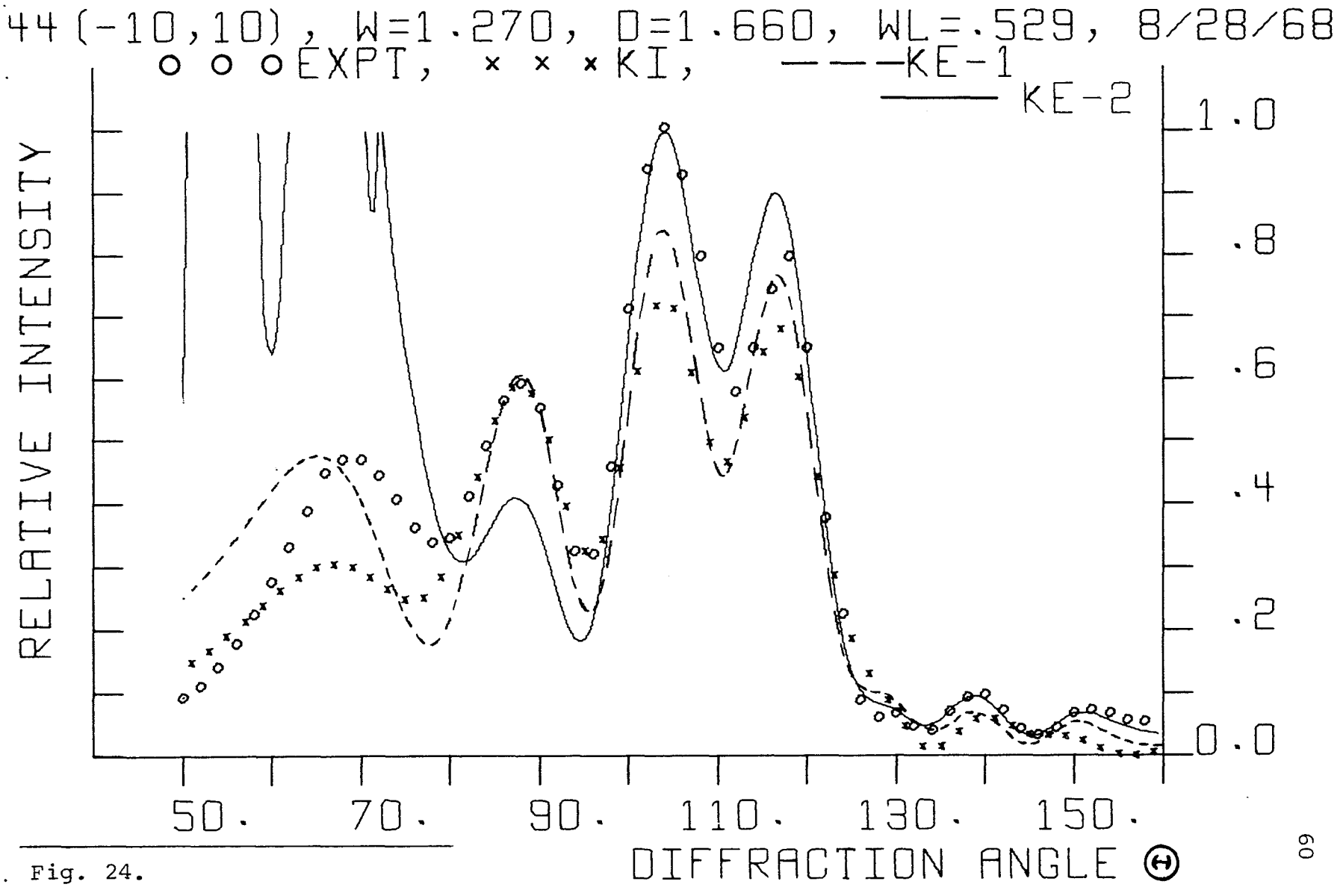
44 (-10,10), W=1.270, D=1.660, WL=.529, 8/28/68
o o o EXPT, x x x KI, — — — KE-1
KE-2
RELATIVE INTENSITY
1.0
.8
.6
.4
.2
0.0
50.
70.
90.
110.
130.
150.
DIFFRACTION ANGLE Θ

Fig. 24.

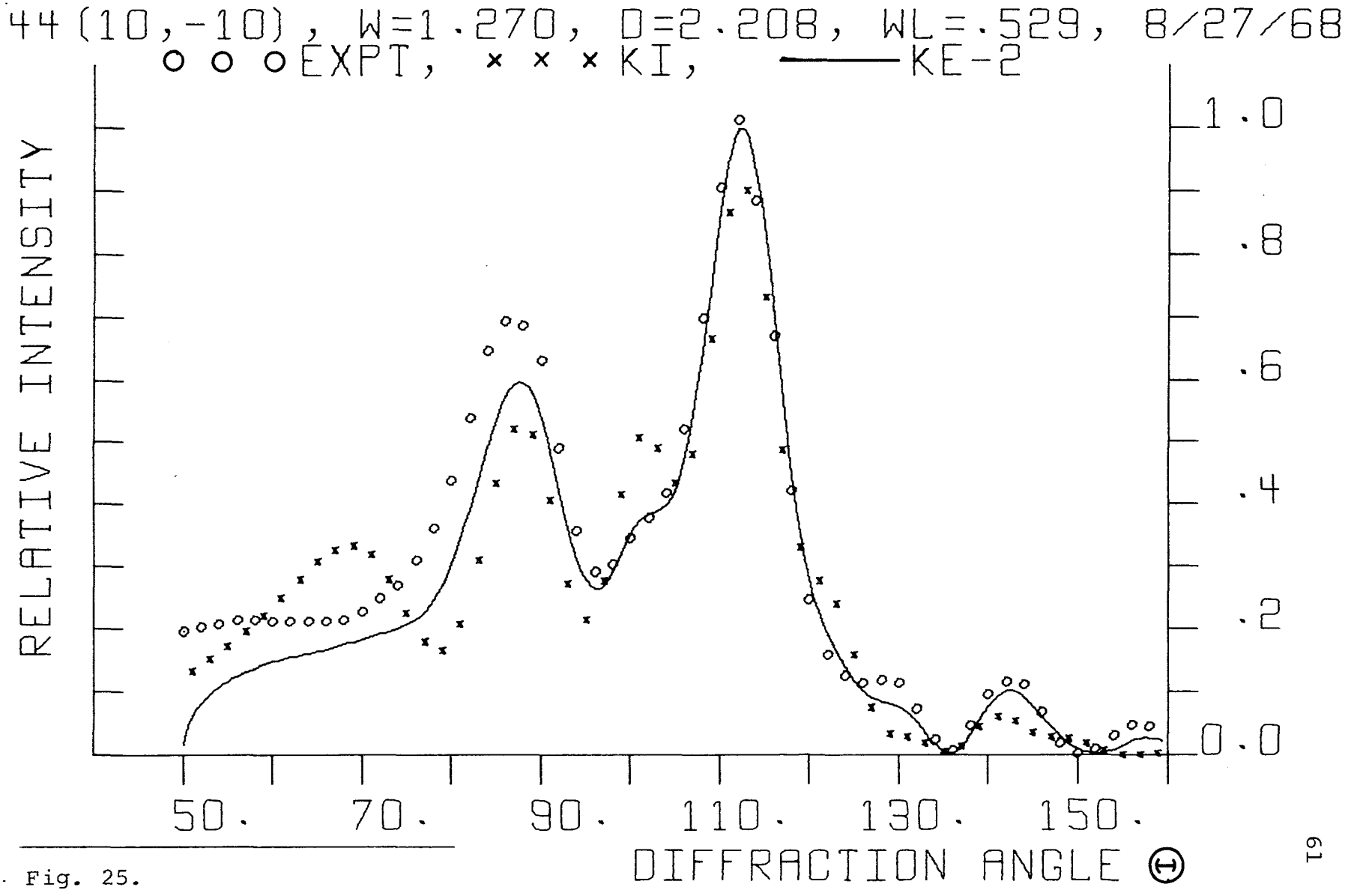
44 (10,-10), W=1.270, D=2.208, WL=.529, 8/27/68
O O O EXPT, × × × KI, —— KE-2
RELATIVE INTENSITY
1.0
.8
.6
.4
.2
0.0
50.
70.
90.
110.
130.
150.
DIFFRACTION ANGLE Θ

Fig. 25.

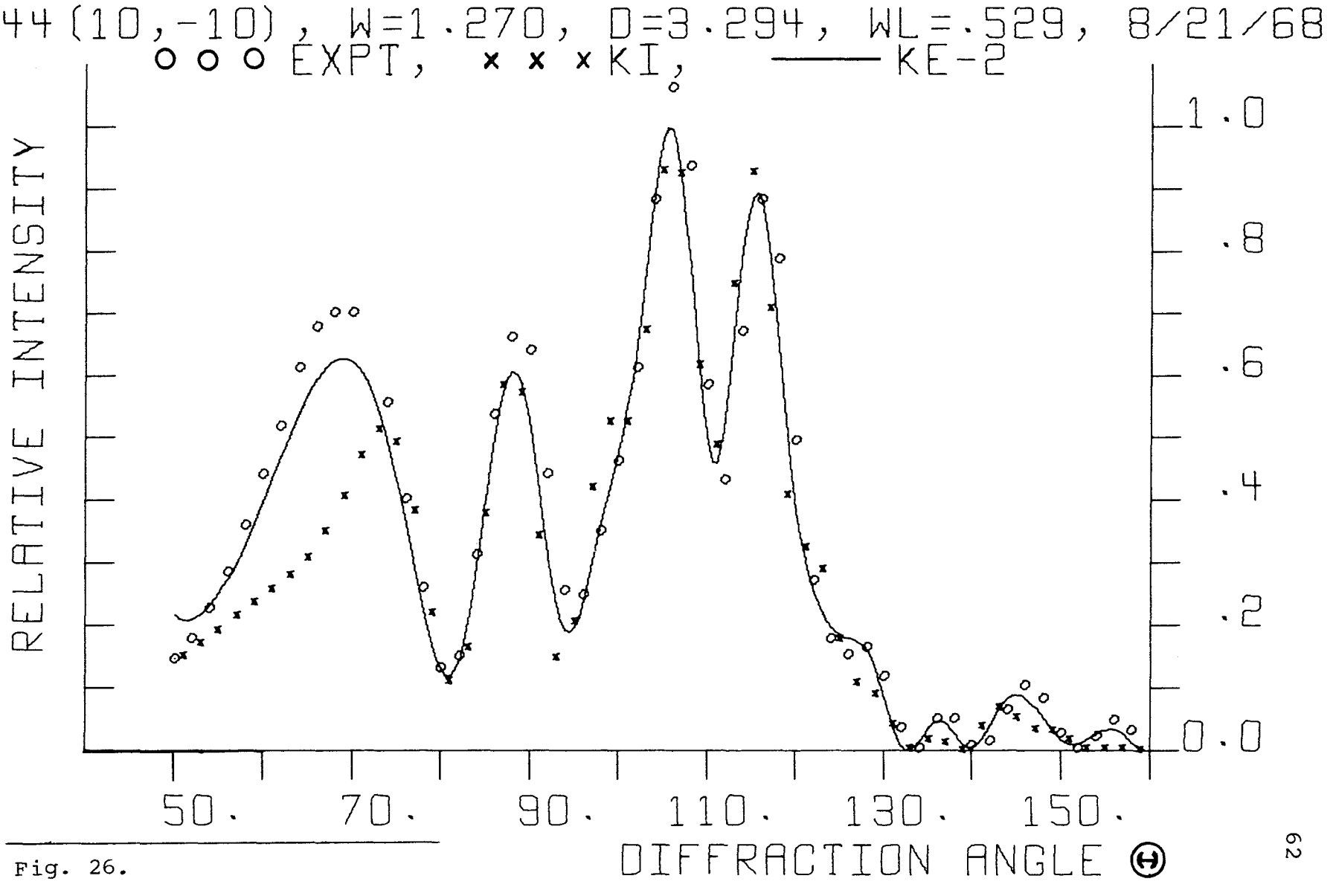
44 (10,-10), W=1.270, D=3.294, WL=.529, 8/21/68
o o o EXPT, x x x KI, —— KE-2
RELATIVE INTENSITY
1.0
.8
.6
.4
.2
0.0
50.
70.
90.
110.
130.
150.
DIFFRACTION ANGLE Θ

Fig. 26.

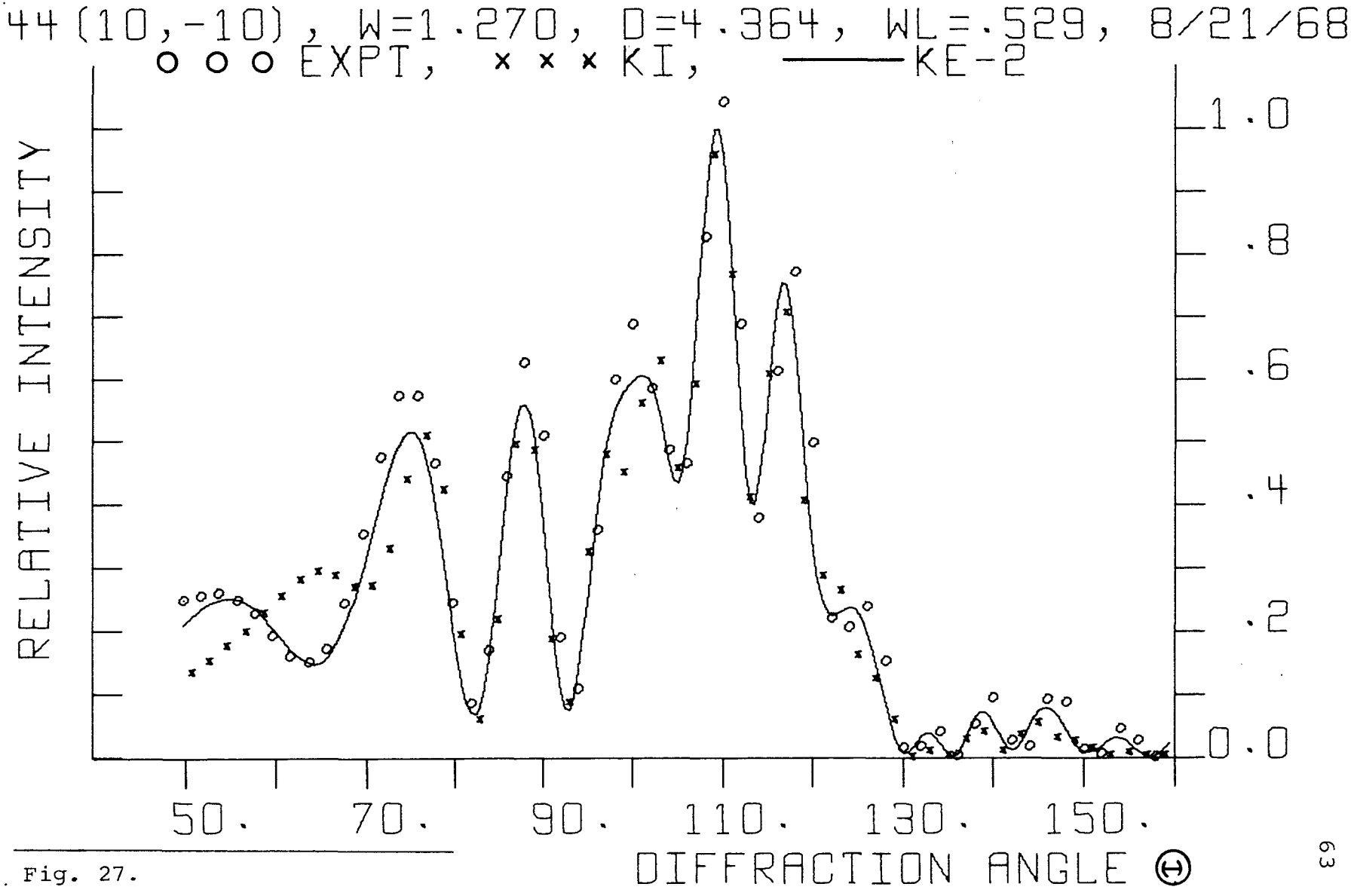
44 (10,-10), W=1.270, D=4.364, WL=.529, 8/21/68
o o o EXPT, x x x KI, ——— KE-2
RELATIVE INTENSITY
1.0
.8
.6
.4
.2
0.0
50.
70.
90.
110.
130.
150.
DIFFRACTION ANGLE Θ

Fig. 27.

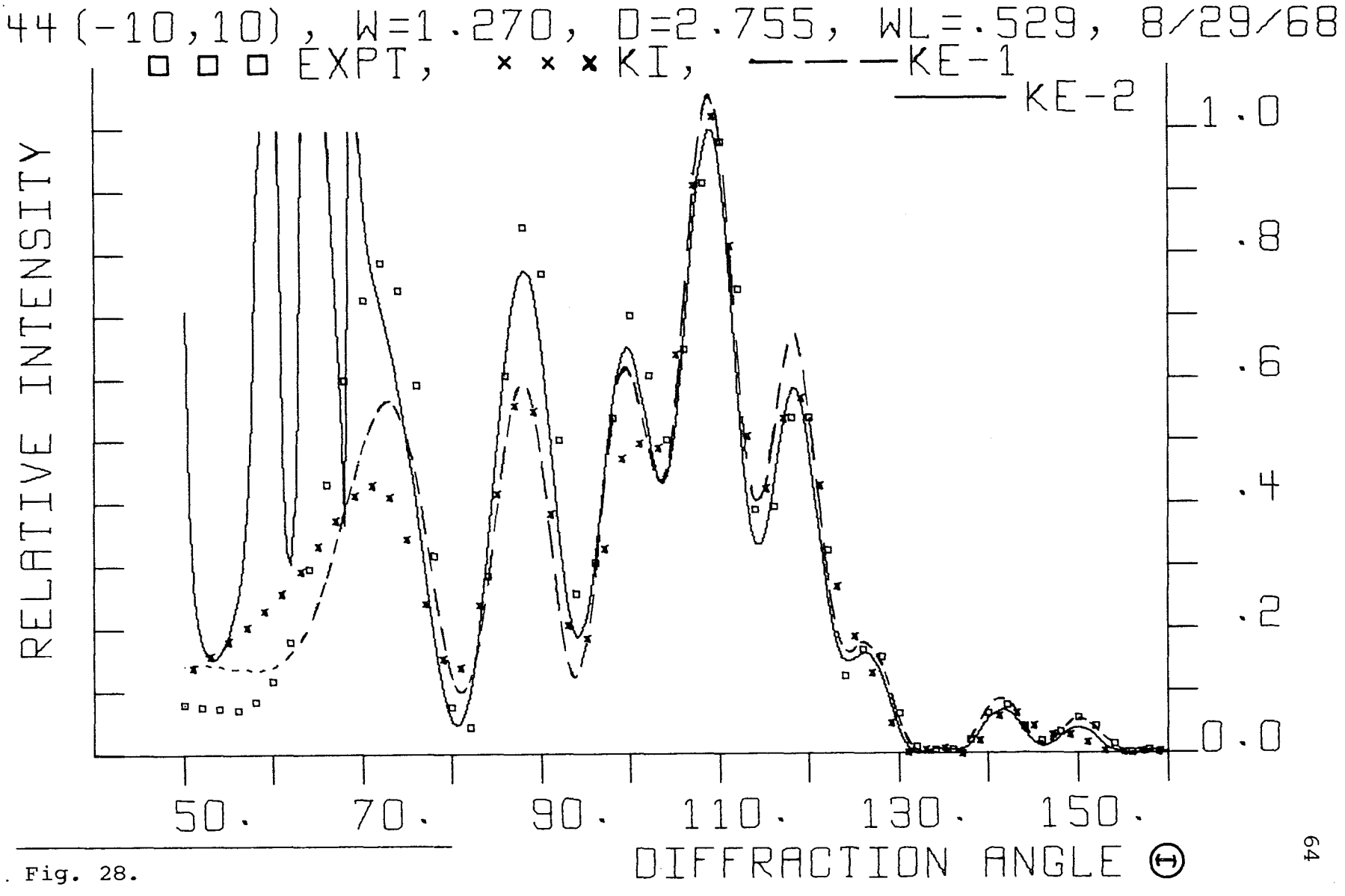
44 (-10,10), W=1.270, D=2.755, WL=.529, 8/29/68
□ □ □ EXPT, × × × KI, — — — KE-1
——— KE-2
RELATIVE INTENSITY
1.0
.8
.6
.4
.2
0.0
50.
70.
90.
110.
130.
150.
DIFFRACTION ANGLE Θ

Fig. 28.

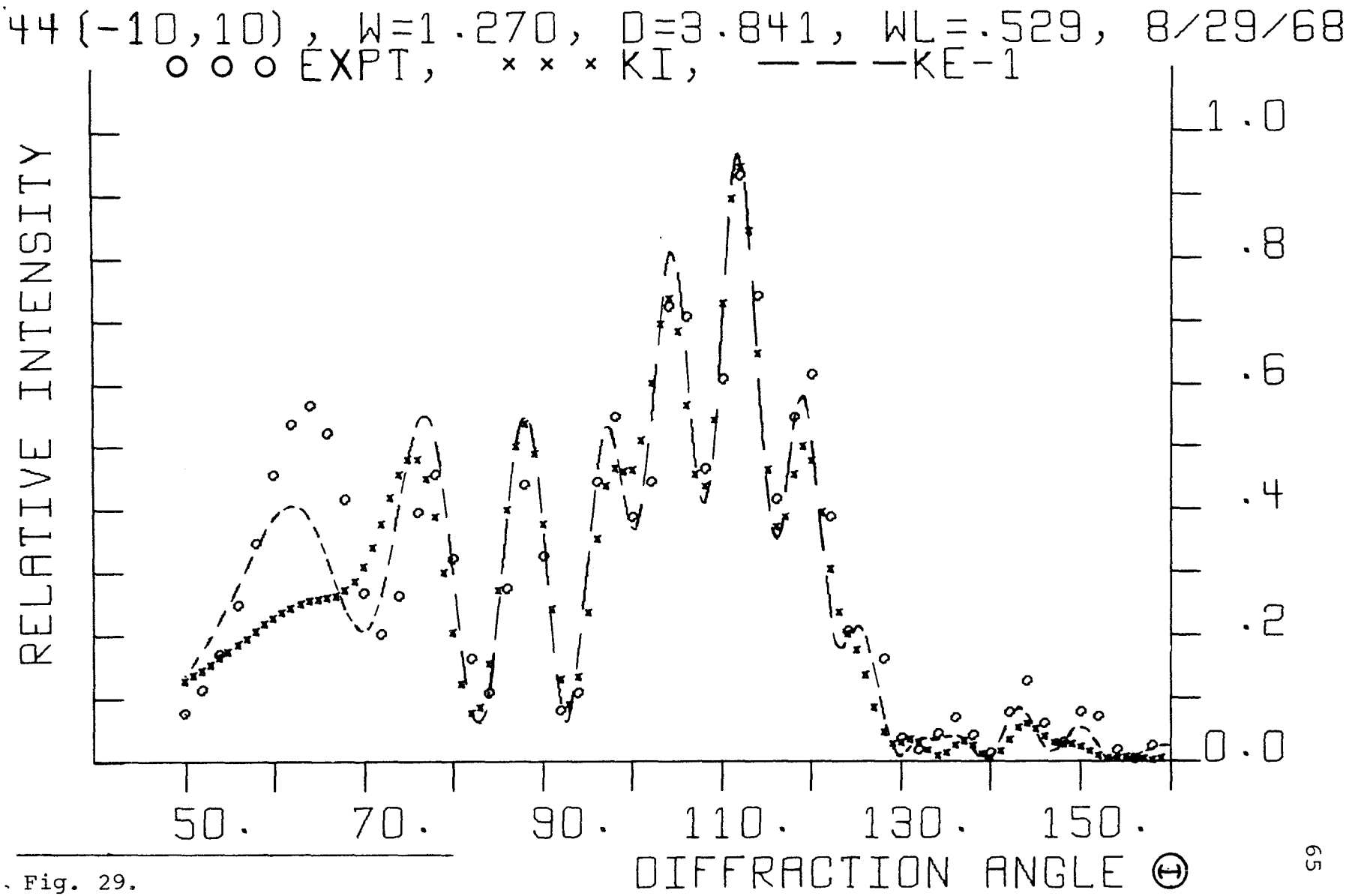
44 (-10,10), W=1.270, D=3.841, WL=.529, 8/29/68
o o o EXPT, × × × KI, — — —KE-1
RELATIVE INTENSITY
1.0
.8
.6
.4
.2
0.0
50.
70.
90.
110.
130.
150.
DIFFRACTION ANGLE Θ

Fig. 29.

D. Inclined Strips - Large Angle

The last orientations considered were for strips whose planes make an angle of 60° with respect to each other. In the diagrams of this section, it must be noted that the region of theoretical interest extends from $\Theta = 74^{\circ}$ to $\Theta = 160^{\circ}$. This is because we are behind one of the strips when $\Theta = 74^{\circ}$ and the Kirchhoff formulation as used here is not applicable in this region. The Keller theory would be valid in this region except that in part of the range ($50^{\circ} < \Theta < 74^{\circ}$), one of the first-order edge diffracted rays and one of the second-order rays would have to pass through a strip in order to reach the observation point. Since the latter penetration is not allowed, and because of the inapplicability of the Kirchhoff results in this region, a marker is drawn at the 74° location in Figs. 30 to 36 and 40 to 42.[21] Results, both theoretical and experimental, have been included from $\Theta = 50^{\circ}$ because it might be of interest to note the extent to which disparities do or do not exist.

Fig. 30 presents the case of two strips (w = 1.270 cm)

---

[21] For the small angle case (Figs. 21 to 27), the region of theoretical applicability actually extends from $\Theta = 54^{\circ}$. This was not noted in the discussion there because of the small region involved. A consequence can be seen in Fig. 11 where the "small" discontinuity at approximately $\Theta = 54^{\circ}$ results because we cross a shadow boundary for one of the doubly diffracted rays of the Keller second-order.

whose faces are inclined away from each other (44(30,-30) case) with a separation of approximately 3λ (D = 1.509 cm). Comparison between first- and second-order Keller indicates that the second-order corrections are small for this case, even though the strips are close (the distance between closest edges is 0.5λ). Comparison between either Keller order and the Kirchhoff results indicates better agreement with Keller in both cases.

Figs. 31 to 33 compare Kirchhoff and second-order Keller theories with experiment for separations of approximately 4λ, 6λ, and 8λ (D = 2.057, 3.143 and 4.213 cm respectively). Second-order Keller corrections are quite small at these separations in the region where $\Theta > 74^{\circ}$, so that either first- or second-order curves could have been used on the graphs. As the strips are separated to greater distances, both theories predict greater detail in the patterns, but the Keller results are better able to predict the results obtained experimentally, especially at the far right of the pattern. The latter may be explained in part by considering the single strip patterns of the strips involved in the above cases. One strip has radiation incident upon it at a glancing angle of $u = 14^{\circ}$ ($\theta_i = 76^{\circ}$). Appendix II indicates that the single strip Kirchhoff theory predictions for such a small glancing angle are poor for strips of width comparable to

that used here. This is especially true at large values of Θ, where the Kirchhoff intensities are consistently too small (see Fig. A7).

Figs. 34 to 36 consider two strips (w = 1.270 cm) inclined toward each other (44(-30,30) case) with separations of approximately 3λ, 5λ, and 7λ (D = 1.509, 2.604, and 3.690 cm respectively). Only first-order Keller theory and Kirchhoff theory are included here. Second-order Keller has been omitted because the number of singular points and the size of the anomalous regions are so large that most of the calculated second-order corrections were meaningless. That higher order effects are present is seen from the rather poor agreement between theory and experiment in the region $74^{\circ} < \Theta < 140^{\circ}$. As in the small angle case, the Kirchhoff patterns here are the same in shape as those for non-facing strips. The Keller patterns, however, have changed so that in Fig. 34 (the counterpart of Fig. 30 where the strips are not facing), the Keller results predict the twin peaks observed experimentally. As the strips are further separated (Figs. 35 and 36), the disparity between theory and experiment diminishes somewhat, but nowhere is the agreement between first-order Keller and experiment as good as in previous cases of comparable separation and strip width.

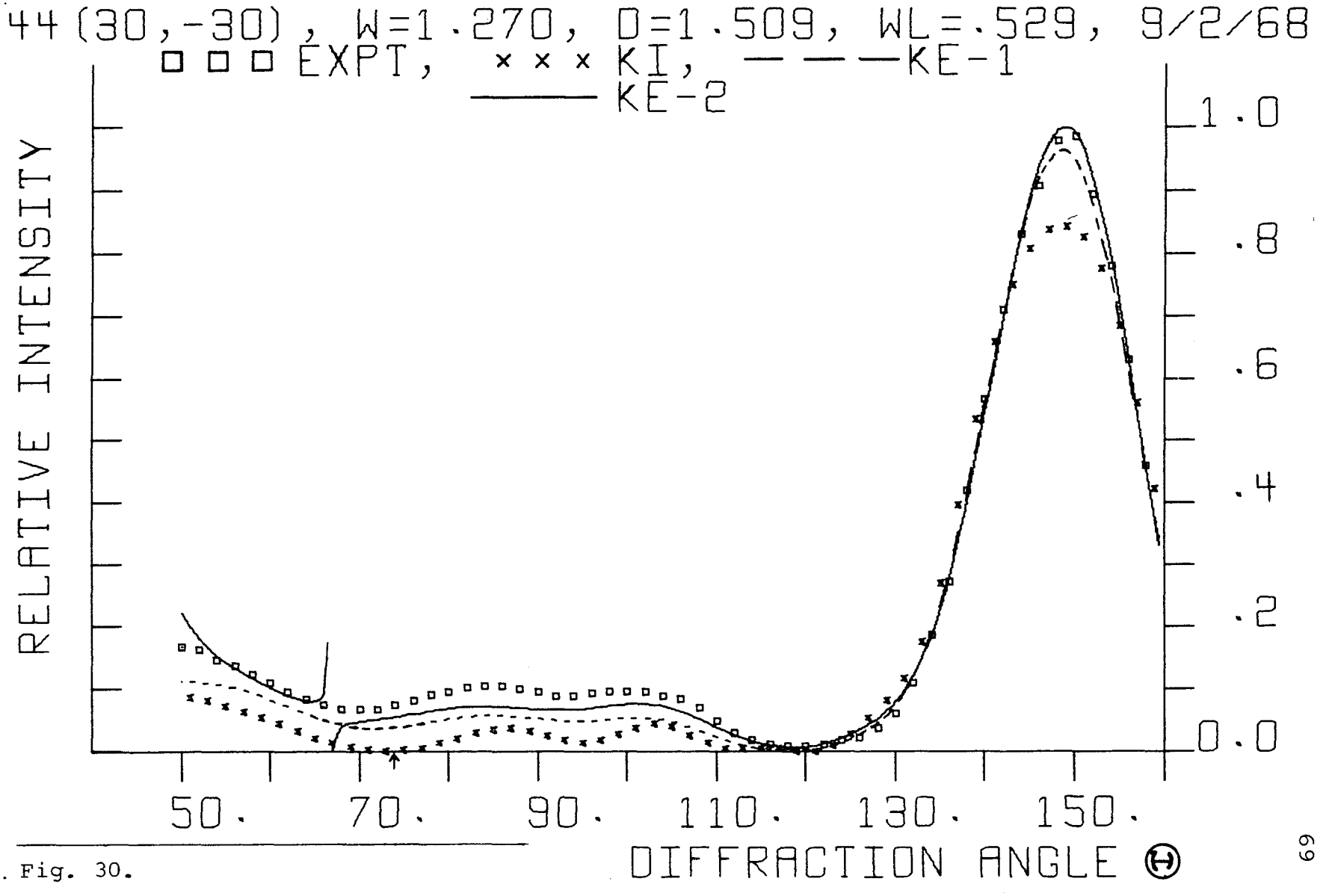
44 (30,-30), W=1.270, D=1.509, WL=.529, 9/2/68
□ □ □ EXPT, × × × KI, — — — KE-1
——— KE-2
RELATIVE INTENSITY
1.0
.8
.6
.4
.2
0.0
50.
70.
90.
110.
130.
150.
DIFFRACTION ANGLE Θ

Fig. 30.

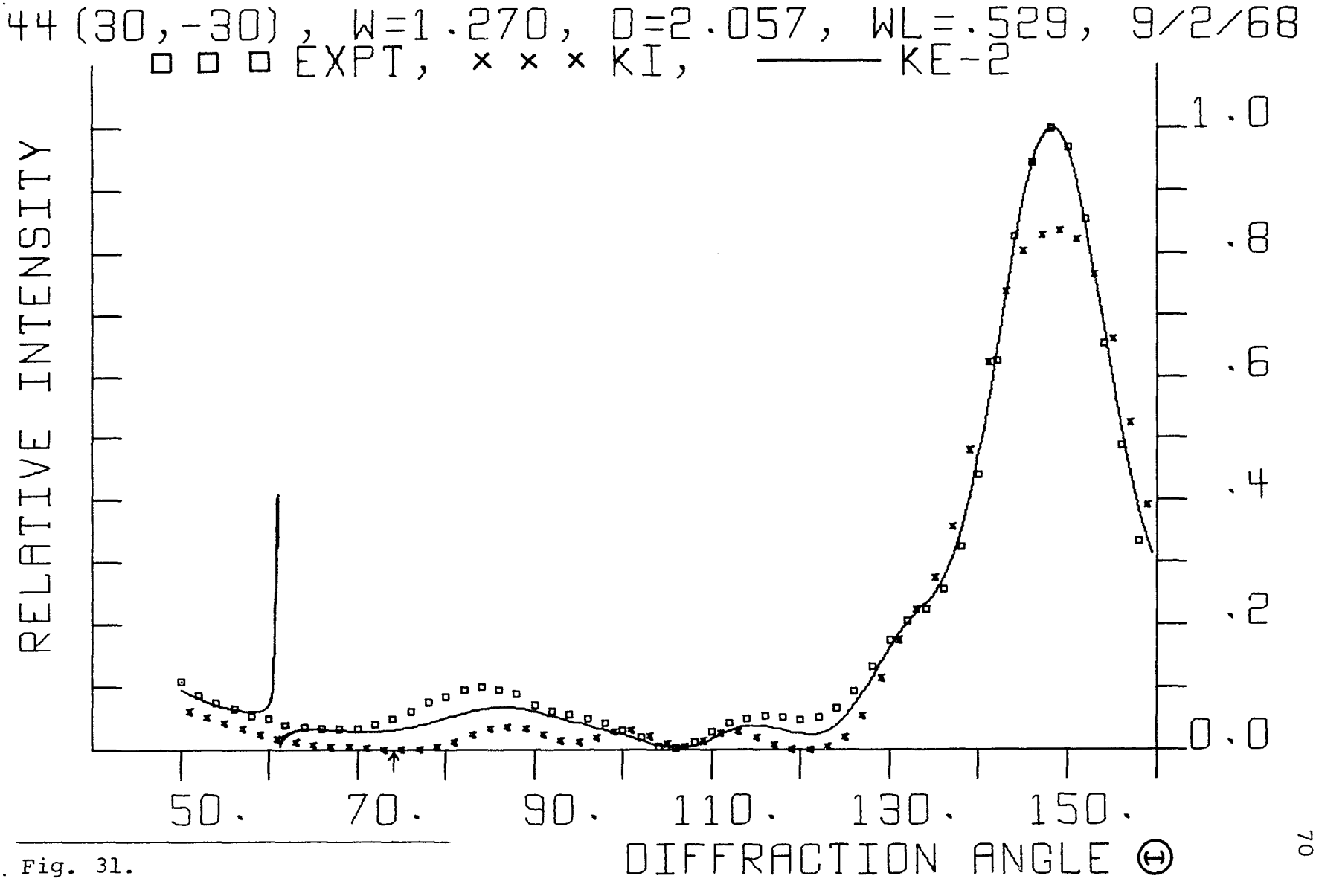
44 (30,-30), W=1.270, D=2.057, WL=.529, 9/2/68
□ □ □ EXPT, × × × KI, ——— KE-2
RELATIVE INTENSITY
1.0
.8
.6
.4
.2
0.0
50.
70.
90.
110.
130.
150.
DIFFRACTION ANGLE Θ

Fig. 31.

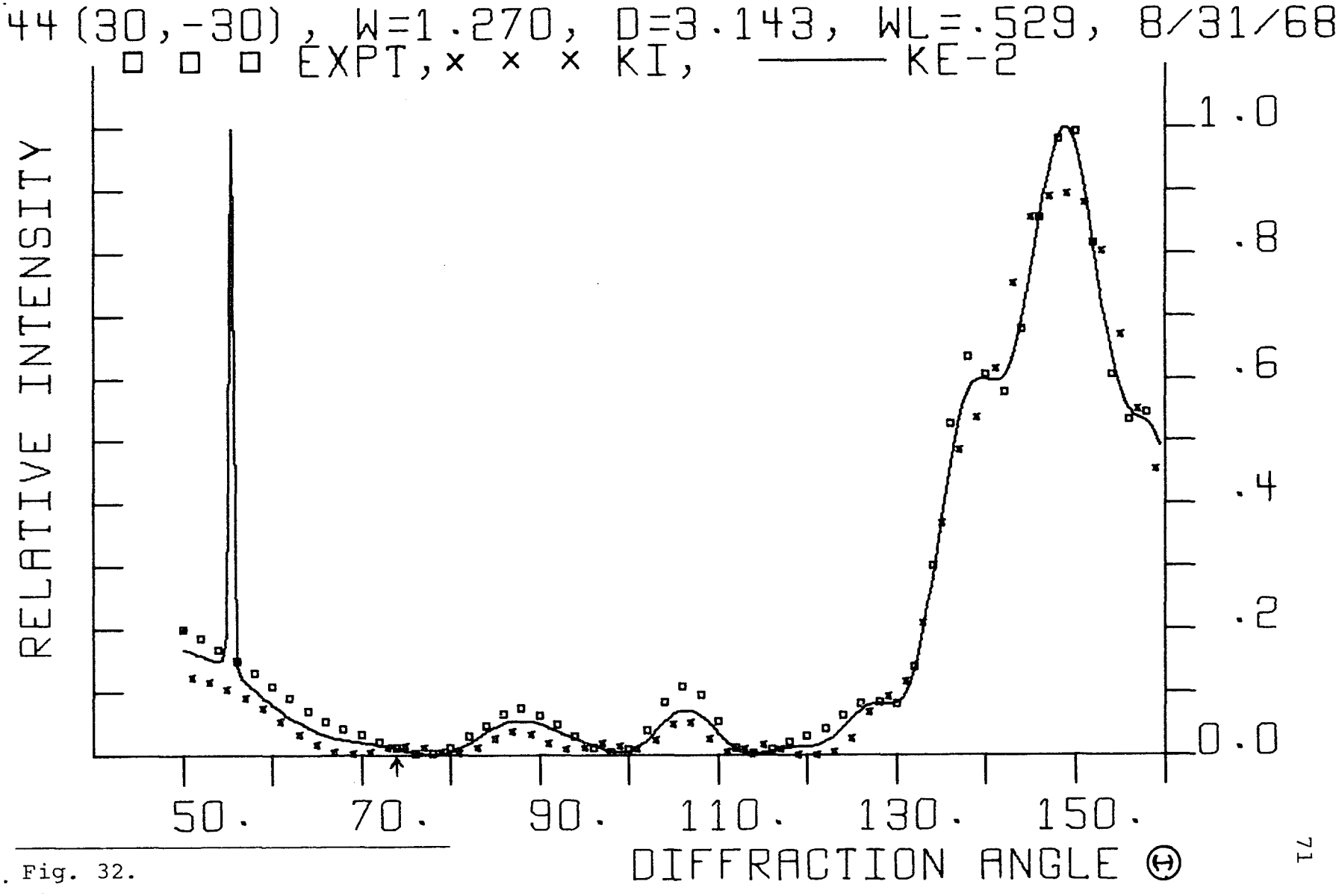
44 (30,-30), W=1.270, D=3.143, WL=.529, 8/31/68
□ □ □ EXPT, × × × KI, ——— KE-2
RELATIVE INTENSITY
1.0
.8
.6
.4
.2
0.0
50.
70.
90.
110.
130.
150.
DIFFRACTION ANGLE Θ

Fig. 32.

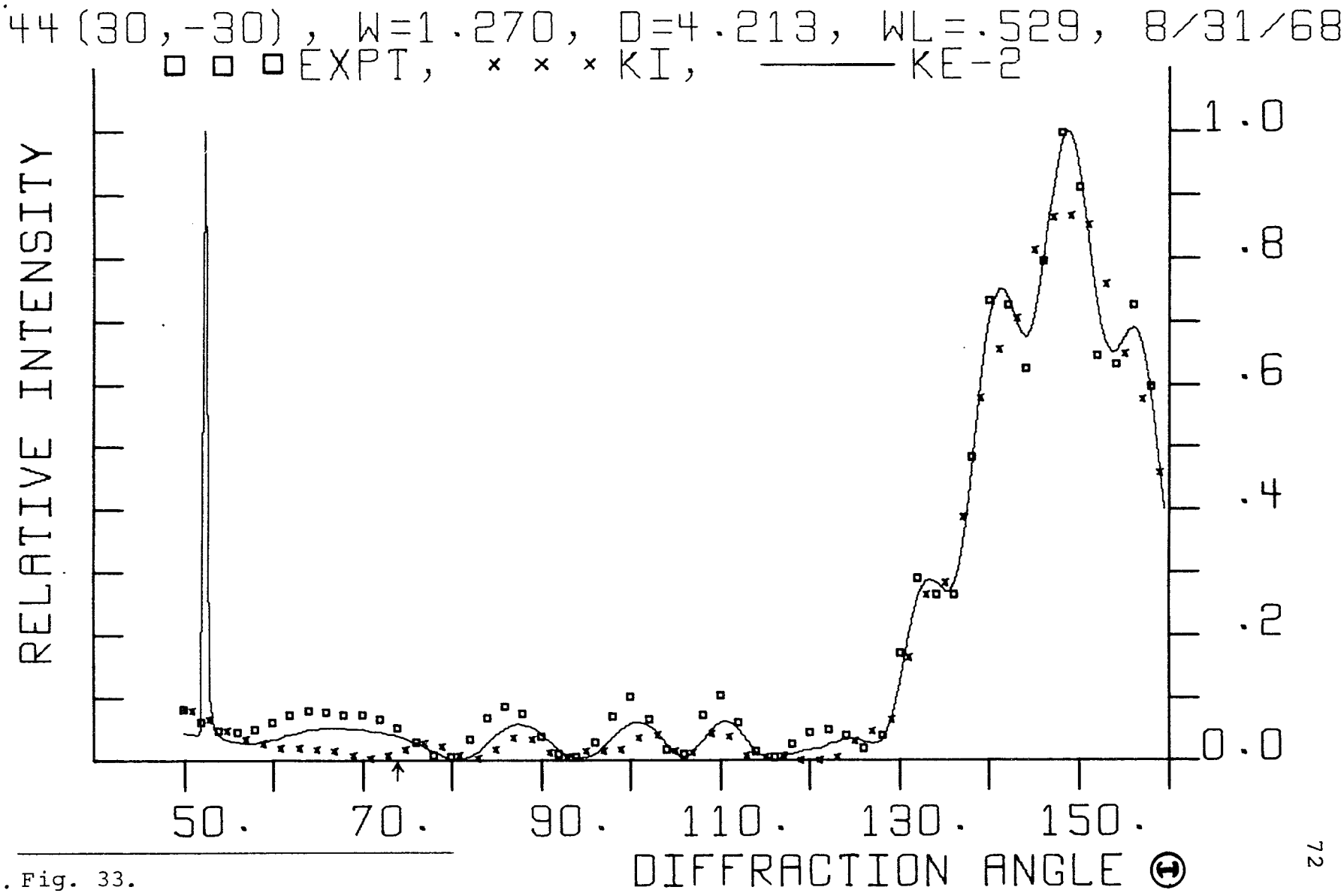
44 (30,-30), W=1.270, D=4.213, WL=.529, 8/31/68
EXPT, KI, KE-2
RELATIVE INTENSITY
1.0
.8
.6
.4
.2
0.0
50.
70.
90.
110.
130.
150.
DIFFRACTION ANGLE Θ

Fig. 33.

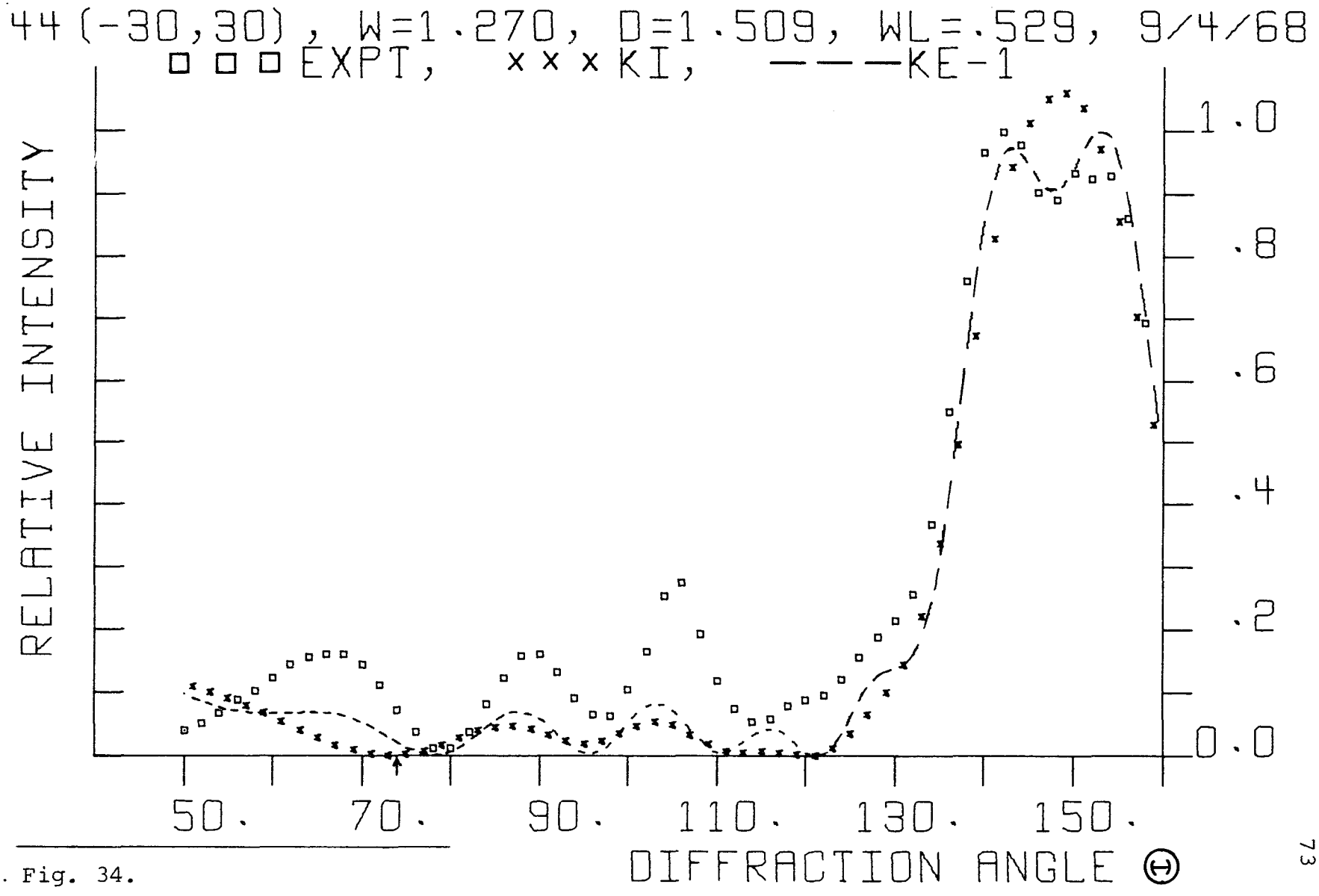
44 (-30,30), W=1.270, D=1.509, WL=.529, 9/4/68
□ □ □ EXPT, x x x KI, ———KE-1
RELATIVE INTENSITY
1.0
.8
.6
.4
.2
0.0
50.
70.
90.
110.
130.
150.
DIFFRACTION ANGLE Θ

Fig. 34.

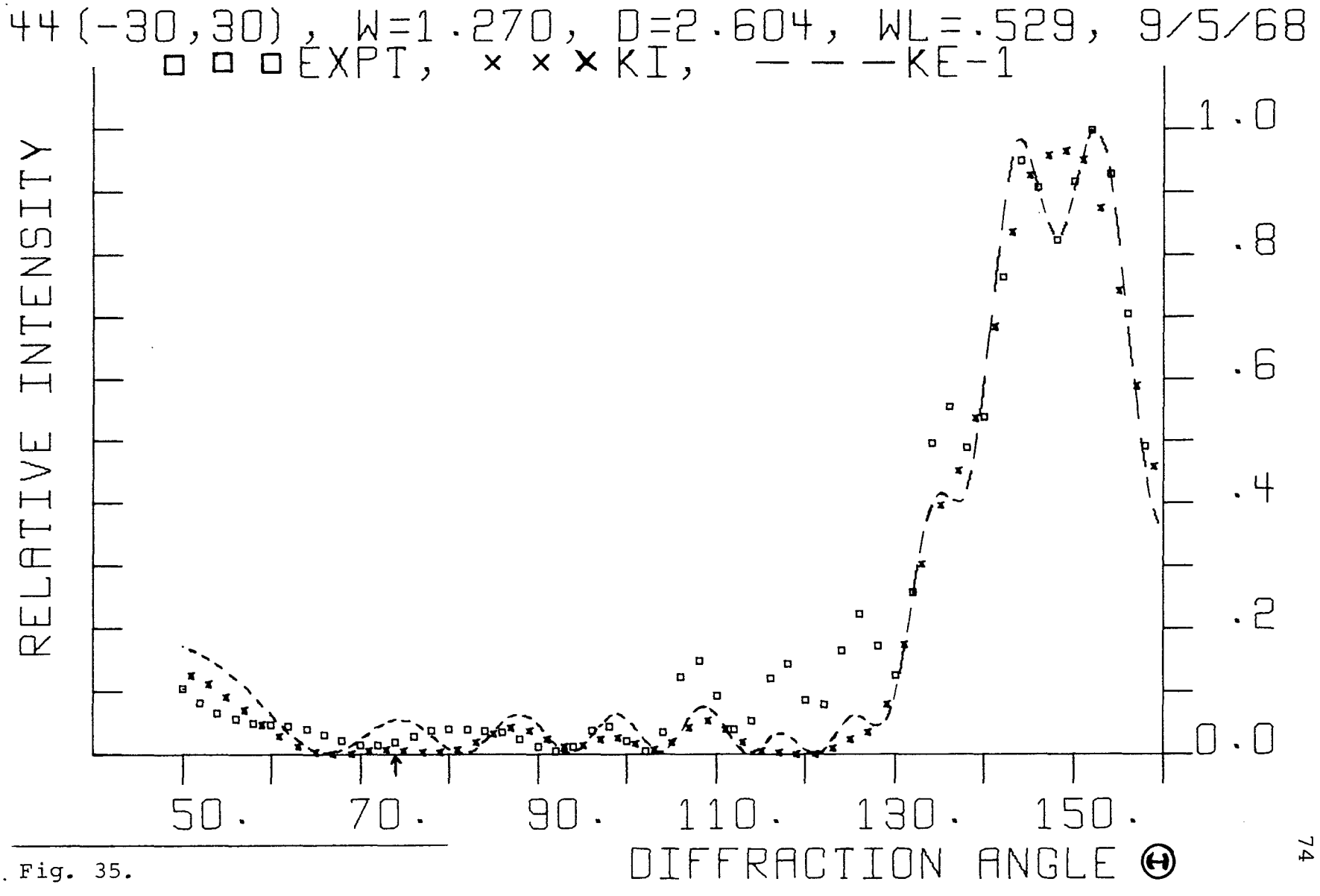
44 (-30,30), W=1.270, D=2.604, WL=.529, 9/5/68
□ □ □ EXPT, × × × KI, — — — KE-1
RELATIVE INTENSITY
1.0
.8
.6
.4
.2
0.0
50.
70.
90.
110.
130.
150.
DIFFRACTION ANGLE Θ

Fig. 35.

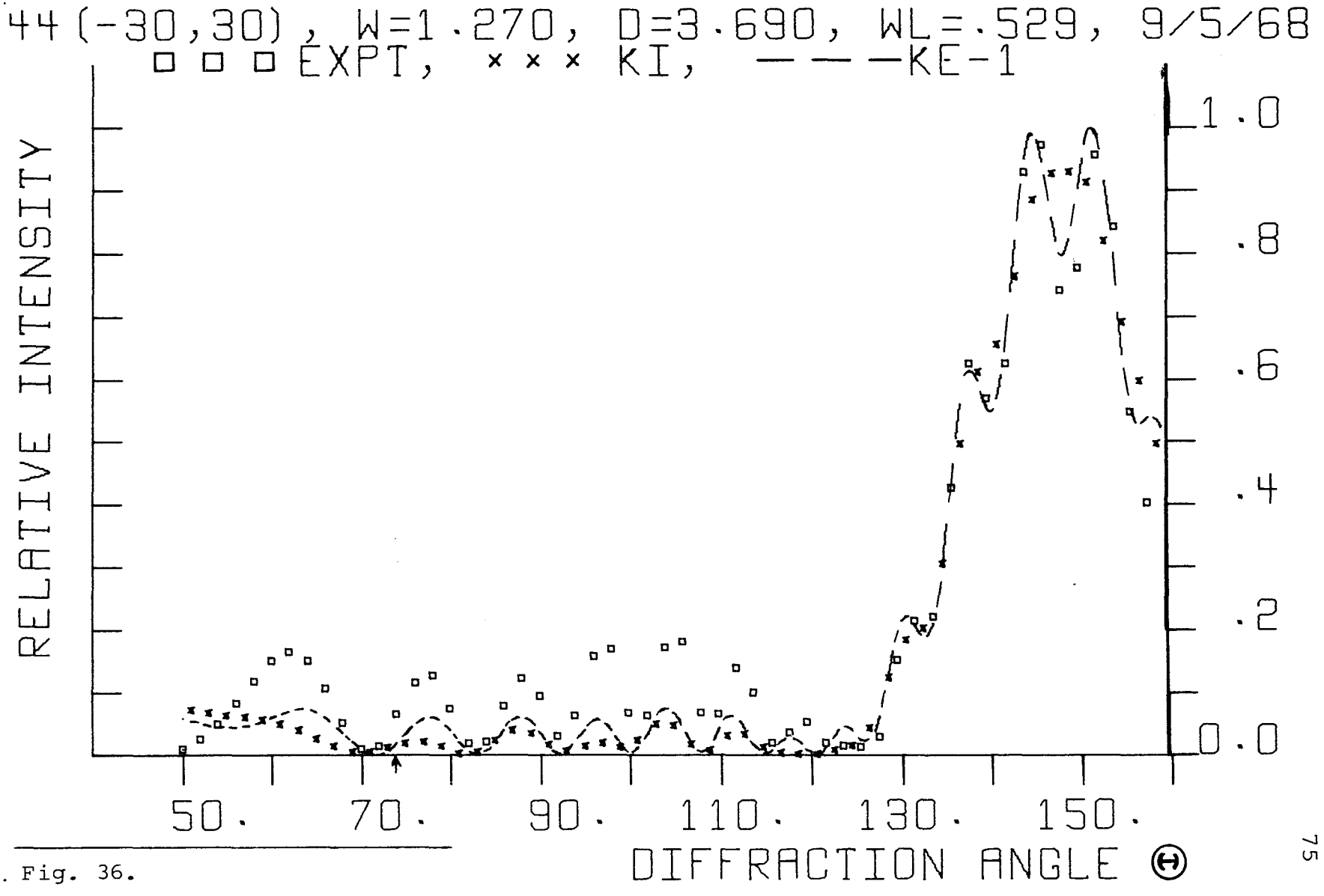
44 (-30,30), W=1.270, D=3.690, WL=.529, 9/5/68
□ □ □ EXPT, × × × KI, — — —KE-1
RELATIVE INTENSITY
1.0
.8
.6
.4
.2
0.0
50.
70.
90.
110.
130.
150.
DIFFRACTION ANGLE Θ

Fig. 36.

E. Additional Miscellaneous Results

Figs. 37 to 42 present results for various cases with strip widths and orientations different from those presented above. They represent further verification of the above results in that they confirm that Keller theory, even to first-order, is better able to describe the results obtained experimentally and that the second-order corrections of the Keller theory are able to account for some of the interactions between strips.

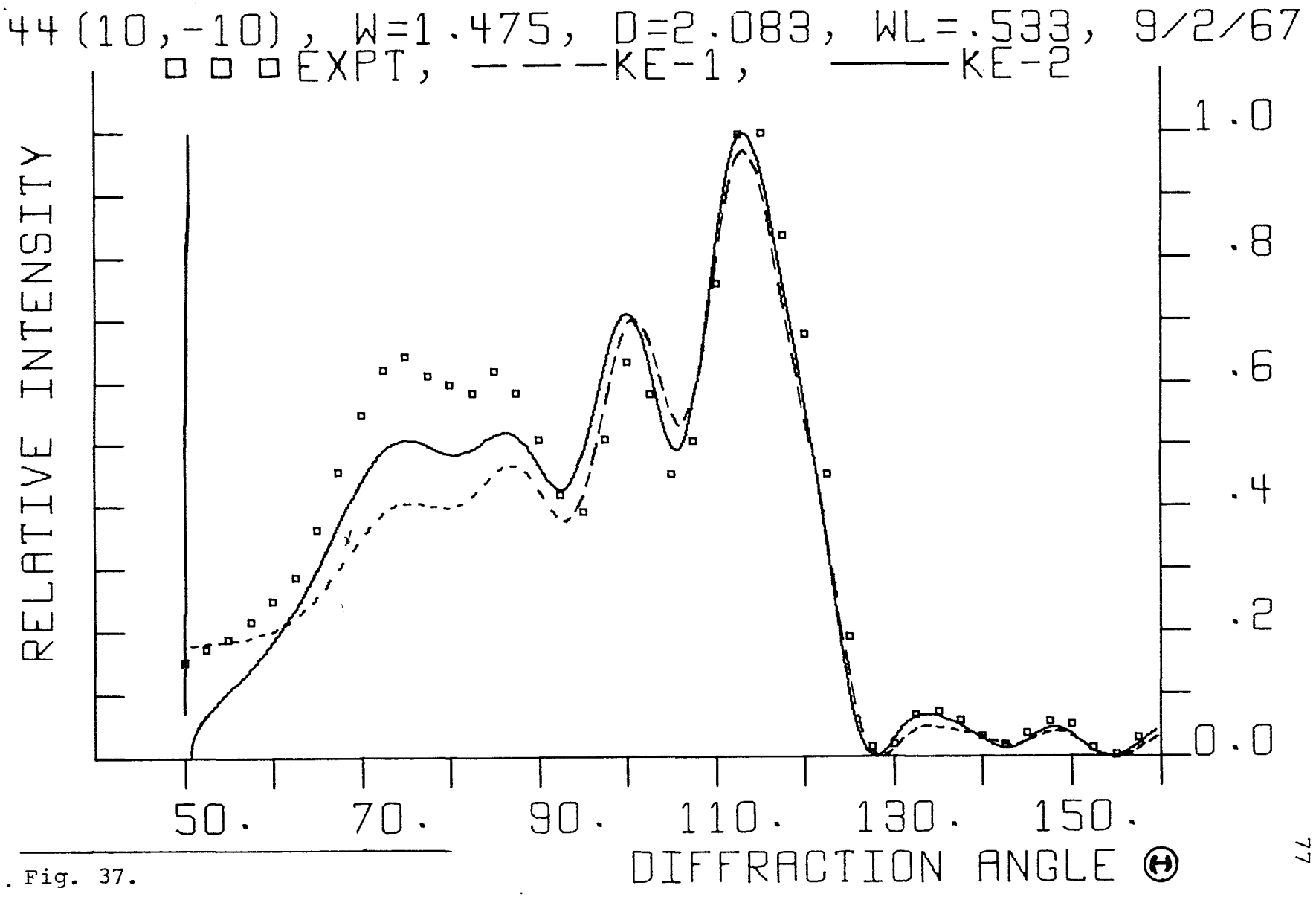
44 (10,-10), W=1.475, D=2.083, WL=.533, 9/2/67
□ □ □ EXPT, — — — KE-1, ——— KE-2
RELATIVE INTENSITY
1.0
.8
.6
.4
.2
0.0
50.
70.
90.
110.
130.
150.
DIFFRACTION ANGLE Θ

Fig. 37.

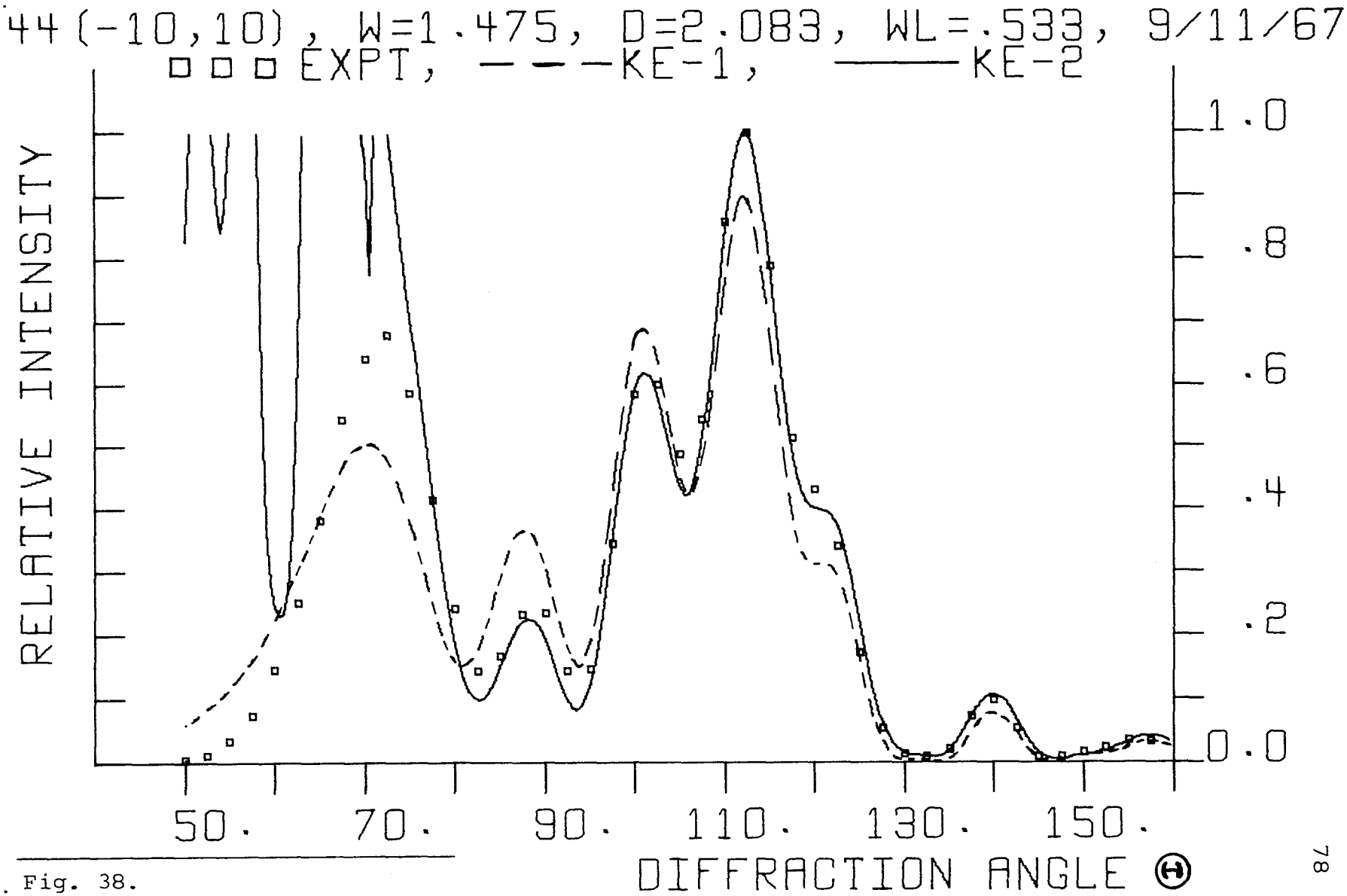
44 (-10,10), W=1.475, D=2.083, WL=.533, 9/11/67
□ □ □ EXPT, — — — KE-1, ——— KE-2
RELATIVE INTENSITY
1.0
.8
.6
.4
.2
0.0
50.
70.
90.
110.
130.
150.
DIFFRACTION ANGLE Θ

Fig. 38.

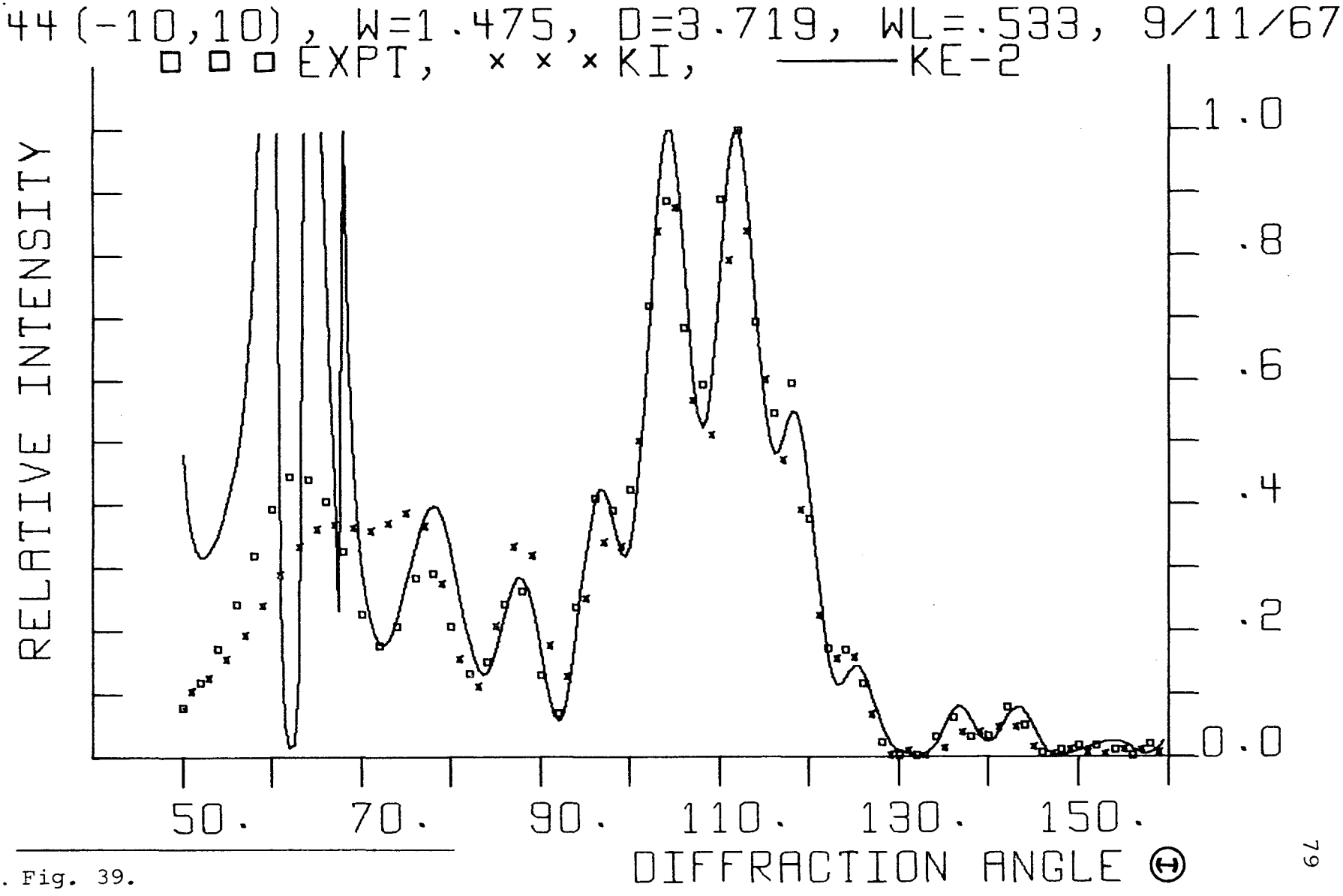
44 (-10,10), W=1.475, D=3.719, WL=.533, 9/11/67
□ □ □ EXPT, × × × KI, ——— KE-2
RELATIVE INTENSITY
1.0
.8
.6
.4
.2
0.0
50.
70.
90.
110.
130.
150.
DIFFRACTION ANGLE Θ

Fig. 39.

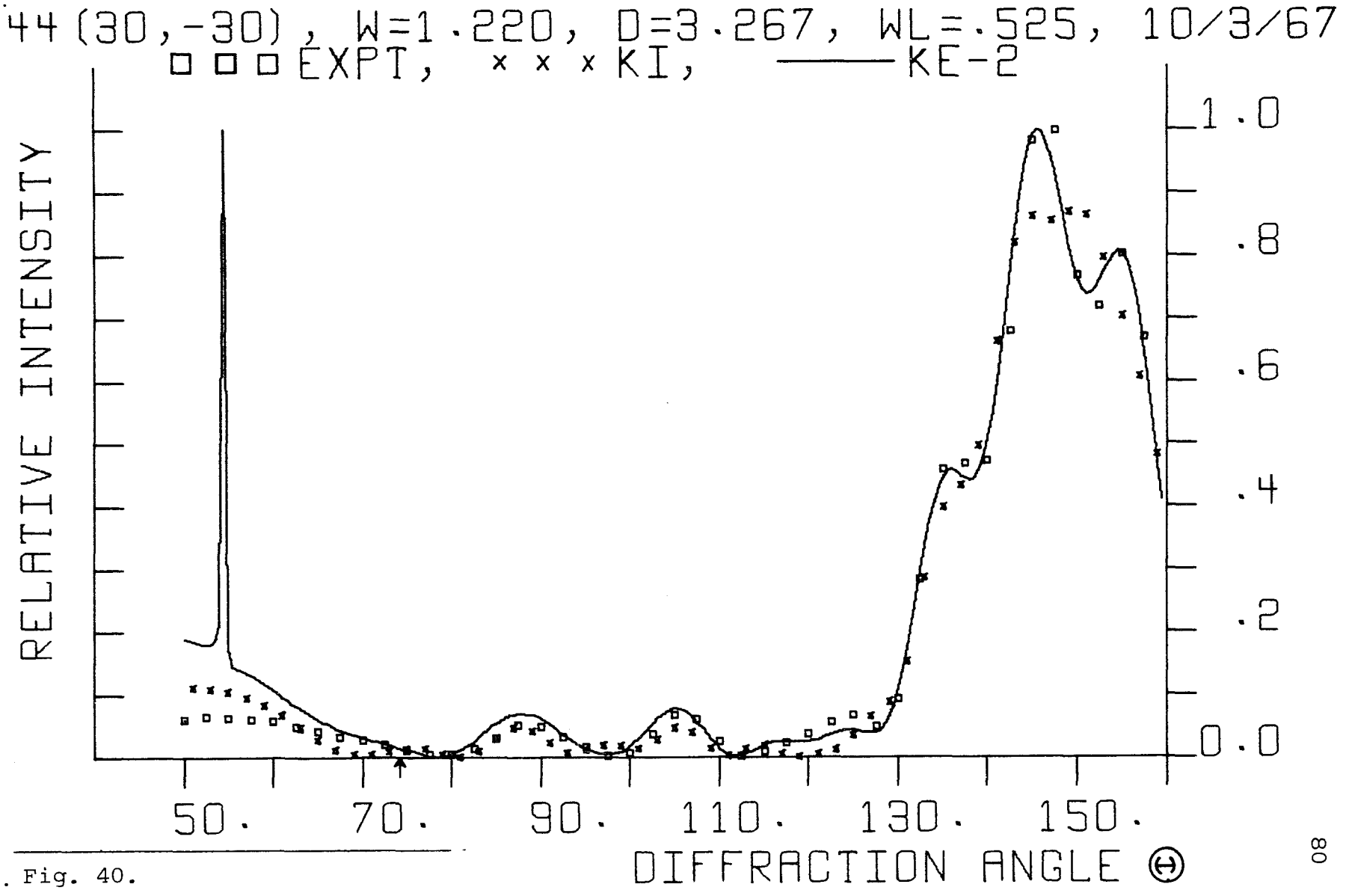
44 (30,-30), W=1.220, D=3.267, WL=.525, 10/3/67
□ □ □ EXPT, x x x KI, ——— KE-2
RELATIVE INTENSITY
1.0
.8
.6
.4
.2
0.0
50.
70.
90.
110.
130.
150.
DIFFRACTION ANGLE Θ

Fig. 40.

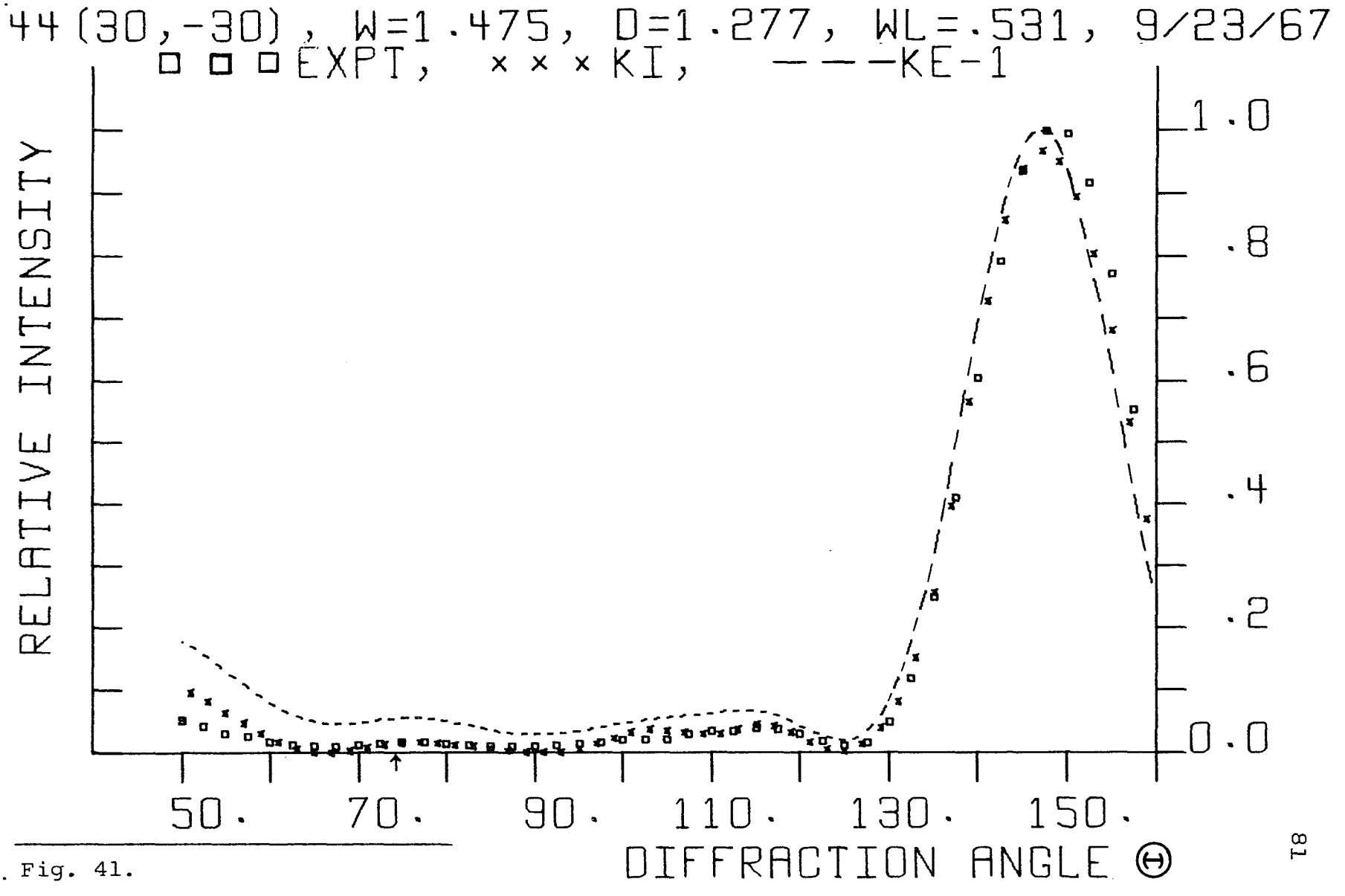
44 (30,-30), W=1.475, D=1.277, WL=.531, 9/23/67
□ □ □ EXPT, × × × KI, — — —KE-1
RELATIVE INTENSITY
1.0
.8
.6
.4
.2
0.0
50.
70.
90.
110.
130.
150.
DIFFRACTION ANGLE Θ

Fig. 41.

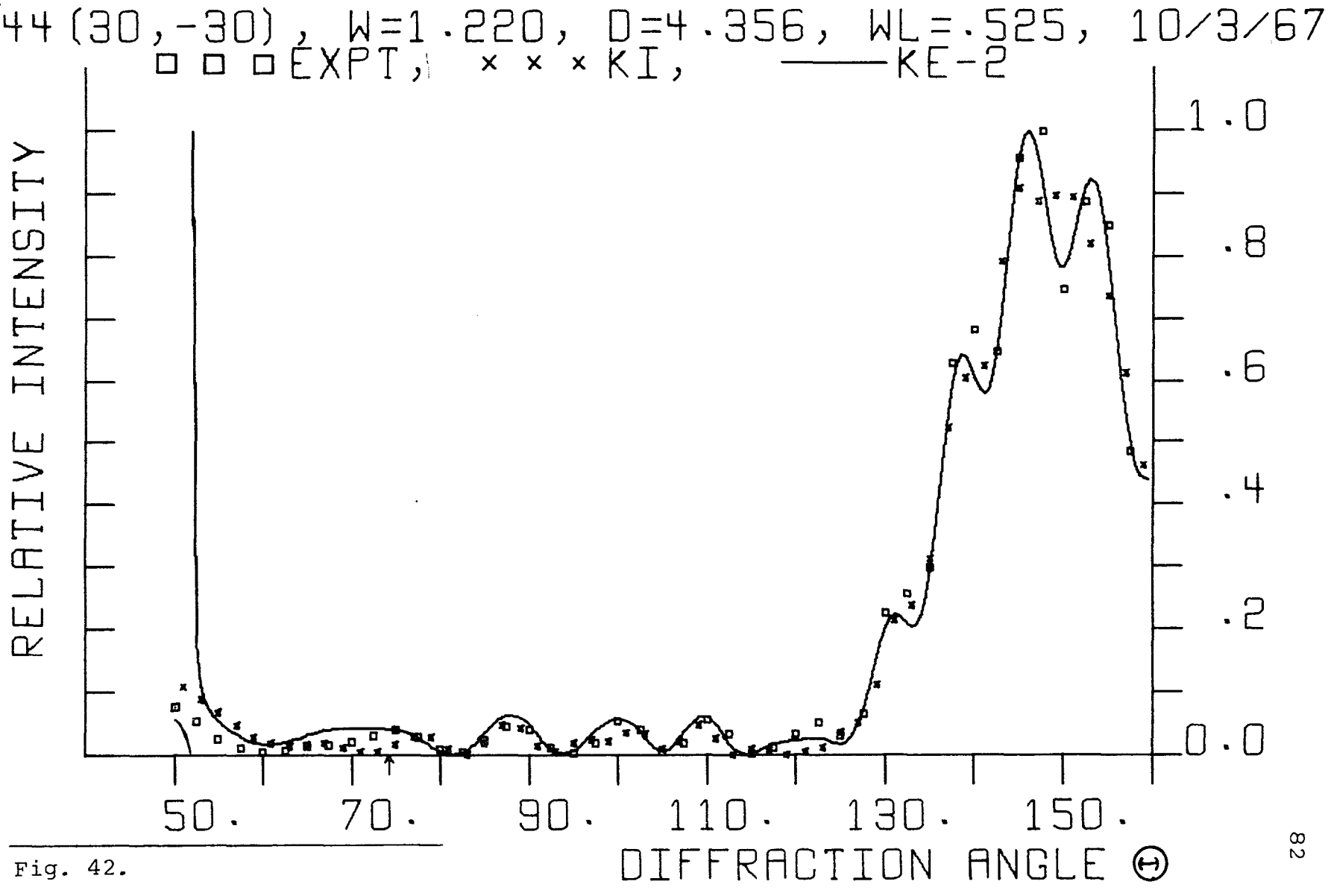
44 (30,-30), W=1.220, D=4.356, WL=.525, 10/3/67
□ □ □ EXPT, × × × KI, ——— KE-2
RELATIVE INTENSITY
1.0
.8
.6
.4
.2
0.0
50.
70.
90.
110.
130.
150.
DIFFRACTION ANGLE Θ

Fig. 42.

5. Discussion

We shall consider here the sources of experimental error associated with various aspects of the experimental apparatus and procedures, and indicate some estimation of the limits of accuracy of the results. A summary of the general conclusions which can be drawn from the results is then given.

A. Limits of Accuracy

The experimental apparatus can be considered as composed of three distinct elements: source system, detection system, and diffracting strips. The errors associated with aspects of each will be considered. A fourth source of error in the form of spurious reflections (or "echoes") is the chamber in which the experiments were conducted, including parts of the spectrometer arm and strip supporting frame. Tests for radiation noise were made with (and without) the frame in place by scanning the angular region of interest when no strips were in place. These tests indicated that the noise level of the room was less than the noise level of the crystal-detector and amplifier combination. This level was in general 30 db or more below typical values at diffraction pattern maxima. Therefore, the walls, ceiling, floor, spectrometer arm and strip frame can be neglected as sources of radiation due to reflections.

The determination of diffraction angle Θ was made mechanically using the angle encoder and spur gears. This determination was recorded and found reproducible to within 0.1^{o}. The wedges used to hold the strips at various angles with the frame (and thereby with respect to each other) were machined to better than 0.1^{o}. The angular positioning of the frame with respect to the direction of the incident radiation was good to within 0.3^{o} and in most cases appeared to be better than 0.2^{o}.

The square-law response of the detector crystals was not tested directly but was inferred by the good agreement between theory and experiment for the case of single strip diffraction which was used as the basic test of the system and its alignment. Also, several crystals and two amplifiers were used interchangeably during the course of the experiments with no noticeable difference in the results.

The frequency meter used to determine the wavelength of the radiation was calibrated to 0.2% accuracy and was very sharp in its response. It allowed the determination of wavelength to well below 1% of the values quoted.

Three different strip widths were used: 1.220 cm, 1.475 cm, and 1.270 cm. The first two were sheared from a three-foot square sheet of aluminum of 0.020 inch

thickness.[22] Some difficulties were encountered in the shearing process due to uneven edges, crimping, and non-uniform width. Approximately 90% of the strips sheared were rejected for one or more of the latter reasons. For the 1968 series of readings, it was decided to shear new strips, as the ones used previously had become permanently distorted.[23] However, the shear had become sufficiently dulled in the meantime so that the strips produced were unsuitable. As an alternative, steel gauge stock was chosen. It was available in 0.5 inch (1.270 cm) widths and a variety of thicknesses. For consistency, the same 0.020 inch thickness (as the aluminum strips) was chosen. The widths of the aluminum, measured with a micrometer, are good to within approximately 0.008 cm while the gauge stock width was far better. The gauge stock also proved more resilient and it yielded more consistent results.

Of the sources of error considered thus far, none is believed to have been a major one. Those to be discussed in the following are considered to be significantly greater

---

[22]The thickness of 0.020 inch = .051 cm which is slightly less than one-tenth of a wavelength; theoretically, the strips are infinitesimally thin.

[23]It was discovered that the old strips had developed a slight twist between the center and the ends of approximately 0.5^{o}. This became apparent when alignment checks were made because the maxima of the single strip test patterns were shifted approximately 1^{o} from their positions in previously obtained results.

in importance to the extent that the above are negligible in comparison. The first of these concerns the amplitude distribution across the incident beam. As mentioned several times above, the strips-in-a-plane patterns taken first were used as a test of the incident radiation's phase and amplitude (section 4 B). The good agreement between theory and experiment with respect to the location of maxima and minima serves as evidence that the incident radiation was indeed plane. But how good a test are these patterns of the amplitude distribution across the beam?[24] In order to check this, the computer programs used to calculate the Keller (and Kirchhoff) patterns were modified to allow for different amplitudes incident upon the two strips. In Fig. 43 we consider the two strips in a plane considered earlier in Fig. 20 ($w = 1.220$ cm, $D = 3.264$ cm) except that here, we have also included for comparison two second-order Keller theory curves which result when the incident radiation is assumed to have different amplitudes upon the strips. The ratio of the amplitudes is indicated in the legend: a ratio of 1.3 indicates that the amplitude on one of the strips is 30% higher than on the other. All curves are normalized

---

[24] It should be noted here that attempts were made to directly measure the intensity distribution across the width and height of the incident beam. These attempts, however, proved inconclusive because of apparent interactions, mostly in the form of standing waves, between the receiver horn and the waveguide source.

relative to their maximum intensity so that the curves are not being compared with each other but with the experimental results which are also normalized in the same way. It is readily seen that an amplitude difference of 30% to 50% could be present and not be readily detected by these patterns. In order to obtain a more direct measure of the amplitude distribution, the following alternative method was employed. A single strip was moved across the beam at intervals of approximately 0.5 inches and the intensity at pattern maximum was recorded. Over that part of the beam that was used, the variation of intensity was no more than approximately 19% of its maximum value; this limits the possible variation in amplitude to no more than 10% of its maximum value. This value will be discussed again below.

A second major source of error concerns the frame and the mounting of the strips onto it. As depicted in Fig. 1, the frame was itself mounted atop the main shaft support and axis of rotation of the spectrometer arm. The strips were held laterally against the frame, or against wedges placed on the frame, and stretched vertically along their lengths between the bottom face of the frame and a plate mounted in the ceiling. Elastic bands between the strips and the ceiling supplied the tension. The central shaft, a 2-inch diameter circular steel rod, was not entirely

rigid, and as the arm was rotated, a certain amount of flexibility would cause the frame to shift slightly toward the longer section of the arm. In order to minimize this effect, counterweights were hung from the short arm, but this did not entirely remove the effect. The results of this motion were two-fold. Firstly, the frame with strips in place was adjusted to vertical before each run. As the arm was rotated, however, the vertical condition would not entirely maintain. In most cases, this did not appear to be a very serious problem because the amount of change was small and is not readily observable in the single strip patterns. Secondly, since the strips were held at one end by connection to the ceiling, and since the frame was shifting, the direction of the stretching support changed as the arm was rotated. This sometimes appeared as a "bowing" of the strips toward or away from each other, thereby changing the distance between the strips from what it was originally set to be. In order to minimize these effects, the initial adjustments of the strips in the frame were made with the arm at the center of its angular range. Also, checks were made at intermediate points during some runs to test the verticality of the strips and the spacing between them. It is estimated that for the cases presented here, the distance D between the strip centers should be good to approximately 0.01 cm or better.

Finally, the supporting of the strips under a tension presented some experimental difficulties. Sufficient tension had to be applied to obtain as flat a strip as possible along a length of approximately twenty-two inches, but care had to be taken to avoid distorting the strips by twisting them about an axis perpendicular to their lengths. Such a distortion would cause one side of the strip to be stretched more than the other and prevent the strip from being plane along its length. For single strip patterns, distortions resulting in a twist of 0.3° or more were detectable because the location of the principal maximum of the pattern would shift approximately 0.6° from its expected position. For the results given here, it is estimated that the error in strip orientations with respect to the incident radiation is approximately 0.2°. This would yield a maximum error in the value of β, the angle between the planes of the strips, of approximately 0.4°.

In order to investigate the effects of each of the above sources of error on a typical pattern when the strips are inclined with respect to each other, we shall consider in detail the case of two strips (w = 1.270 cm, D = 3.841 cm) whose faces are inclined away from each other (44(10,-10) case). Fig. 44 compares experiment with first- and second-order Keller theory where we have assumed equal amplitude on each strip and all angles and distances as stated.

Fig. 45 compares second-order Keller theory for equal amplitudes on the strips but an 0.2^{o} shift in the value of wedge angle (44(10.2,-10.2) case). No significant change is seen. In Fig. 46 we consider the effect of a change in the distance between strip centers by an amount equivalent to one-tenth wavelength (0.1λ = 0.053 cm) making D equal to 3.788 cm. Most of the effect is seen to be located to the right of the principal maximum where the location and heights of the minima and maxima are slightly changed. Although the locations of maxima and minima obtained experimentally compare favorably with those predicted by Keller theory, the small discrepancies evident in some of the graphs may find their explanation in such small variations of the distance between the strips.

In Fig. 47 we consider the effect of a 10% difference in the amplitude of the radiation incident upon each strip. For this case, the effect upon the pattern is significant and larger than any of the others considered, and its effect is almost entirely on the maxima to the left of the principal maximum. Here agreement between theory and experiment has been significantly improved. Of the sources of error considered, it appears that this one is probably the most significant for the results presented.

On the basis of the deviations observed in Figs. 45 to 47, experimental points to the left of the principal

maximum of the two strip "small-angle" patterns may have experimental error up to 10% of the pattern maximum. These appear due mostly to non-uniformities in the radiation incident upon the strips. Experimental values to the right of the principal maximum are generally good to within 3% of the maximum intensity. For strips in a plane, or the "large-angle" patterns, the errors were generally observed to be no greater than those stated above, and in many cases appeared to be considerably smaller. In any case, it was found that fluctuations in the value of the relative intensity at a peak did not cause the general characteristics of a pattern to change, i.e., the general shape of the peaks and the locations of the maxima and minima were preserved and found experimentally reproducible. This is why Kirchhoff theory is clearly poorer in some patterns - it predicts curves which do not have the general shape of the patterns observed experimentally (see, for example, Figs. 23, 25 and 29).

Another indication of the limits of accuracy of the experimental results concerns their reproducibility. Figs. 48 to 50 give examples of experimental results obtained at different times for the three categories of diffraction patterns presented above, viz., single strip, coplanar strips, and angled strips. A Keller theory pattern is included on each plot for comparison. Since

the single strip pattern was used as the alignment standard, consistent results were sought for locations of the strip at different parts of the beam, as well as at different times during a series of experiments. Fig. 48 considers two single strip test patterns ($u = 44^{o}$, $w = 1.475$ cm, $\lambda = .529$ cm) taken at the beginning of the summer 1968 series of experiments when the system's alignment was being checked. The theoretical curve is obtained from single strip Keller theory, and all curves are normalized relative to their maximum intensity. Fig. 49 compares results for the planar strip case considered in Fig. 17 ($w = 1.475$ cm, $D = 2.106$ cm, 44(0,0) case). The patterns were taken approximately eleven months apart and the wavelength is slightly different as indicated in the legend. Here, a second-order Keller theory curve is included for comparison and again all curves are normalized with respect to their maximum values. In Fig. 50 we consider the angled strips ($w = 1.270$ cm, $D = 3.841$ cm, $\lambda = .529$ cm, 44(10,-10) case) considered in detail above (Figs. 44 to 47) in the discussion of the sources of error and their effects. In this figure, the experimental results are normalized differently: the boxes represent normalization relative to maximum intensity whereas the points denoted by zeros are normalized relative to a single strip value. The difference here is negligible.

Also, it is noticed that the lack of complete agreement between theory and experiment for the secondary maxima to the left of the principal maximum is confirmed. As mentioned above, the patterns were readily reproducible with respect to location of maxima and minima and this is seen in the above cases. Some slight deviations in the relative intensities of the maxima and minima can also be observed in Fig. 50.

The final item to be discussed concerns the methods used to compare theories with each other and with experiment. When the experimental work was started, all patterns were normalized relative to their maximum intensity. This method is commonly used and its utility has been established. This resulted, however, in comparisons between experiment and each of the theoretical patterns and offered no comparison between the theoretical curves themselves. Also, the choice of the pattern maximum placed seemingly unwarranted importance upon the value at a single point. For the single strip cases, there was little choice but to use this method since any absolute measurement of the intensity of the diffracted radiation was not feasible. Having once decided to use the single strip patterns as the standard, however, a method of normalization based upon single strip results could then be used. Normalization of the double strip readings

relative to single strip values, as described in section 4 A, offered no theoretical difficulties since the required single and double strip values could be readily evaluated, and this was done. Experimentally, however, a considerable amount of data had already been accumulated which was normalized relative to the maximum intensity and this could not be easily renormalized. This is why two methods of normalization were used. The results here affirm the validity of normalization relative to maximum value since, in most cases, the difference between the methods of normalization proved almost negligible; the maxima of the experimental patterns normalized relative to the single strip proved to have values close to unity anyway (cf., Figs. 24, 25, 26, 27, 29, 44 and 50). In general, the normalization relative to the single strip is preferable since it makes all curves independent of each other. This independence proved important in cases where there was significant difference between the predictions of the theories due to the proximity of the strips (cf., Figs. 15, 16, 23 and 24). In these cases, the normalization relative to the single strip permitted a better quantitative comparison between first- and second-order Keller theory, Kirchhoff theory, and experiment. The results

presented here indicate that both normalization procedures are of approximately equal value as long as the strips' interactions are not large and higher order effects do not significantly change the values at the principal maximum of the pattern.

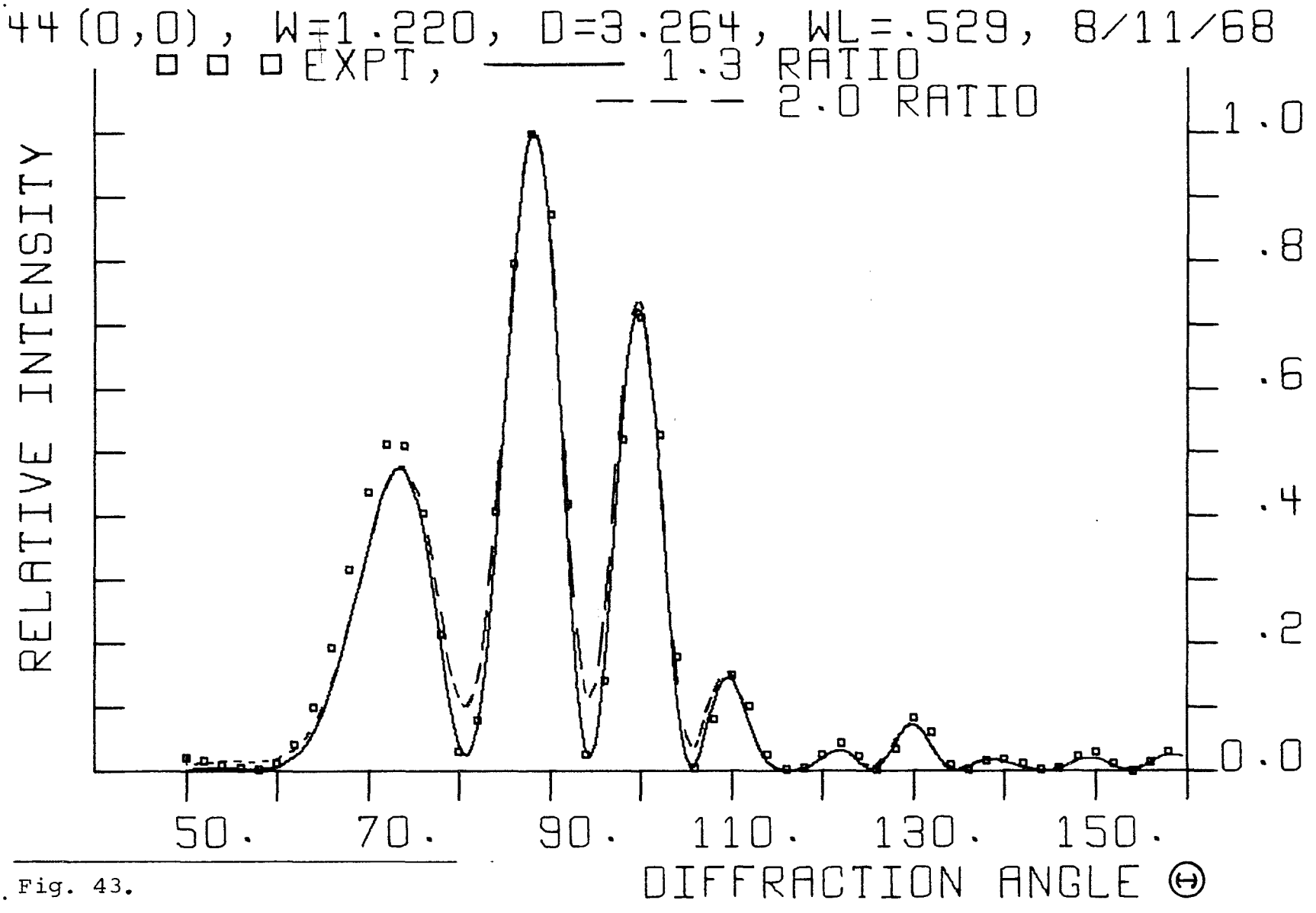
44 (0,0), W=1.220, D=3.264, WL=.529, 8/11/68
EXPT, 1.3 RATIO
2.0 RATIO
RELATIVE INTENSITY
1.0
.8
.6
.4
.2
0.0
50.
70.
90.
110.
130.
150.
DIFFRACTION ANGLE Θ

Fig. 43.

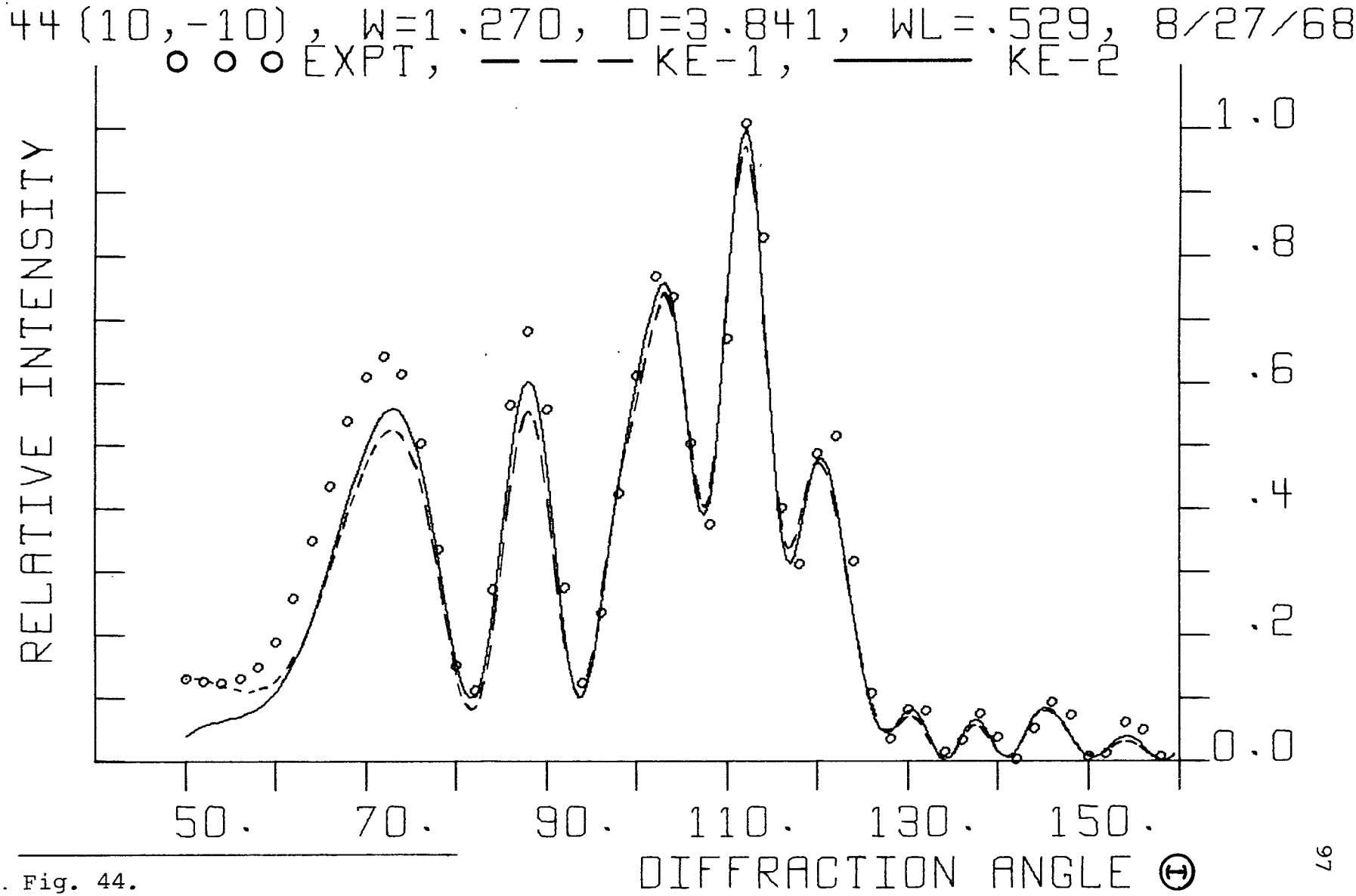
44 (10,-10), W=1.270, D=3.841, WL=.529, 8/27/68
o o o EXPT, — — — KE-1, ——— KE-2
RELATIVE INTENSITY
1.0
.8
.6
.4
.2
0.0
50.
70.
90.
110.
130.
150.
DIFFRACTION ANGLE Θ

Fig. 44.

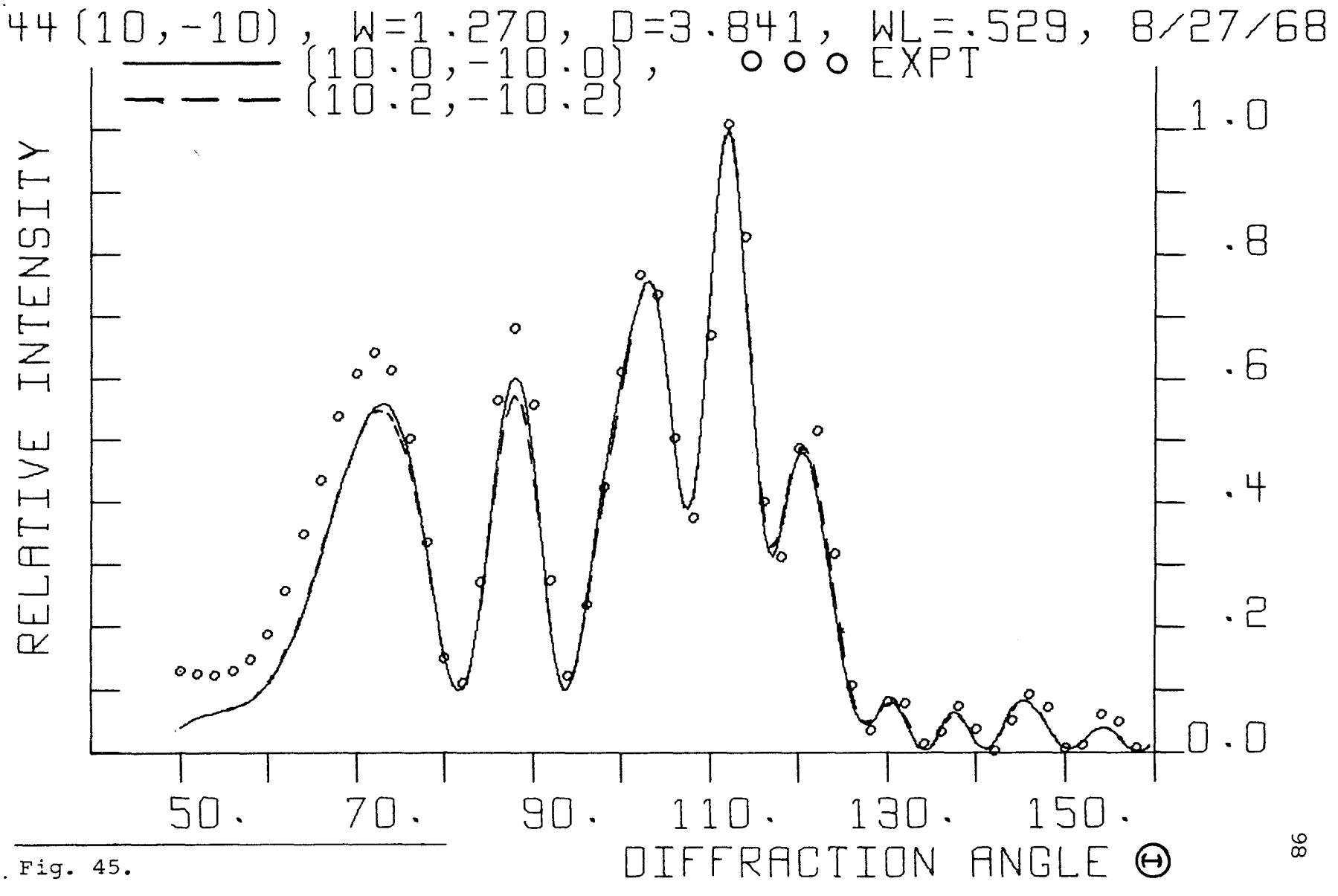
44 (10,-10), W=1.270, D=3.841, WL=.529, 8/27/68
(10.0,-10.0), o o o EXPT
(10.2,-10.2)
RELATIVE INTENSITY
1.0
.8
.6
.4
.2
0.0
50.
70.
90.
110.
130.
150.
DIFFRACTION ANGLE Θ

Fig. 45.

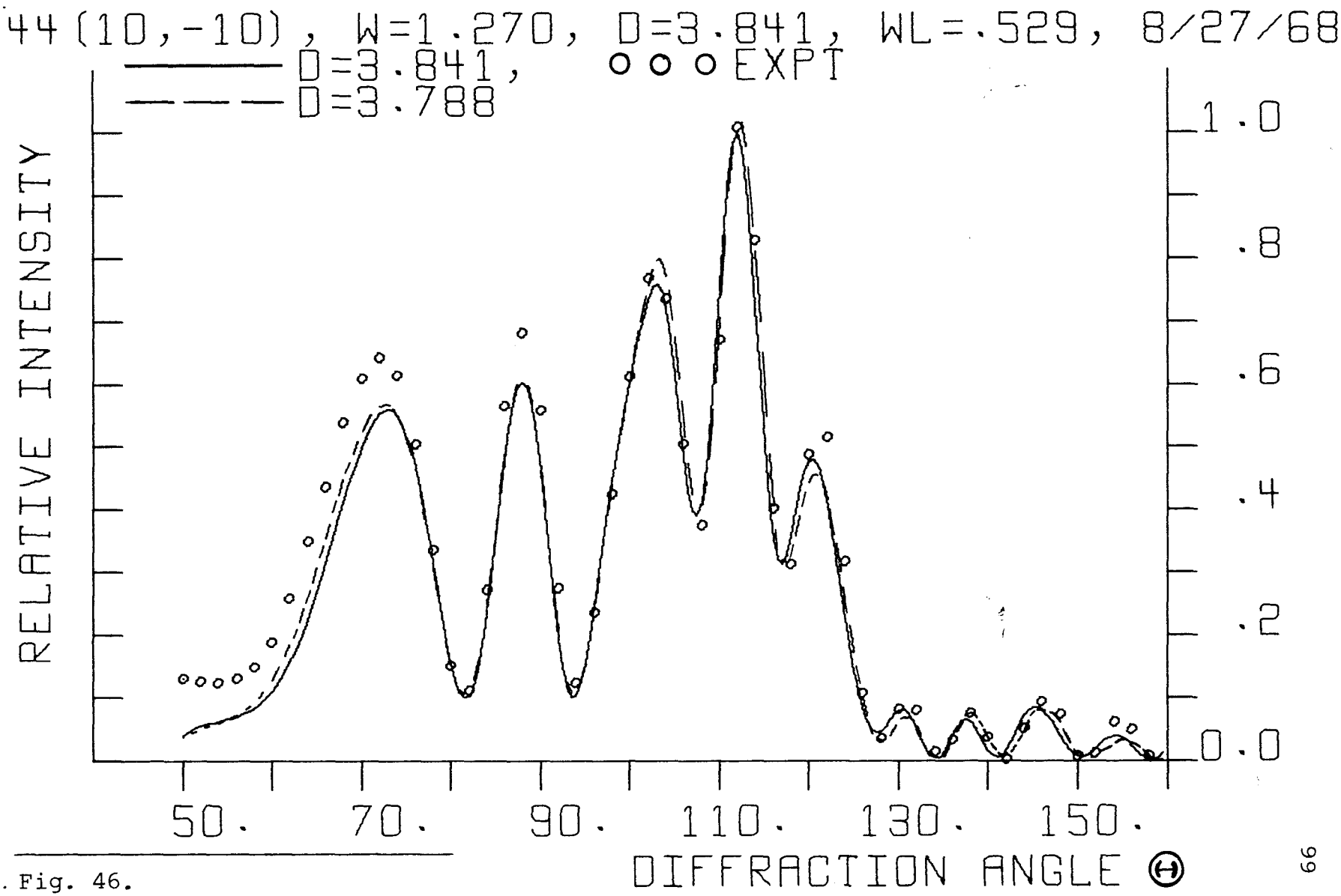
44 (10,-10), W=1.270, D=3.841, WL=.529, 8/27/68
D=3.841, o o o EXPT
D=3.788
RELATIVE INTENSITY
1.0
.8
.6
.4
.2
0.0
50.
70.
90.
110.
130.
150.
DIFFRACTION ANGLE Θ

Fig. 46.

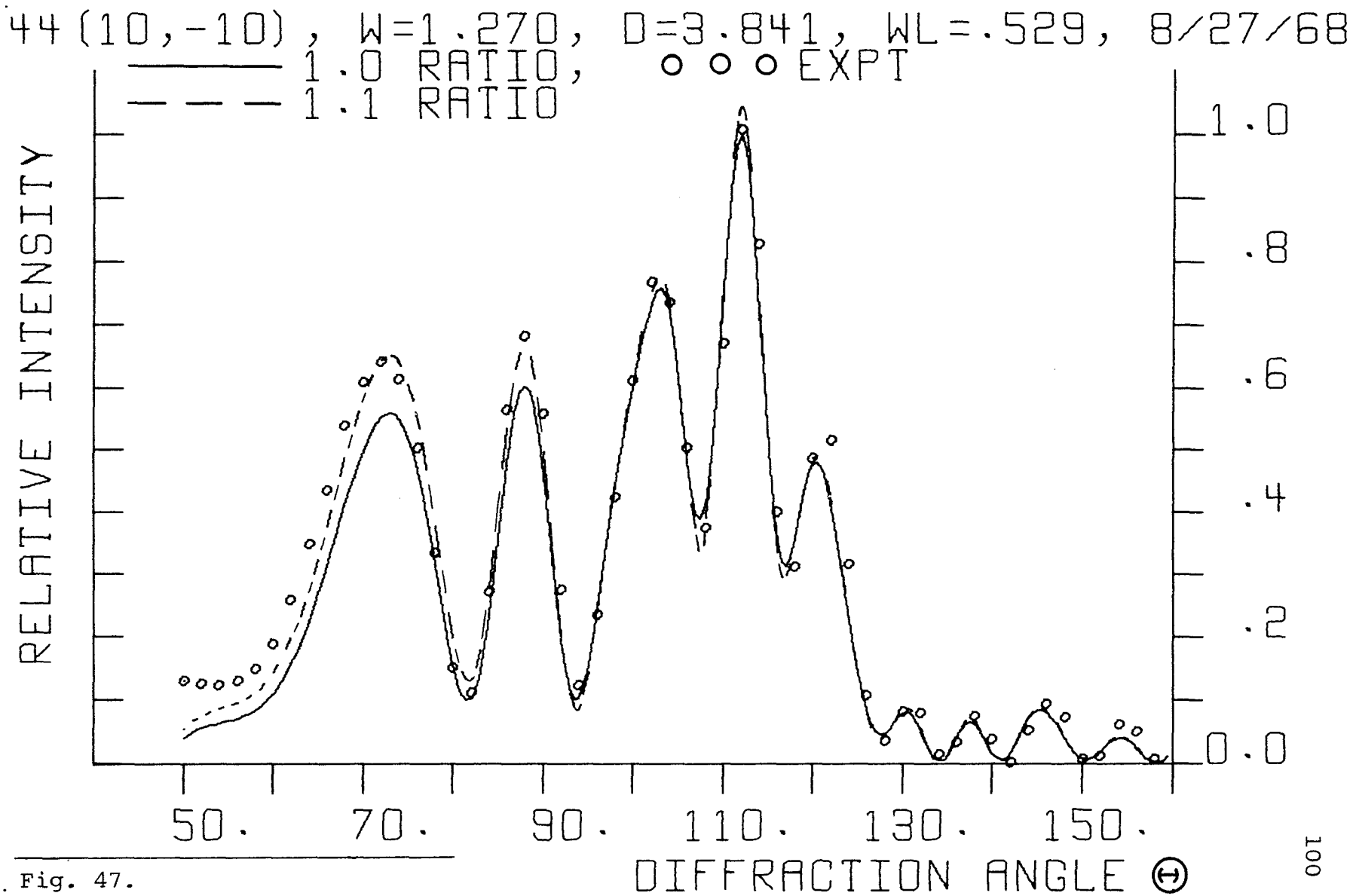
44 (10,-10), W=1.270, D=3.841, WL=.529, 8/27/68
1.0 RATIO, O O O EXPT
1.1 RATIO
RELATIVE INTENSITY
1.0
.8
.6
.4
.2
0.0
50.
70.
90.
110.
130.
150.
DIFFRACTION ANGLE Θ

Fig. 47.

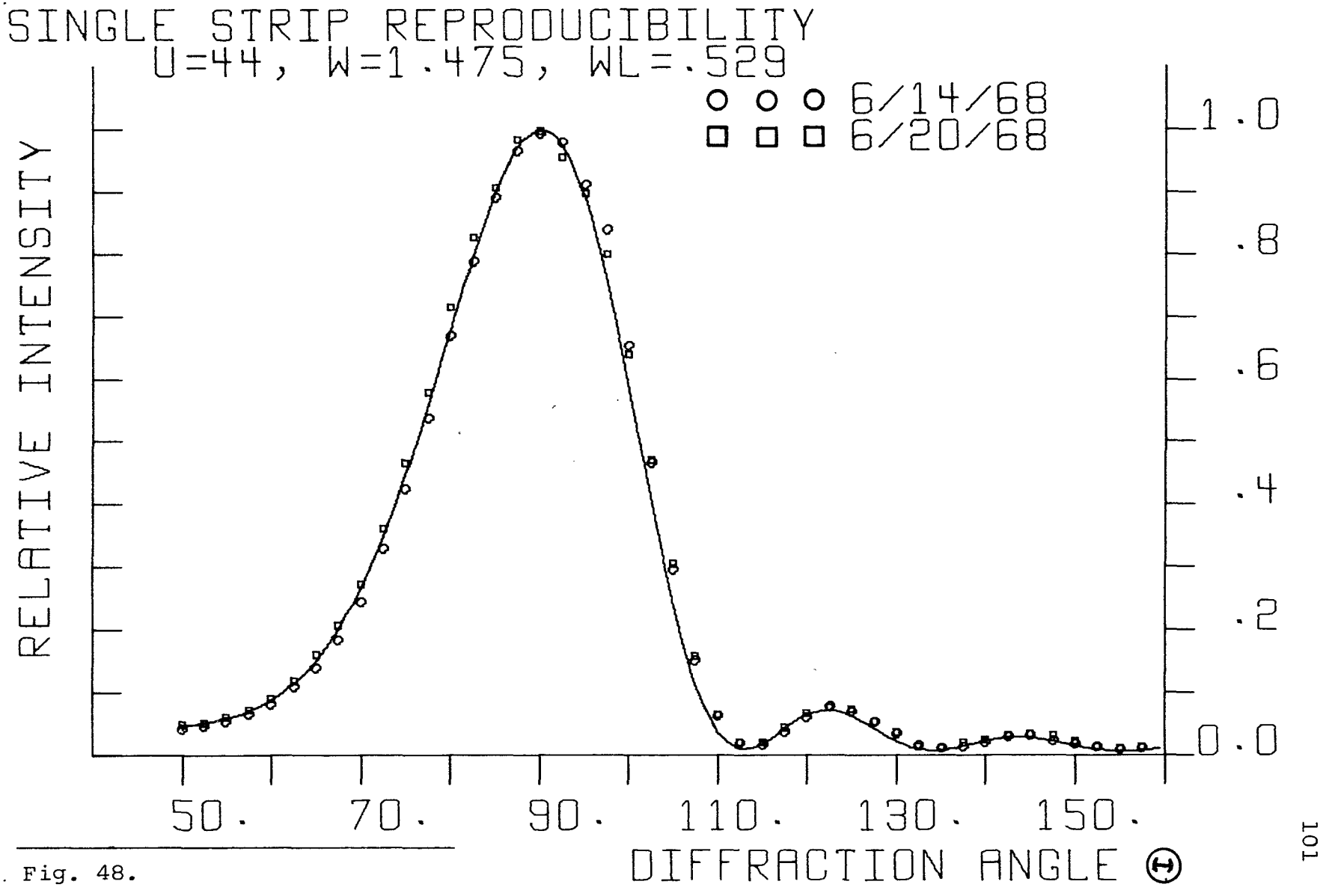
SINGLE STRIP REPRODUCIBILITY
U=44, W=1.475, WL=.529
6/14/68
6/20/68
RELATIVE INTENSITY
1.0
.8
.6
.4
.2
0.0
50.
70.
90.
110.
130.
150.
DIFFRACTION ANGLE Θ

Fig. 48.

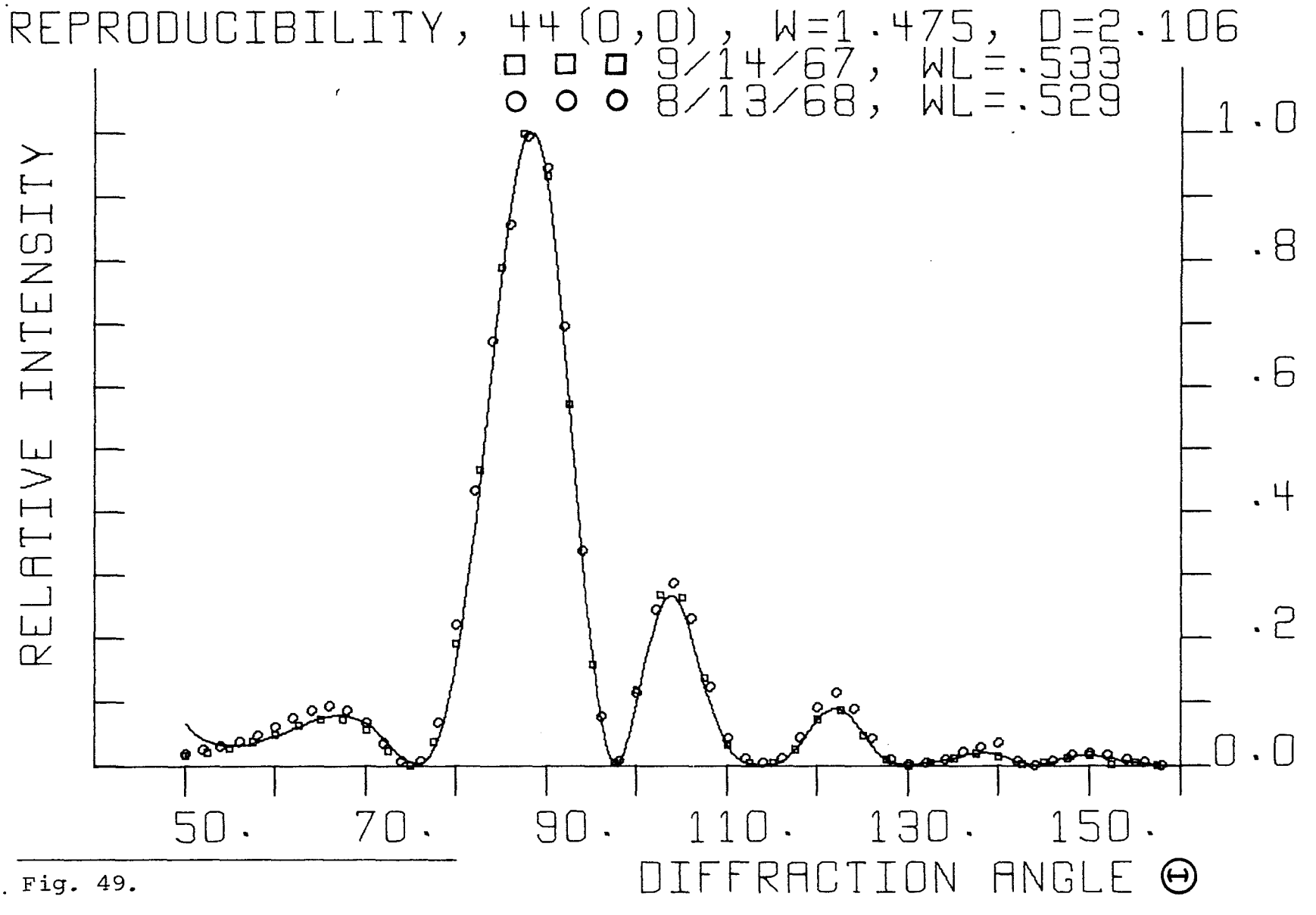
REPRODUCIBILITY, 44(0,0), W=1.475, D=2.106
9/14/67, WL=.533
8/13/68, WL=.529
RELATIVE INTENSITY
1.0
.8
.6
.4
.2
0.0
50.
70.
90.
110.
130.
150.
DIFFRACTION ANGLE Θ

Fig. 49.

REPRODUCIBILITY, 44)10,-10) M=1.270, D=3.841
○ □ 8/27/98, ML=.5529
○ □ 8/21/98, ML=.5525
RELATIVE INTENSITY
0.0
0.2
0.4
0.6
0.8
1.0
50.
70.
90.
110.
130.
150.
DIFFRACTION ANGLE ①

Fig. 50.

B. Conclusions

The aims of this project were two-fold. First, to develop an experimental facility for the study of electromagnetic diffraction problems in the microwave region, and second, to use this facility to compare the diffraction theories of Kirchhoff and Keller. Both of these objectives have been achieved. Equipment has been assembled and a chamber prepared which together are capable of investigating diffraction, under both Fresnel and Fraunhofer conditions, by multiple obstacles in proximity whose dimensions and separation are of the order of the wavelength of the incident polarized radiation. This equipment was used to carry out an investigation of Fraunhofer diffraction by two long, thin, parallel, conducting strips with incident radiation polarized parallel to the strip axes. The experimental results were compared with the scalar Kirchhoff theory, and the more recently developed Keller geometrical theory of diffraction. The results presented above clearly indicate that the geometrical theory, even to first-order, is better able to describe the results obtained experimentally. Moreover, second-order Keller theory, which considers interactions between the strips due to "doubly diffracted rays," is found to improve the agreement between theory and experiment in most cases,

as long as the strip separation is not too small (closest edges less than approximately a wavelength apart). The analysis of second-order effects in Appendix III indicates that the largest second-order contributions result from interactions between the edges which are closest and from doubly diffracted rays which are travelling in directions close to those of the singly diffracted rays which caused them. On this basis, it does not appear that third-order terms would appreciably improve the Keller results in the regions we have considered. Finally, although no detailed study was made here of the effects of conductivity upon the double strip patterns, the results from two types of strips used (aluminum and steel) indicated no evidence of any conductivity dependence (the conductivity of aluminum is approximately six times that of steel).

APPENDIX I

Measurement of the Focal Length of a Parabolic Mirror

The large parabolic mirror used as a collimator in the experiment was a government surplus searchlight mirror with an aperture of approximately 36 inches and a focal length whose value of 14 5/16 inches was etched near the rim of the mirror. The following analysis was made to determine how true the parabolic shape of the mirror was and at the same time to verify the focal length given.

The general equation of a parabola symmetric with respect to the y-axis and with a vertex which passes through the origin is $y = x^2/(4F)$ where F is the focal length of the parabola. Let (x_i,y_i) and (x_j,y_j) be two points which lie on the parabola. The "first difference" in y for these points is defined as

$$(\Delta y) = y_j - y_i = \frac{1}{4F}(x_j^2 - x_i^2) = \frac{1}{4F}(x_j - x_i)(x_j + x_i). \quad \text{(A1)}$$

Consider three consecutive points, (x_1,y_1), (x_2,y_2), (x_3,y_3). Then

$$(\Delta y)_1 = y_2 - y_1 = \frac{1}{4F}(x_2 - x_1)(x_2 + x_1)$$
$$(\Delta y)_2 = y_3 - y_2 = \frac{1}{4F}(x_3 - x_2)(x_3 + x_2) \quad \text{(A2)}$$

The "second difference," $\Delta^2 y$, for these three points is

given by

$$(\Delta^2 y) = (\Delta y)_2 - (\Delta y)_1$$
$$= \frac{1}{4F}\left[(x_3-x_2)(x_3+x_2) - (x_2-x_1)(x_2+x_1)\right] \tag{A3}$$

Let the x-intervals be equal and denoted by Δx. Then,

$$(\Delta^2 y) = \frac{\Delta x}{4F}(x_3 - x_1) = \frac{2(\Delta x)^2}{4F} \tag{A4}$$

Solving for the focal length F, we get

$$F = \frac{(\Delta x)^2}{2(\Delta^2 y)} \tag{A5}$$

This last result was used to evaluate the focal length of the mirror. In order to effect this, coordinates of points on the surface of the mirror must be measured. Actually, only the changes in the coordinates need be measured since only differences appear in equation (A5). The measurements were made by mounting the mirror, with its axis vertical, on a milling table. A feeler gauge was rigidly mounted above the mirror surface. Starting at the edge of the mirror, the mirror was moved horizontally at intervals of one inch relative to the gauge. After each horizontal movement, the table was raised until the feeler gauge contacted the surface. The change in the vertical displacement was recorded and a typical set of points is given in Table A1, along with the corresponding first and second differences.

The relatively good agreement between the various values in the second difference column indicate that the mirror is indeed parabolic. Table A2 considers a set of values that would be obtained from a spherical mirror with a focal length of 14 5/16 inches. As is readily seen, the second difference for a spherical mirror has a constantly increasing value which would have been detectable with the measuring procedure used.

The average value of the second difference in Table A1 was found to be 0.0349 inches with an average deviation of $\pm$ 0.0004 inches. The mirror was rotated 90^{o} and another set of readings was taken. This second set yielded average values of 0.0353 $\pm$ 0.0004 inches. Using these average values in equation A5, with $\Delta x = 1.0$ inches, the focal length F is found to be

$$F = 14.25 \pm 0.16 \text{ inches}$$

The value 14 5/16 is 14.31 inches.

x (in.)	Δy (in.)	$\Delta^2 y$ (in.)
0	-	
1	.4472	
		.0347
2	.4125	
		.0349
3	.3776	
		.0348
4	.3428	
		.0350
5	.3078	
		.0352
6	.2726	
		.0343
7	.2383	
		.0355
8	.2028	
		.0351
9	.1677	
		.0351
10	.1326	
		.0342
11	.0984	
		.0361
12	.0623	
		.0344
13	.0279	
	AVERAGE	.0349

Table A1. Measured values and first and second differences for the parabolic mirror used.

x (in.)	Δy (in.)	$\Delta^2 y$ (in.)
0	-	
1	.0175	
		.0350
2	.0525	
		.0351
3	.0876	
		.0357
4	.1233	
		.0359
5	.1592	
		.0366
6	.1958	
		.0374
7	.2332	
		.0383
8	.2715	
		.0396
9	.3111	
		.0407
10	.3518	
		.0426
11	.3944	
		.0444
12	.4388	
		.0467
13	.4855	

Table A2. Calculated values of first and second differences for a spherical mirror with a focal length of 14 5/16 inches.

APPENDIX II

Single Strip Diffraction - Comparison Between Keller and Kirchhoff Theories and Exact Solution of Maxwell's Equations*

The case of diffraction by a single, infinitely long conducting strip is one of those few cases where exact solution of Maxwell's Equations is possible. The solution is given in detail elsewhere**; we will only indicate here that the general solution may be obtained by considering a two-dimensional boundary value problem in elliptic coordinates. The strip is considered as a special case of an ellipse whose minor axis goes to zero. The solution so obtained is in terms of an infinite series of Mathieu functions. Evaluation of this solution was made at New York University by Lazar and Hatcher[+] for various angles of incidence.

The Keller theory diffraction pattern for a single strip can be obtained from the general two-strip results given in equations 16 and 17 by setting both β and D equal to zero. The resulting expression for the intensity

---

*DeAcetis and Lazar, III.

**Lazar

[+]Lazar and Hatcher, unpublished.

of the radiation diffracted into angle θ is then given by

$$I_{KE} = B \left\{ \frac{\cos^2[kw(\sin\theta - \sin\theta_i)/2]}{\cos^2[(\theta+\theta_i)/2]} + \frac{\sin^2[kw(\sin\theta - \sin\theta_i)/2]}{\sin^2[(\theta+\theta_i)/2]} \right\} \quad \text{(A6)}$$

where B is independent of direction and θ_i is the angle of incidence (Fig. A1).

The corresponding Kirchhoff solution for the single strip can be obtained from equation 11 in the same way. With β and D set equal to zero there, we get

$$I_{KI} = B'w^2(\cos\theta_i + \cos\theta)^2 \frac{\sin^2[kw(\sin\theta_i - \sin\theta)/2]}{[kw(\sin\theta_i - \sin\theta)/2]^2} \quad \text{(A7)}$$

where B' is independent of direction, and θ and θ_i are as defined in Fig. A1.

Equations (A6) and (A7) were evaluated on an IBM 1620 computer and the results were plotted using the IBM 1627 Plotter. The exact theory values were punched onto cards and plotted with the above results. Figures A2 to A19 compare the Keller, Kirchhoff, and exact theory results for various strip widths and angles of incidence. Each plot considers the intensity distribution in the 180° region on the same side of the strip as the incident radiation. The diffraction angle, Θ, is measured relative to the direction

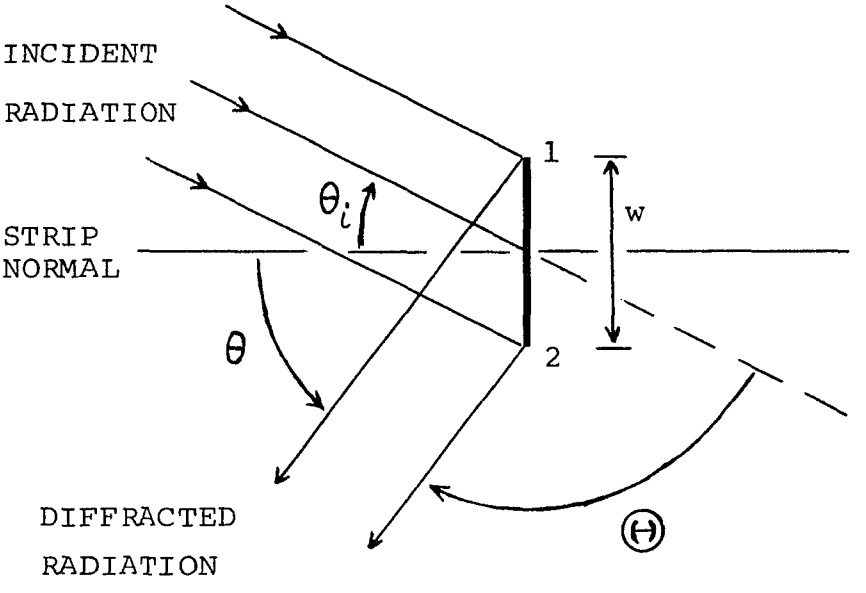

Fig. A1. Diffraction by a single strip--definition of angular quantities used.

of the incident radiation (Fig. A1), and is given in terms of θ and θ_i by $\Theta = 180^o - \theta - \theta_i$.

The curves are compared and normalized as follows. For Figs. A2 to A8, the intensity of each theory at a given point was divided by the maximum value predicted by the theory for the case $\theta_i = 6^o$ (compared in Fig. A2); the value of the exact solution maximum so obtained was then taken as unity and all other values adjusted accordingly. The same procedure was followed for Figs. A9 to A13. Figs. A14 to A19 compare the patterns as a function of strip width with θ_i kept at 46^o. For this latter series of curves, the maximum for the case where $W=3.1831\lambda$ and $\theta_i = 46^o$ was used as the divisor.

A comparison of the patterns plotted indicated that, in all cases, Keller theory more closely agrees with exact theory. For the cases of wide strip width or small angle of incidence, both theories compare favorably with exact theory. However, near glancing incidence or for small strip width, both theories diverge from the exact solution, with Keller theory still in better agreement.

A comparison of the intensity and amplitude at the pattern maximum as a function of angle of incidence is made in Table A3 and Table A4 for the cases of width/wavelength (w/λ) equal to 2.251 and 2.847. The values listed are normalized with respect to the value they have at $\theta_i = 6^o$. As can be seen, Keller theory again

more closely agrees with the exact solution, especially as one approaches larger incident angles.

Table A5 compares the intensity and amplitude at pattern maximum as a function of strip width for an incident angle of 46^{o}. Again, Keller theory is better able to describe the results predicted by exact solution.

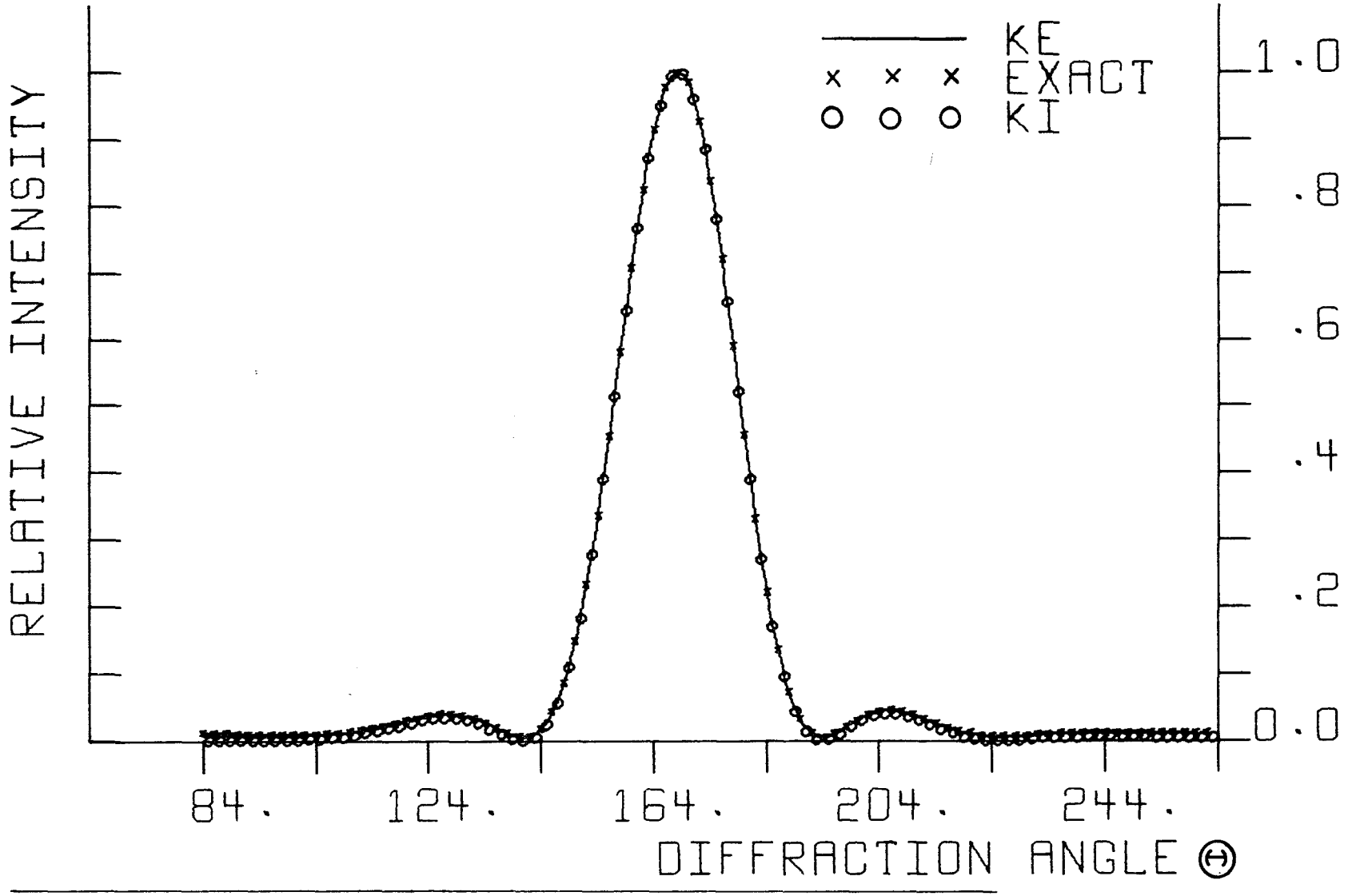

Fig. A2. Single strip diffraction: $w = 2.251\lambda$, $\theta_i = 6^o$.

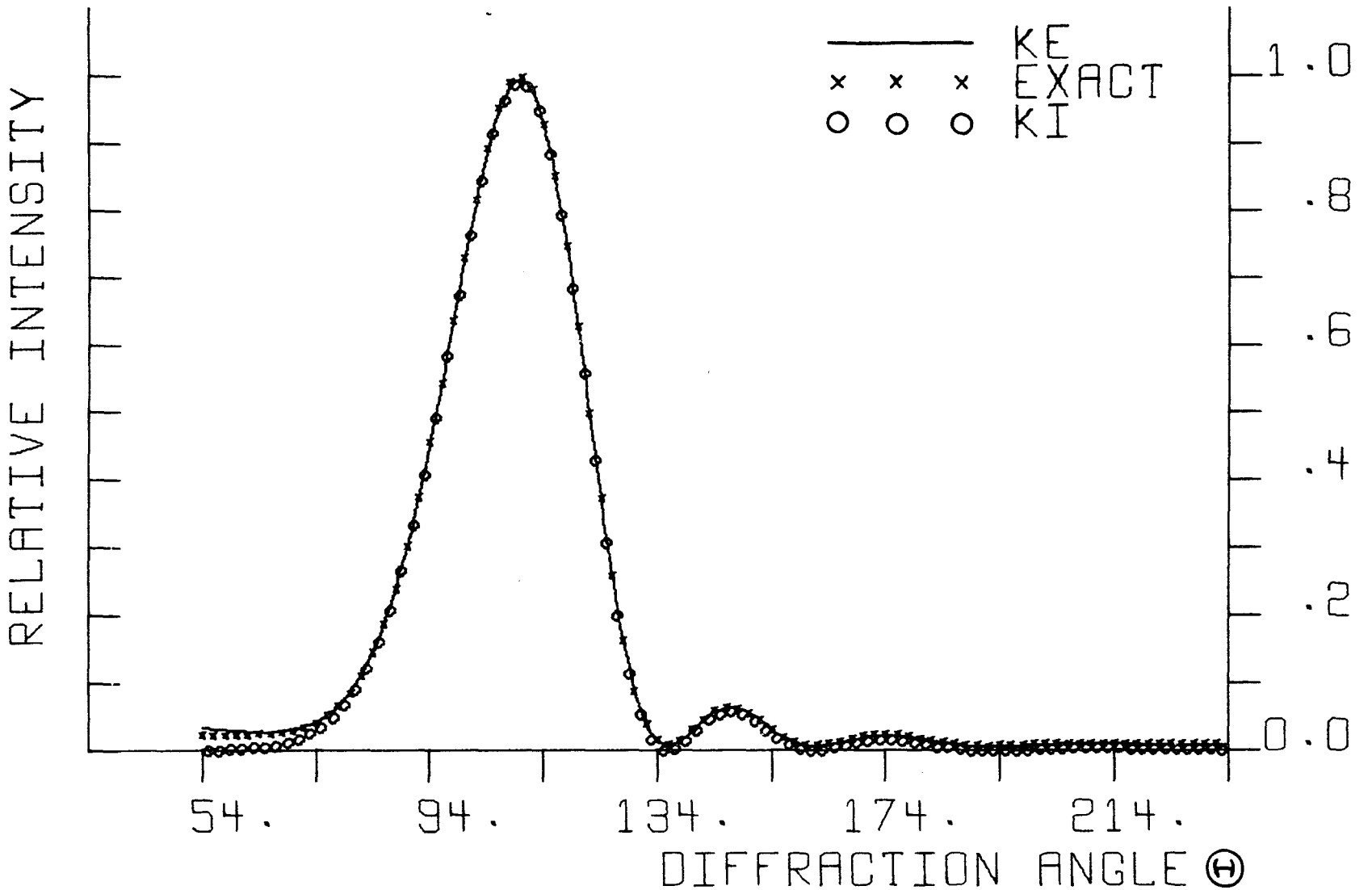

Fig. A3. Single strip diffraction: $w = 2.251\lambda$, $\theta_i = 36^\circ$.

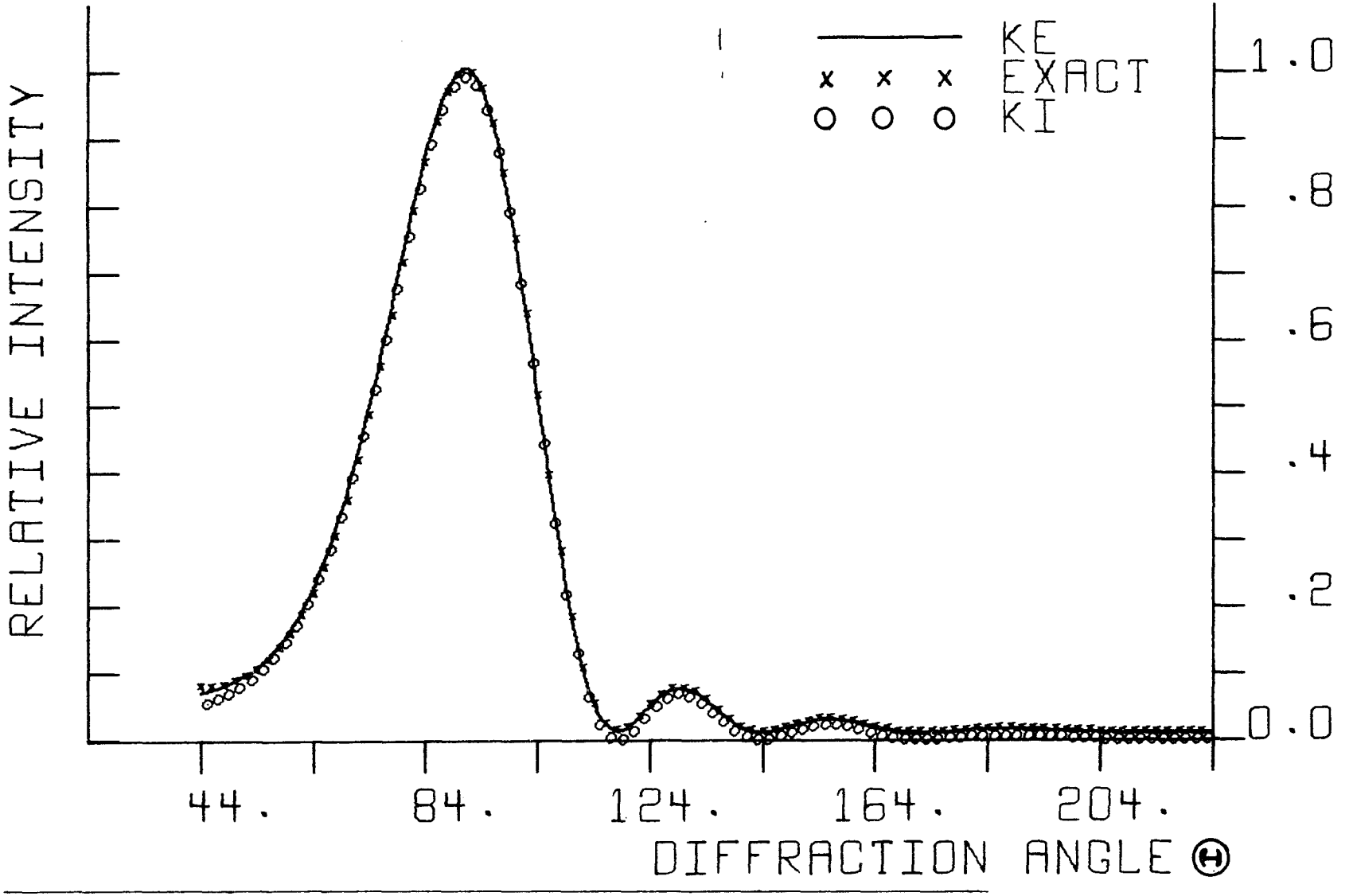

Fig. A4. Single strip diffraction: $w = 2.251\lambda$, $\theta_i = 46^\circ$.

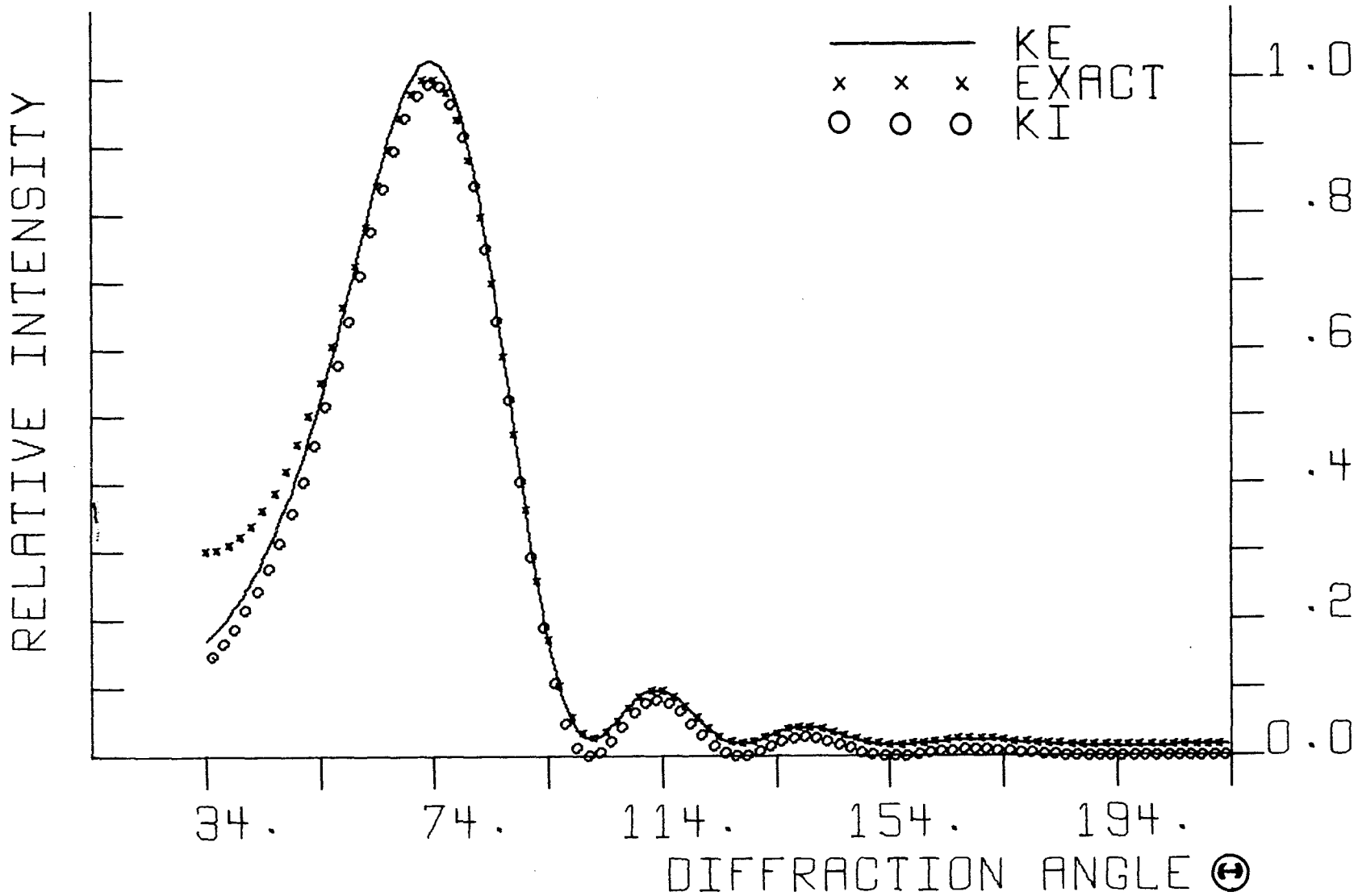

Fig. A5. Single strip diffraction: $w = 2.251\lambda$, $\theta_i = 56^\circ$.

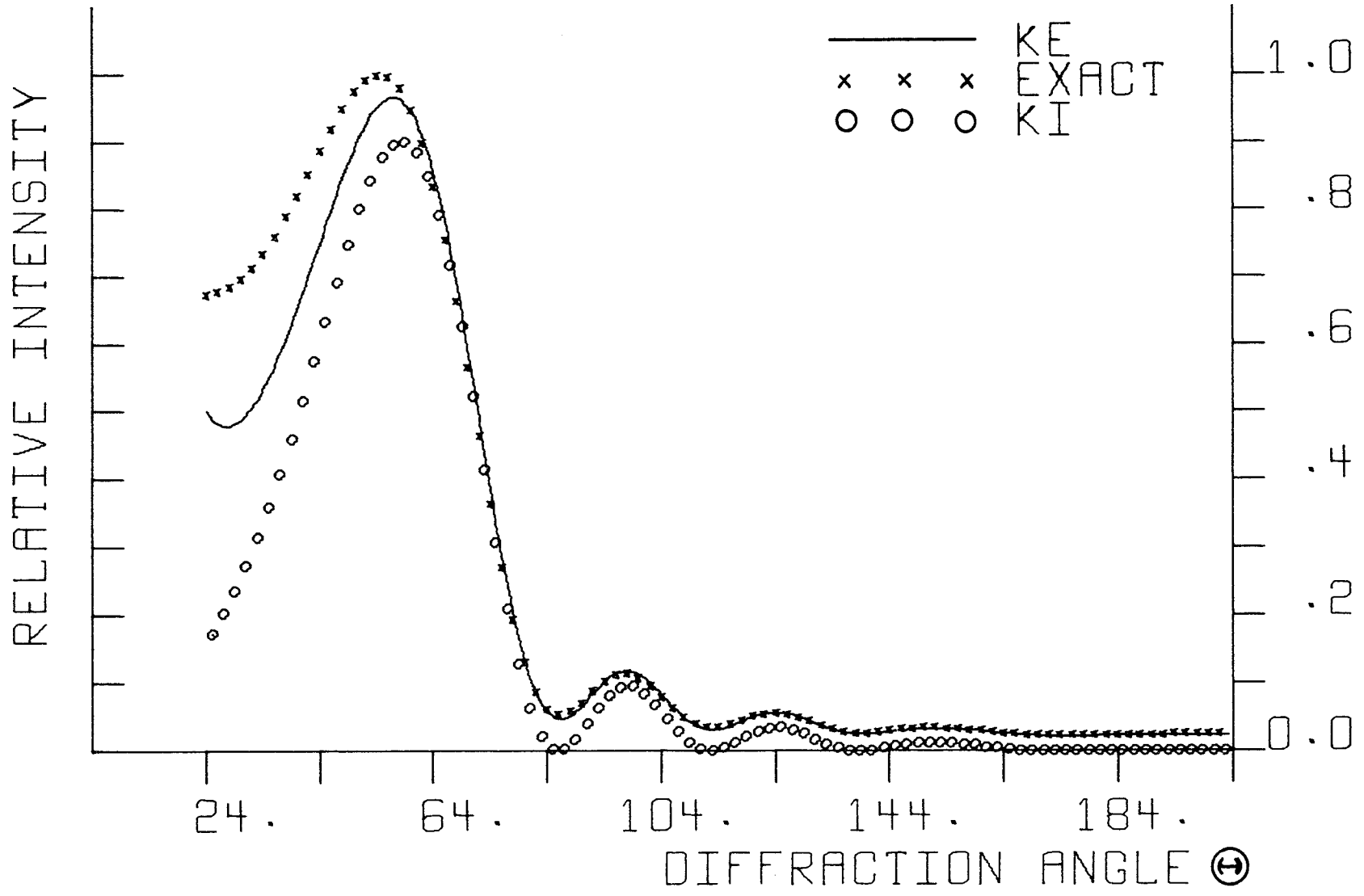

Fig. A6. Single strip diffraction: $w = 2.251\lambda$, $\theta_i = 66^\circ$.

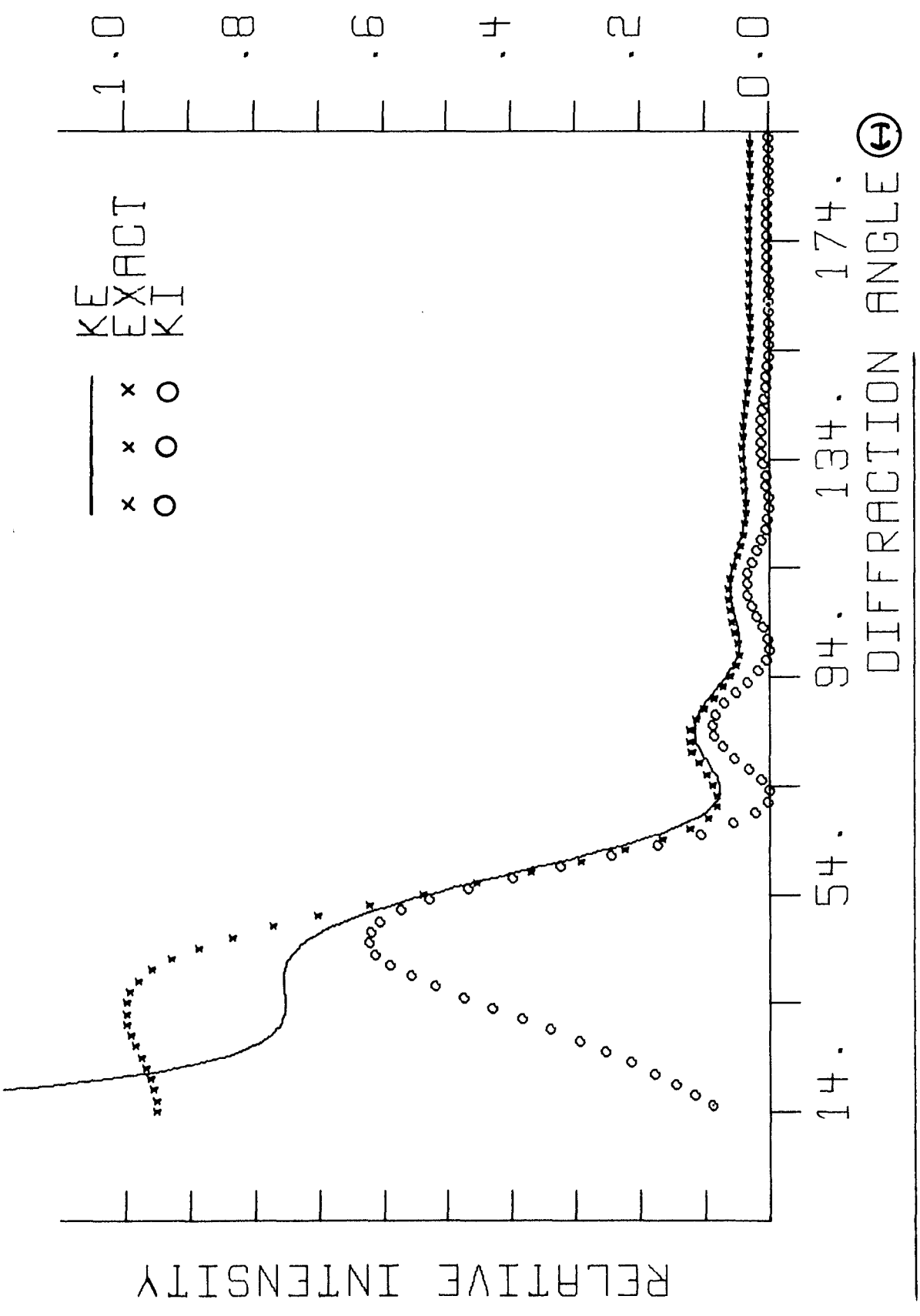

Fig. A7. Single strip diffraction: $w = 2.251\lambda$, $\theta_i = 76^\circ$.

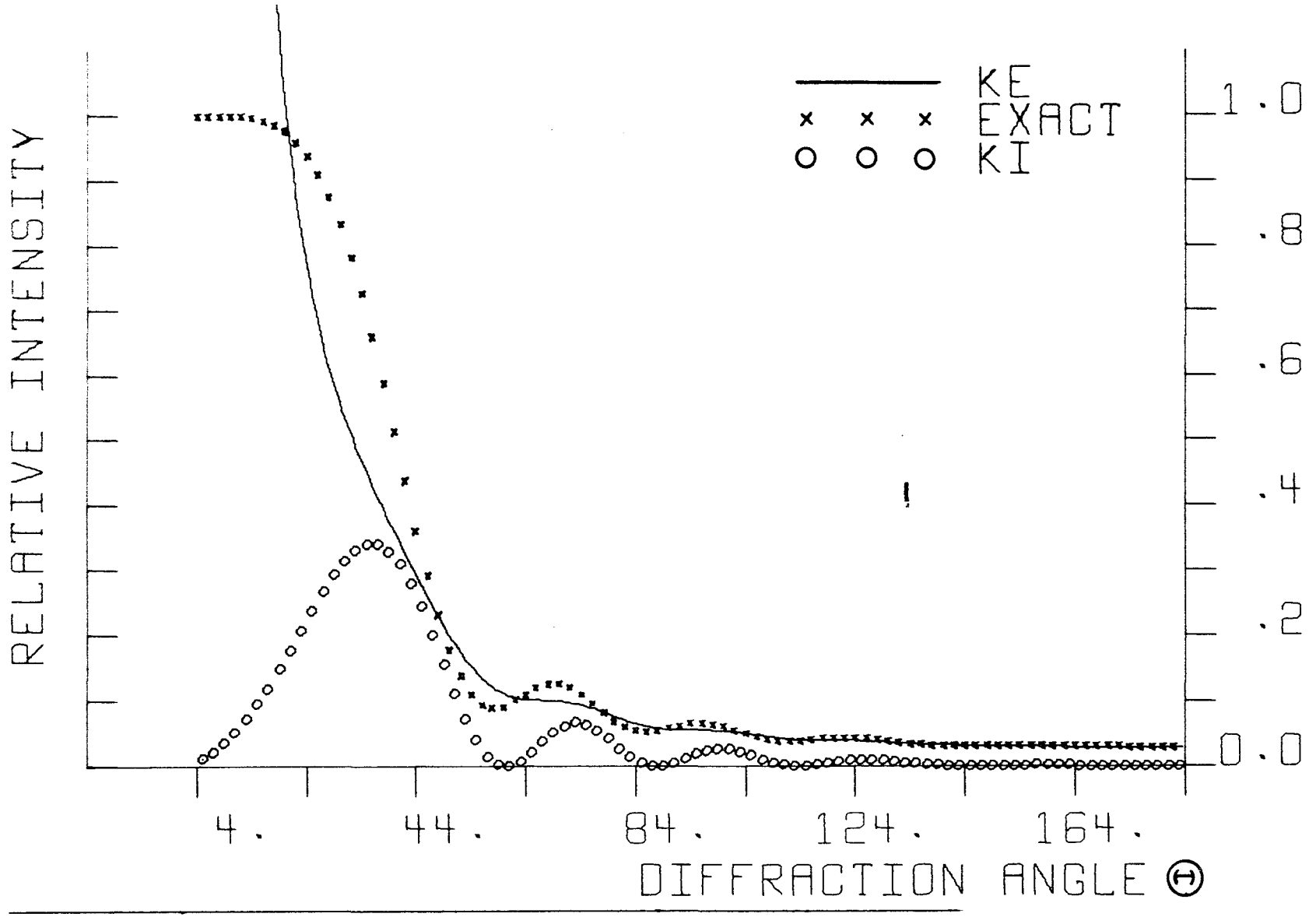

Fig. A8. Single strip diffraction: $w = 2.251\lambda$, $\theta_i = 86^{\circ}$.

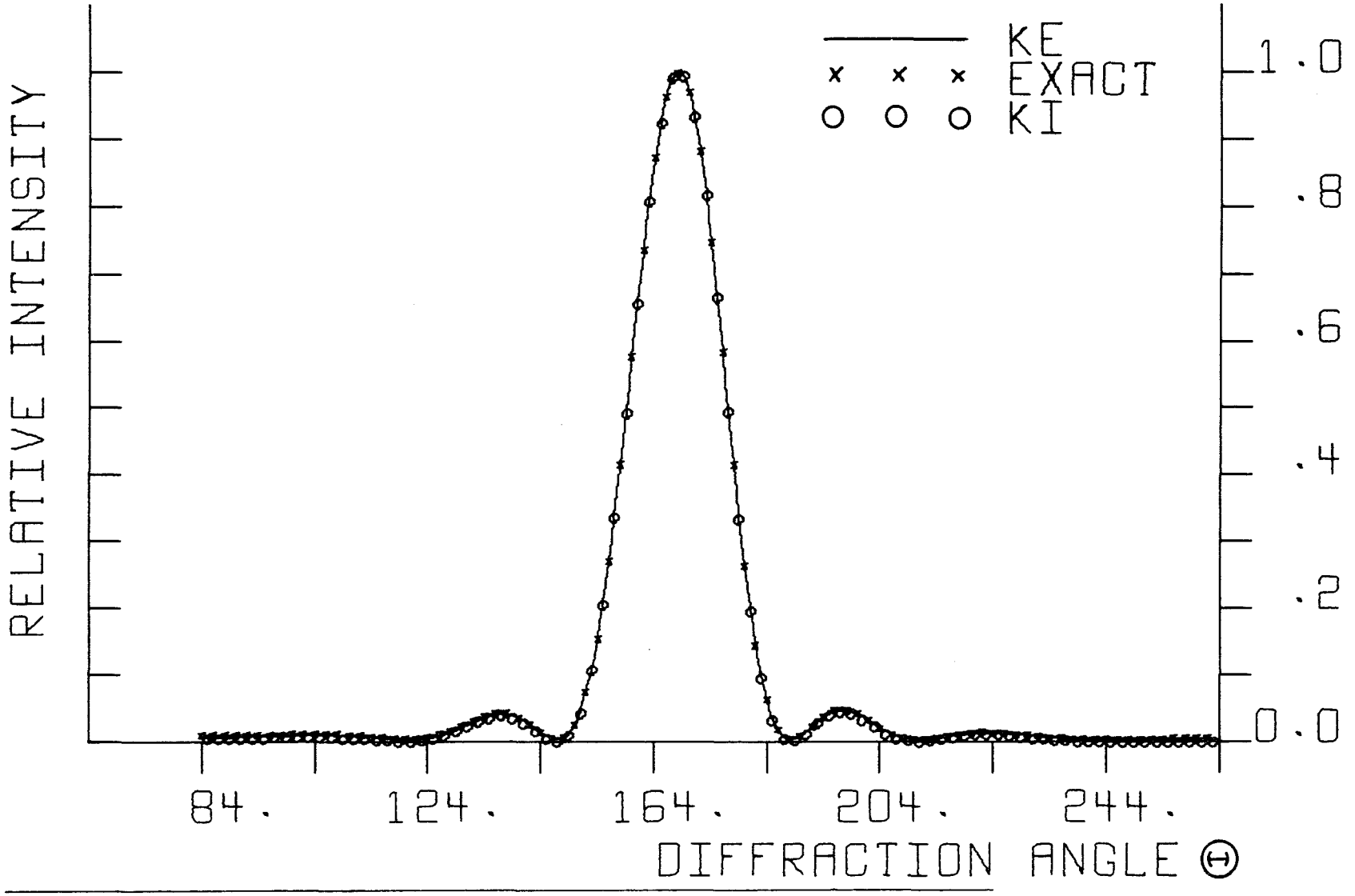

Fig. A9. Single strip diffraction: $w = 2.847\lambda$, $\theta_i = 6^o$.

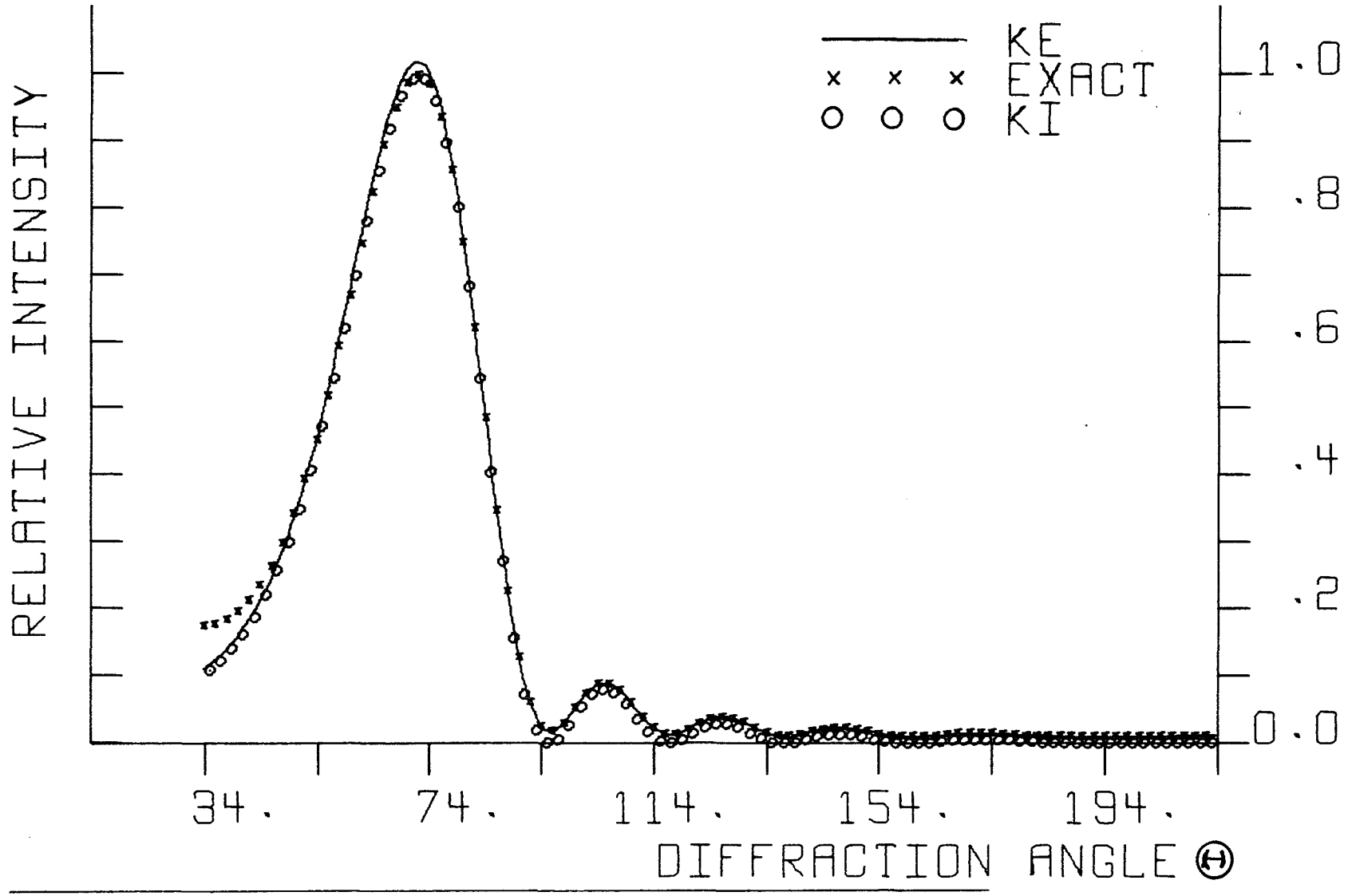

Fig. A10. Single strip diffraction: $w = 2.847\lambda$, $\theta_i = 56^\circ$.

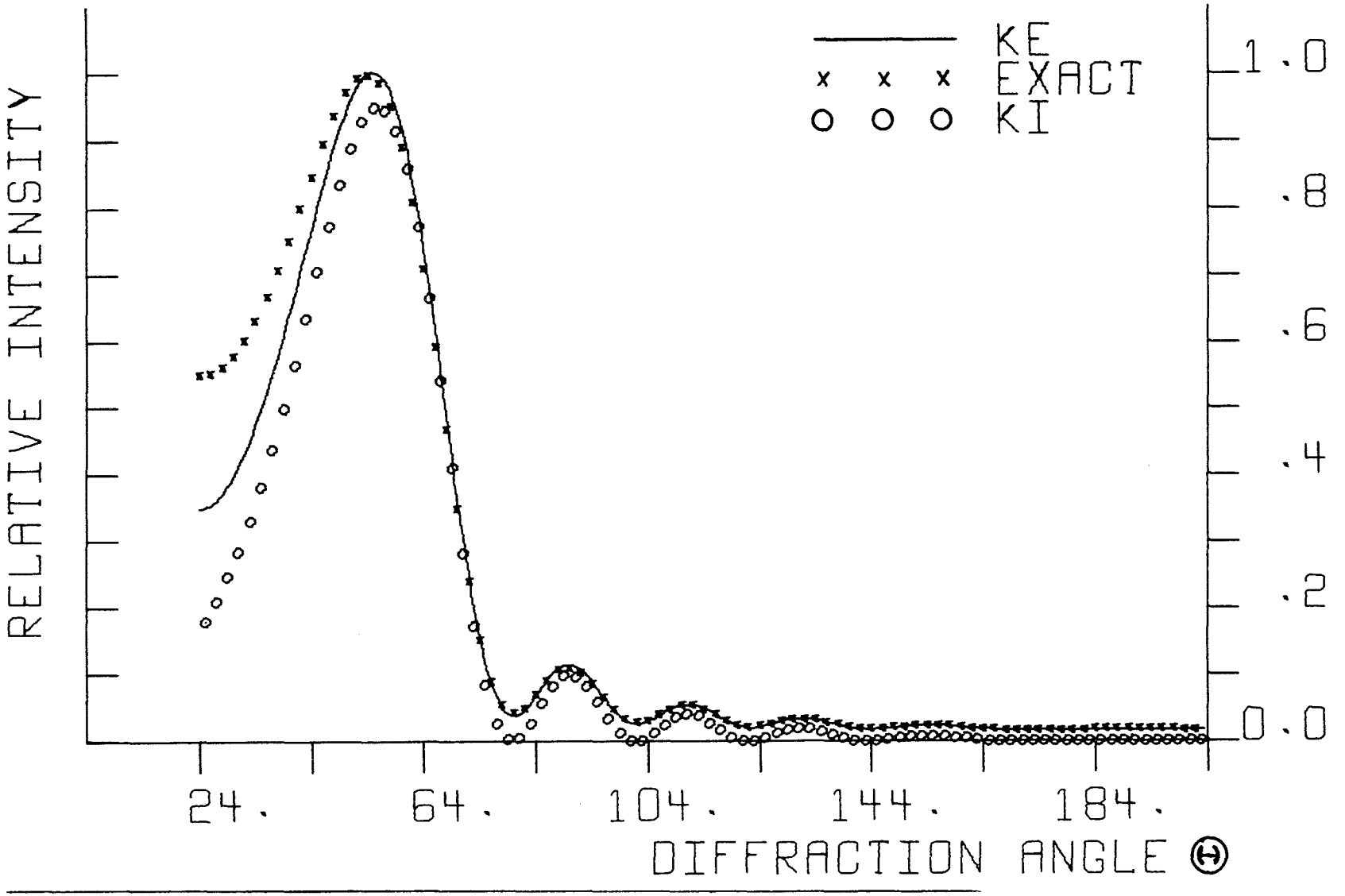

Fig. All. Single strip diffraction: $w = 2.847\lambda$, $\theta_i = 66^\circ$.

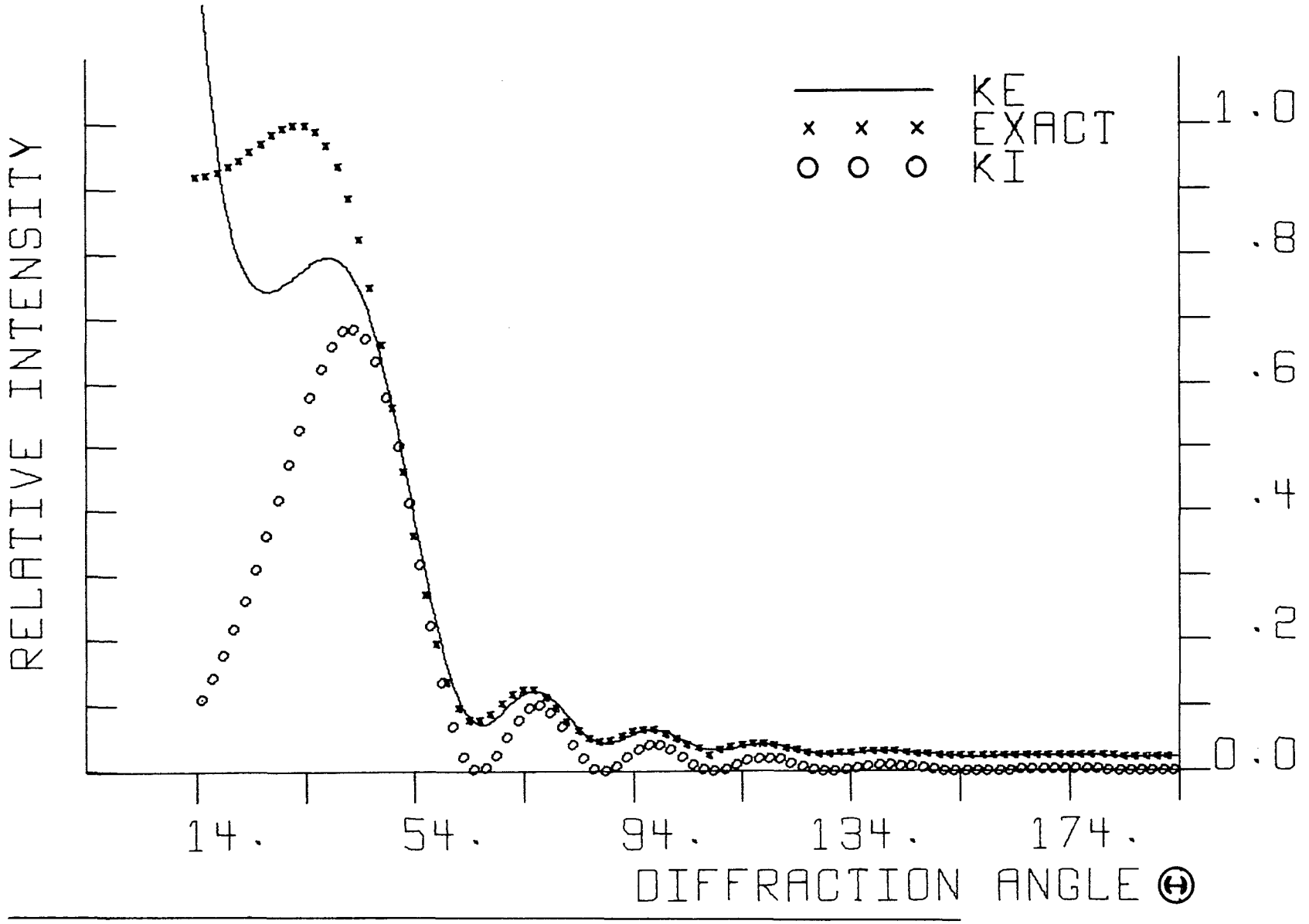

Fig. A12. Single strip diffraction: $w = 2.847\lambda$, $\theta_i = 76^\circ$.

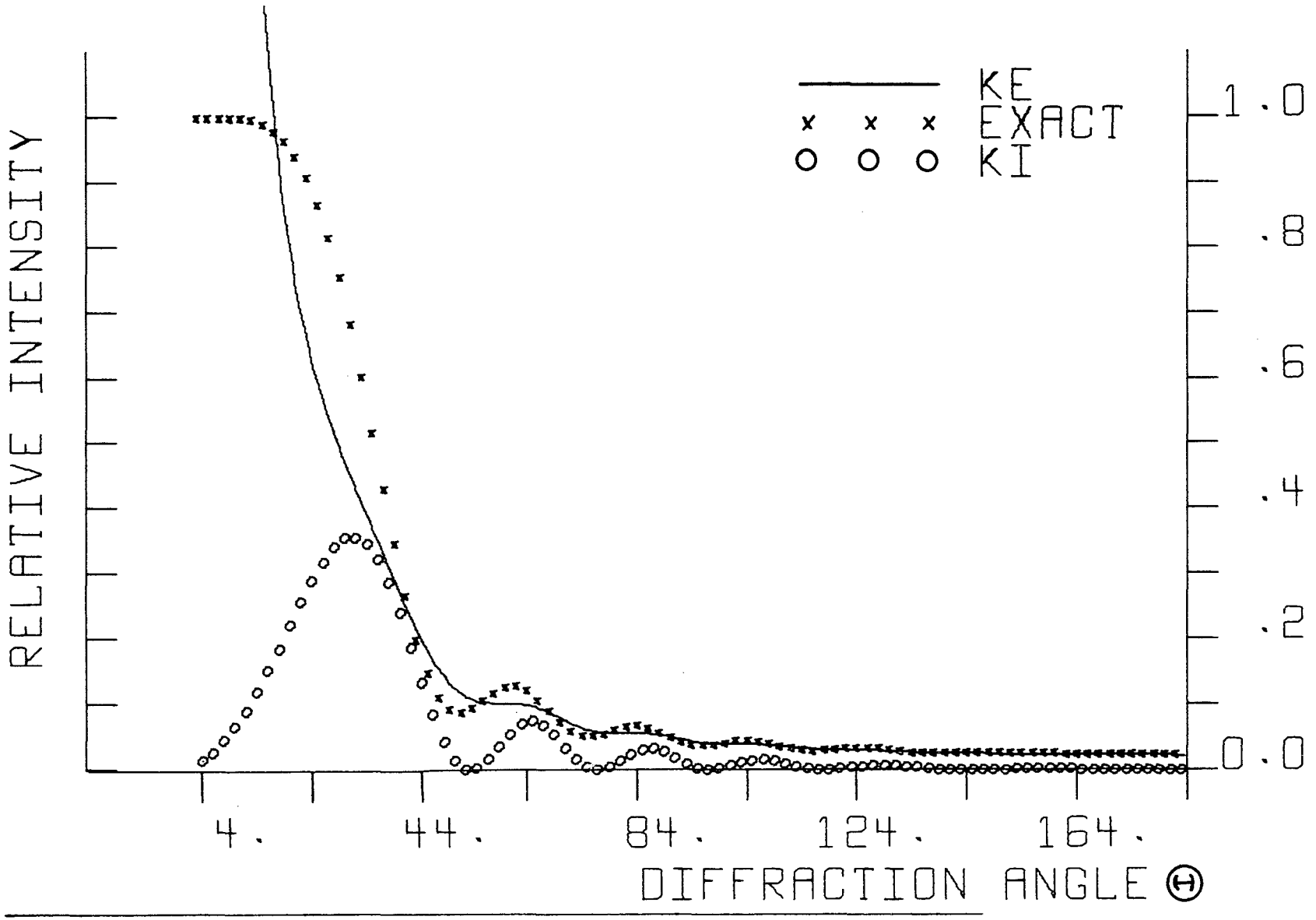

Fig. A13. Single strip diffraction: $w = 2.847\lambda$, $\theta_i = 86^\circ$.

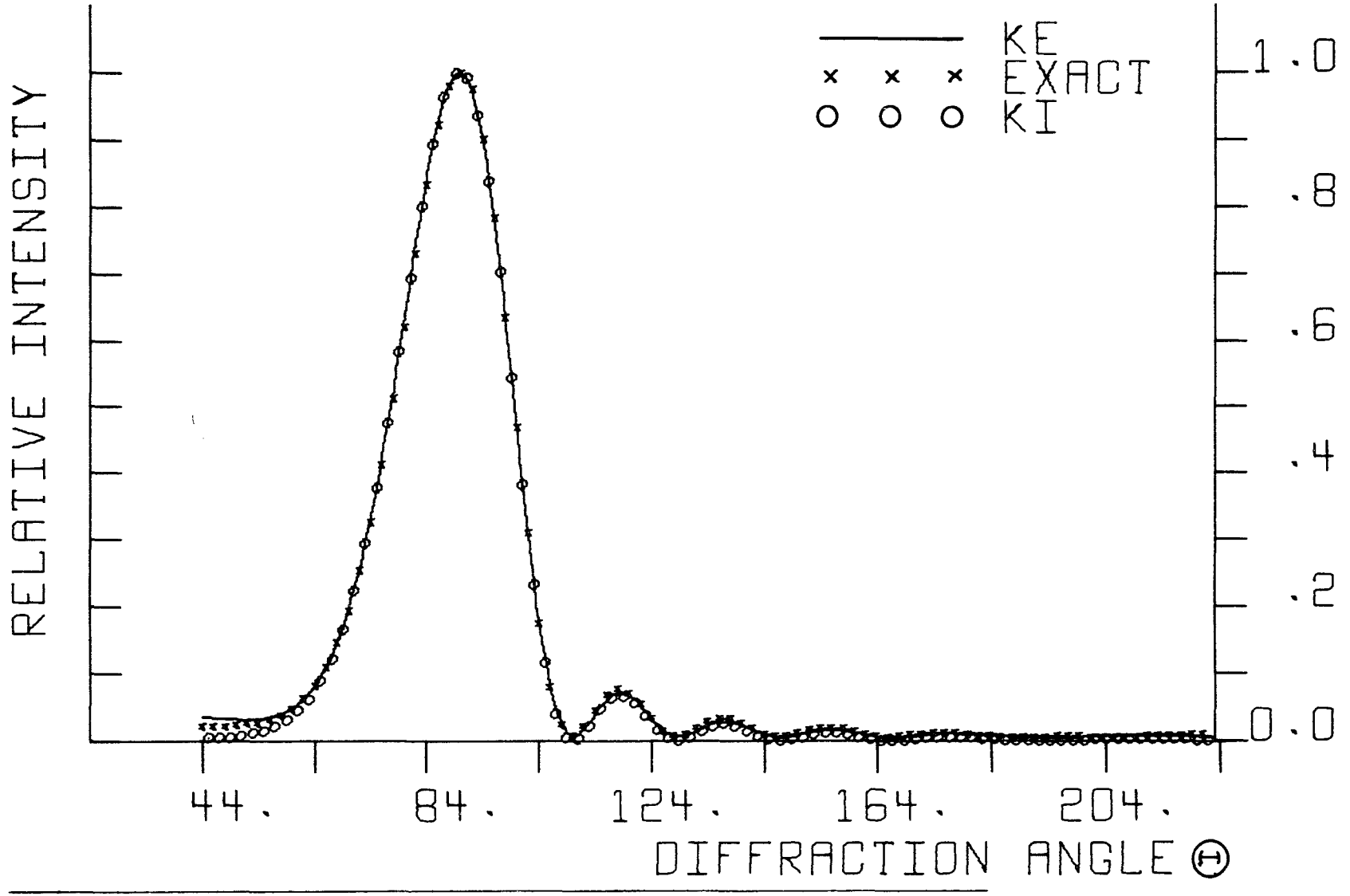

Fig. A14. Single strip diffraction: $w = 3.813\lambda$, $\theta_i = 46^\circ$.

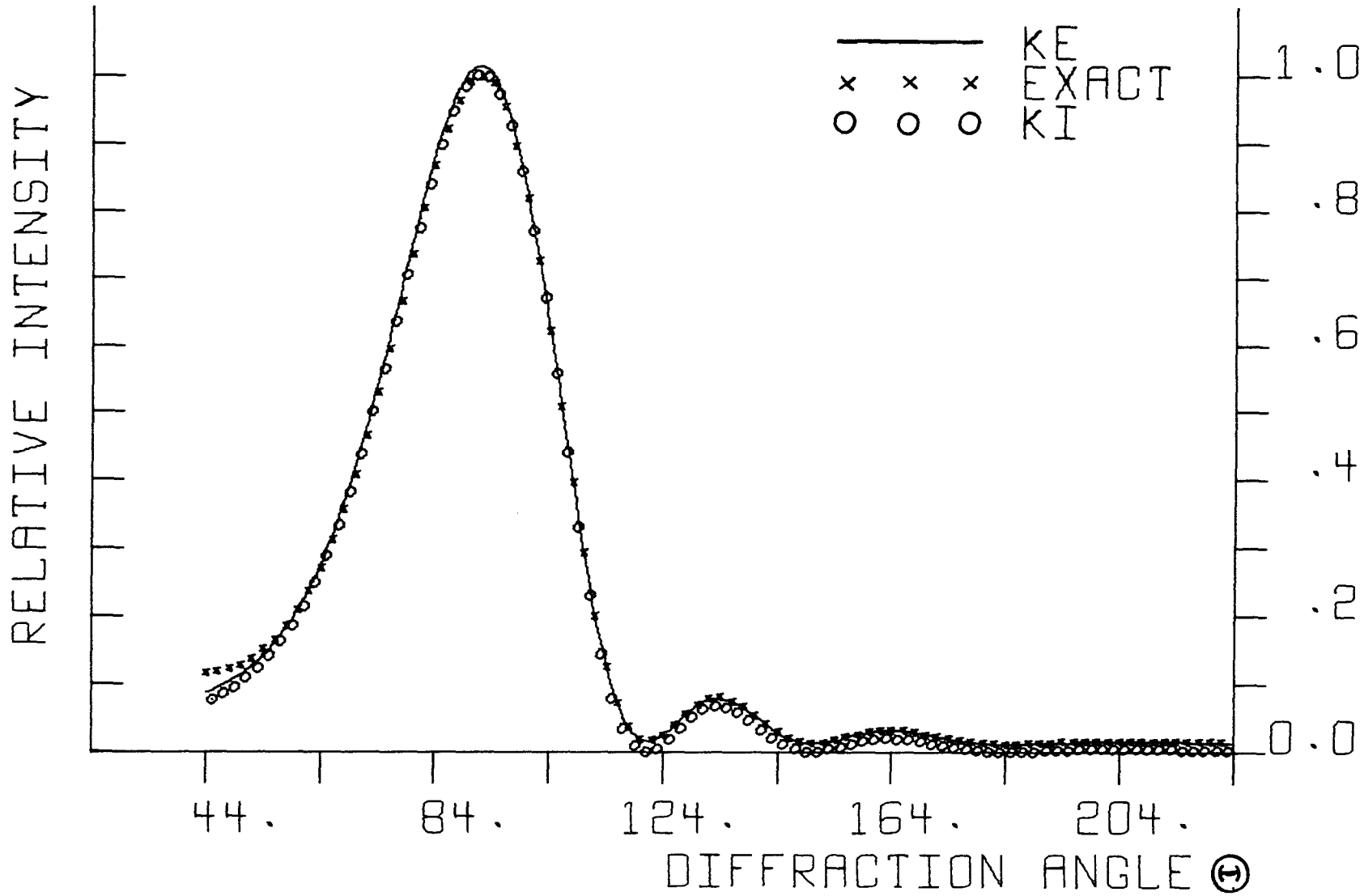

Fig. A15. Single strip diffraction: $w = 2.013\lambda$, $\theta_i = 46^\circ$.

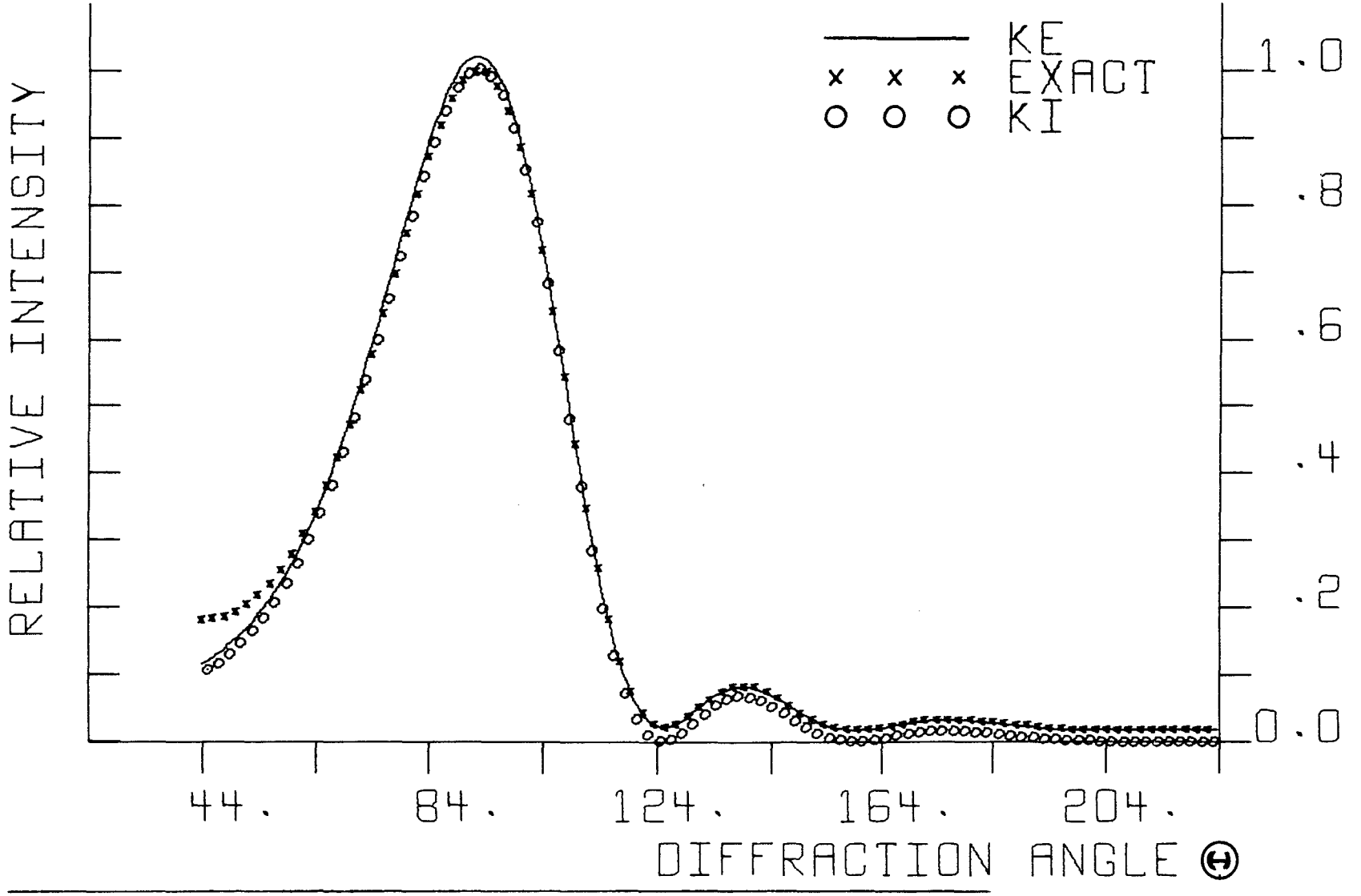

Fig. A16. Single strip diffraction: $w = 1.744\lambda$, $\theta_i = 46^\circ$.

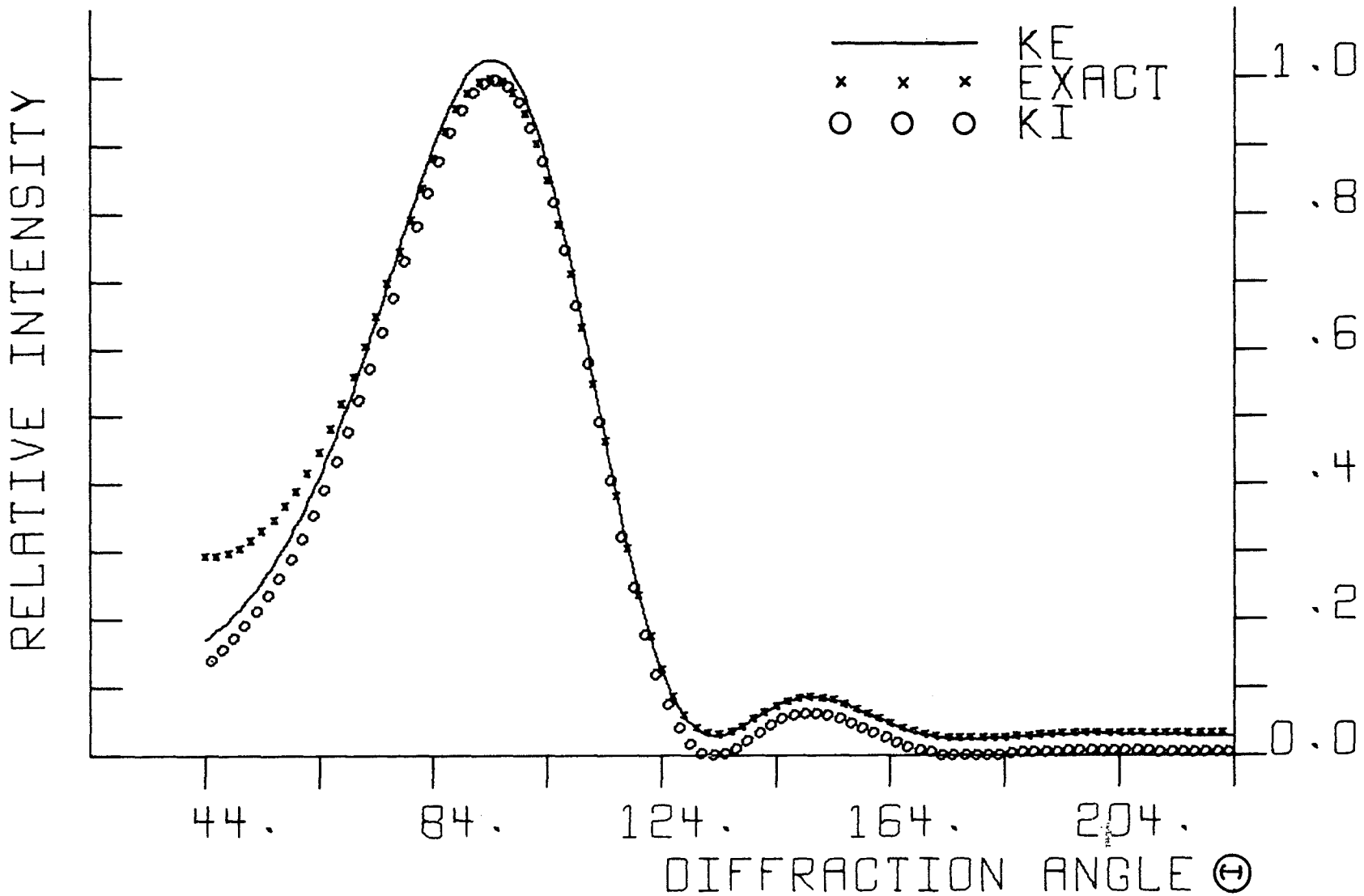

Fig. A17. Single strip diffraction: $w = 1.424\lambda$, $\theta_i = 46^\circ$.

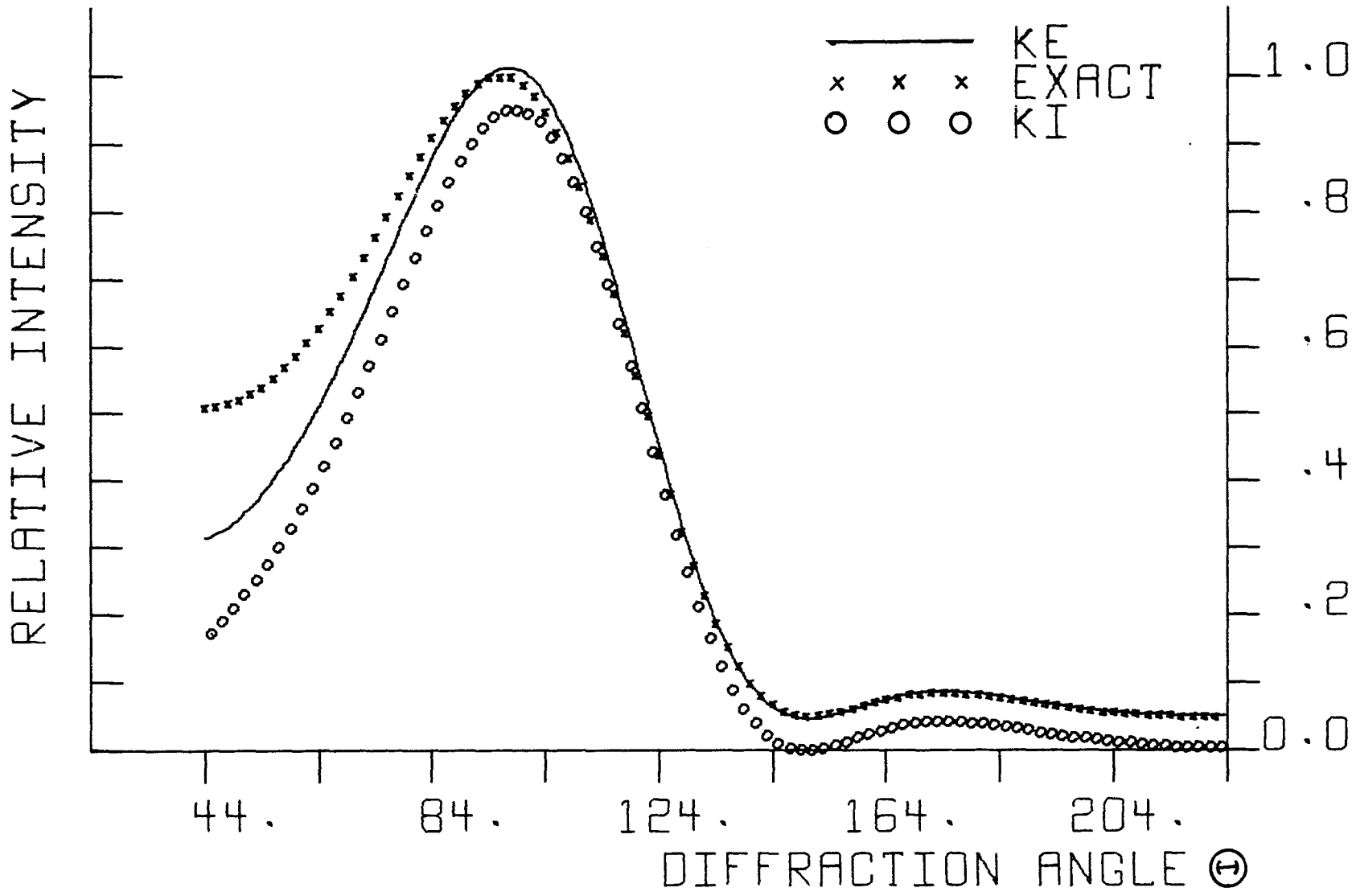

Fig. A18. Single strip diffraction: $w = 1.007\lambda$, $\theta_i = 46^\circ$.

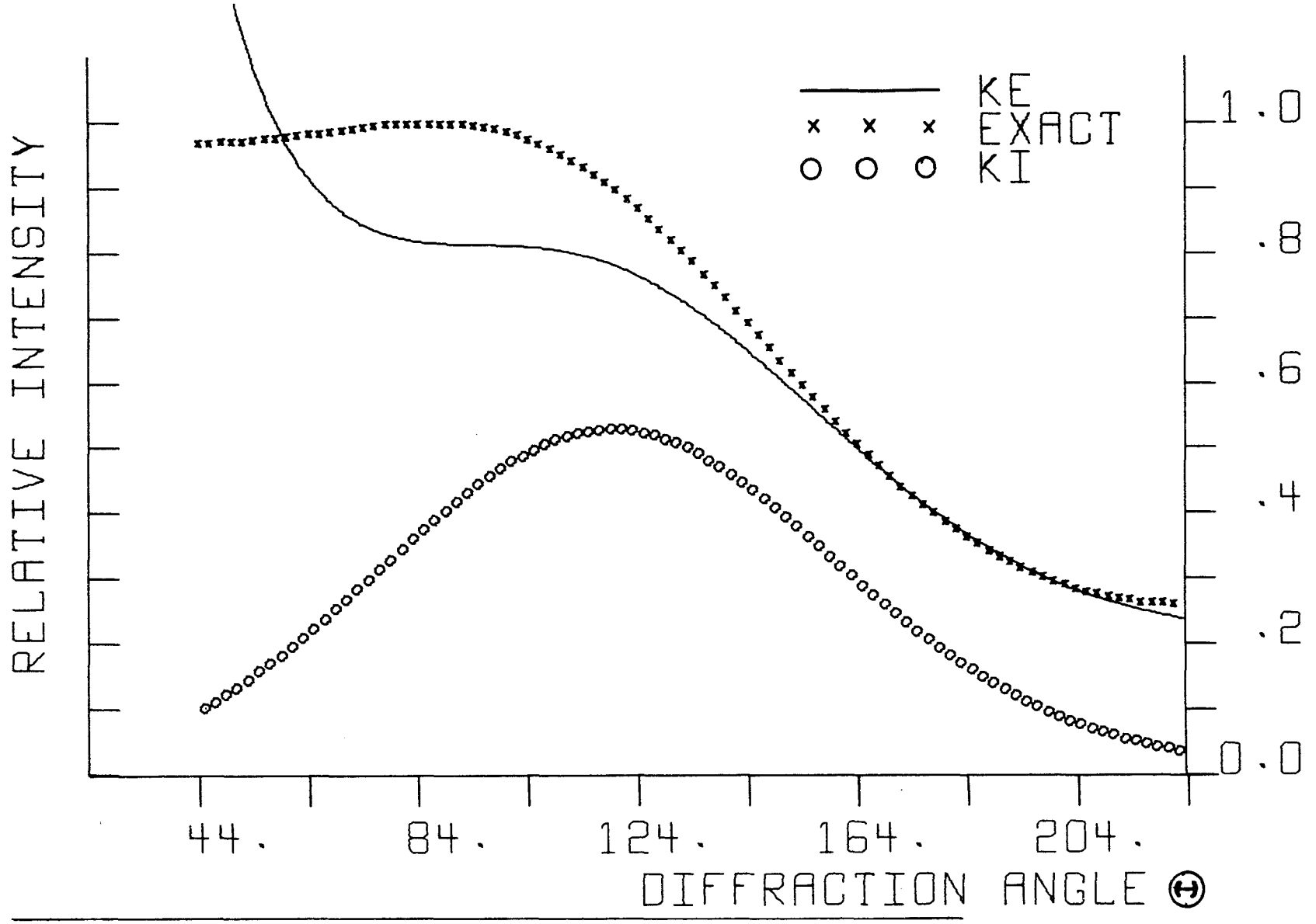

Fig. A19. Single strip diffraction: $w = 0.318\lambda$, $\theta_i = 46^{\circ}$.

θ_i	Exact Theory		Keller Theory		Kirchhoff Theory	
(deg)	Intensity	Amplitude	Intensity	Amplitude	Intensity	Amplitude
6	1.000	1.000	1.000	1.000	1.000	1.000
16	.935	.967	.936	.968	.935	.967
26	.821	.906	.822	.907	.820	.906
36	.676	.822	.673	.820	.669	.818
46	.507	.712	.509	.714	.502	.709
56	.344	.586	.353	.594	.342	.585
66	.232	.482	.225	.474	.209	.457
76	.187	.432	.141	.376	.117	.342
86	.181	.425	---	---	.062	.248

Table A3. Relative intensity and amplitude of the principal maximum as a function of angle of incidence for a single strip with $w/\lambda = 2.251$.

θ_i	Exact Theory		Keller Theory		Kirchhoff Theory	
(deg)	Intensity	Amplitude	Intensity	Amplitude	Intensity	Amplitude
6	1.000	1.000	1.000	1.000	1.000	1.000
16	.935	.967	.935	.967	.934	.966
26	.819	.905	.820	.906	.818	.905
36	.669	.818	.669	.818	.667	.816
46	.504	.710	.502	.708	.497	.705
56	.335	.579	.341	.584	.334	.578
66	.208	.456	.209	.457	.198	.444
76	.152	,389	.121	.347	.104	.322
86	.143	.379	---	---	.051	.226

Table A4. Relative intensity and amplitude of the principal maximum as a function of angle of incidence for a single strip with $w/\lambda = 2.847$.

w/λ	Exact Theory		Keller Theory		Kirchhoff Theory	
	Intensity	Amplitude	Intensity	Amplitude	Intensity	Amplitude
1.0066	.115	.338	.116	.341	.109	.330
1.4235	.210	.458	.216	.465	.209	.458
1.7435	.308	.555	.315	.561	.309	.556
2.0132	.407	.638	.413	.643	.408	.639
2.2508	.507	.712	.511	.715	.507	.712
2.4656	.607	.779	.609	.781	.606	.778
2.7009	.726	.852	.726	.852	.724	.851
2.8471	.805	.897	.805	.897	.803	.896
3.0531	.923	.961	.922	.960	.921	.960
3.1831	1.000	1.000	1.000	1.000	1.000	1.000

Table A5. Relative intensity and amplitude of the principal maximum as a function of strip width for an angle of incidence $\theta_i = 46^o$.

APPENDIX III

Analysis of Second-Order Effects in Keller's Theory of Edge Diffraction

The application of Keller's geometrical theory of edge diffraction to the case of diffraction by two long, thin, parallel strips involves the use of four diffracting edges. If the strip faces are inclined with respect to each other, then second-order effects can result from the production of eight "doubly diffracted" rays. The analysis that follows concerns itself with a discussion of which of the second-order rays yield significant corrections to the first-order field, and an indication of the location and extent of singularities in the second-order fields. This information should find use in more complex diffraction cases by allowing theoretical considerations to be limited to those second-order rays which give rise to significant corrections.

1. Evaluation of Second-Order Effects

In order to analyze the effects of the individual second-order rays, the calculations and curves that follow were obtained by considering each doubly diffracted ray in turn. The first-order field, $u^{(1)}$, at a given diffraction angle was added to the field of the appropriate second-order ray, u_{ij}, (see Eq. 18) and the square magnitude (intensity) of the result was found. The

first-order intensity was then subtracted from the latter and the difference was divided by the maximum value of the first-order intensity. Denoting the final result as ΔI_{ij}, the above results are represented mathematically by

$$\Delta I_{ij} = \frac{\left| u^{(1)} + u_{ij} \right|^2 - \left| u^{(1)} \right|^2}{\left| u^{(1)} \right|^2_{max}} \qquad \text{(A8)}$$

Equation A8 was evaluated over the region of interest for each of the second-order rays and the results of several of the calculations are presented graphically below. The legend on the curves identifies the particular second-order rays used to obtain a given result.

2. Singularities

Singularities and associated anomalous regions in the second-order Keller patterns are present at certain angles for either of two reasons: a) a doubly diffracted ray emerges at an angle of specular reflection with respect to the plane of the strip, or b) the diffraction angle is on a shadow boundary of the incident ray. Inspection of Eq. 12 reveals that singularities arise for the cases where $\theta' + \alpha' = 0$ and where $\theta' - \alpha' = \pi$. These correspond respectively to reasons a and b (see also Fig. 9).*

The singularities are a consequence of the approximate nature of the theory: Eq. 12 results from an asymptotic expansion of the exact solution of Maxwell's equations for the case of diffraction by a perfectly conducting half-plane.** The extent to which this approximation and Eq. 12 are valid can be estimated using the following inequalities+

$$\left|\sqrt{2kr}\,\mathrm{Cos}\,\left(\frac{\alpha' - \theta'}{2}\right)\right| > \frac{1}{\epsilon\sqrt{\pi}} \qquad \text{(A9)}$$

$$\left|\sqrt{2kr}\,\mathrm{Cos}\,\left(\frac{\alpha' + \theta' - 3\pi}{2}\right)\right| > \frac{1}{\epsilon\sqrt{\pi}} \qquad \text{(A10)}$$

---

*The reason that these angles do not offer difficulty in the first-order results is that the singularities there occur in pairs and, in the far field case, cancel each other.

**Sommerfeld, P. 247ff.

+Baker and Copson, P. 145ff.

where α', θ' and r are defined in Fig. 8, and ϵ is defined such that $\frac{1}{2}\pi\epsilon^3$ equals the maximum error in the determination of the diffracted field at the observation point. Eq. A9 is used when a shadow boundary is crossed while Eq. A10 is for the case of specular reflection of the incident ray. Eqs. A9 and A10 can also be used to determine the angular extent of the anomalous region near a singularity: if δ represents the angular distance from a singularity (due to either specular reflection or a shadow boundary), within which the error is greater than $\frac{1}{2}\pi\epsilon^3$, then it can be shown that

$$\text{Sin } (\frac{\delta}{2}) = \frac{1}{\epsilon\sqrt{2\pi kr}} \qquad \text{(A11)}$$

Consider the case of two strips (w = 1.270 cm) separated by a distance of approximately 3λ (D = 1.660 cm λ = .529 cm) when their faces are inclined away from each other (44(10,-10) case). This case is considered in the text in Fig. 23. Only three of the eight possible doubly diffracted rays were found to yield any significant contributions to the second-order pattern. Their contributions, as calculated from Eq. A8, are presented in Fig. A20. (The remaining five doubly diffracted rays each yielded corrections of 0.008 or less and were therefore not plotted.) Fig. A21 indicates the strip separation and orientations along with the three rays

considered. As is seen, two of the rays, u_{23} and u_{32}, result from interactions between the closest edges. Since these edges are only about 0.8λ apart, we are considering a case where the validity of the geometrical theory is in doubt. In order to estimate the errors involved in the evaluation of the second-order terms, consider that doubly diffracted ray which yields the largest corrections, viz. u_{32}. This ray results from the diffraction by edge 3 of a singly diffracted ray from edge 2. Using Eq. A9 to evaluate ϵ, we can find the maximum error in the determination of the singly diffracted field which is incident upon edge 3. The calculation indicates an estimated error of up to 24% can occur. This, however, is not the only error which the doubly diffracted ray may have. We must also consider the angular regions about any singularities which may appear when the singly diffracted ray is diffracted again. A shadow boundary exists at $\phi = 44^{\circ}$; this is out of our region of interest, but the effects of this singularity can (and in this case, do) extend into the region $\phi > 50^{\circ}$. If we demand the same accuracy for the doubly-diffracted field as for the incident field, i.e., a maximum error of approximately 24%, then Eq. A11 yields a value for δ of about 45°. Thus, in the region from $\phi = 50^{\circ}$ to approximately $\phi = 90^{\circ}$, a maximum possible error of more than 50%

can occur in the second-order field. Beyond $\Theta = 90^{\circ}$, the maximum possible error diminishes from 50% to approximately 25% at $\Theta = 160^{\circ}$.

Similar considerations of the other two contributing doubly diffracted rays, u_{23} and u_{31}, yields a maximum error of less than 6% over the interval $50^{\circ} < \Theta < 160^{\circ}$ except near $\Theta = 52^{\circ}$ where u_{31} has a singularity due to a shadow boundary. Otherwise, the contribution of u_{31} is negligible and can be ignored.

In Figs. A22 and A23, we consider the same strip separation as in the above case but with the strip faces inclined toward each other (44(-10,10) case). Five of the eight second-order rays now yield large contributions, although for three of these, u_{31}, u_{41}, and u_{42}, most of the contributions are near singular points. Again, the largest general contribution is made by the u_{32} doubly diffracted ray. Using Eq. A9, it is found that the maximum error in the first-order field from edge 2 which is incident upon edge 3 is here approximately the same as before, viz., 24%. The singularity at 64° for the u_{32} ray results from the specular reflection of the singly diffracted ray and its effects extend to values of δ up to 45° if we require a maximum error of about 24%. The maximum error in the amplitude of ray u_{23} is again less than 6%. The effect of ray u_{31} is seen to be small in

general, except at the sharp singularity (due to specular reflection) at approximately 72^{o}. It could therefore be neglected. For the second-order rays which involve edge 4, the value of δ is approximately 20^{o} for the region about the singularities (at $\Theta = 54^{o}$ and 58^{o}) where the maximum error is greater than about 20%. Thus, one cannot make any predictions concerning the contributions of u_{41} and u_{42} except outside the range of their singularities where their predicted contributions are negligible.

As the strips are moved further apart, the second-order effects are found to diminish in importance. In Figs. A24 and A25, we consider the case of two strips (w = 1.270 cm) whose faces are inclined toward each other (44(-10,10) case) at a separation of approximately 6λ (D = 3.294 cm, λ = .529 cm). Table A6 lists some results of error calculations for this case and various other cases considered in the text for strips whose planes make the "small angle" of $\beta = 20^{o}$. As before, the largest interactions are between the closest edges, with the larger contribution again from u_{32}, the ray which is diffracted in the "forward direction," i.e., in a direction close to the original direction of the incident singly diffracted ray. The results in Table A6, based upon Eqs. A9, A10, and A11, give an estimation of the maximum errors in the singly diffracted fields which are incident upon an edge and also an estimate of the range of influence of the singularities

which arise.* The theoretical elimination of these singularities, involving theory other than the Keller theory used above, is described in the literature,[+] and since such calculations were beyond the intent of the present work, they were not pursued.

For the above results, it is evident that the main contributions to second-order effects as predicted by Keller theory are caused by interactions between the nearest edges and by rays which are diffracted in directions close to the direction of the ray incident upon the edge. However, it is evident that one must examine the geometry to be sure that large corrections are not a result of proximity to a singularity.

---

*It must be noted that the maximum errors indicated earlier and those listed in Table A6 can only be called estimates since Eqs. A9, A10, and A11 are obtained from the exact solution of Maxwell's equations for the case of diffraction by the straight edge of an infinite half-plane. Further examination of the extent to which these equations can be applied to diffraction at straight edges of strips would be needed before a more definitive statement of the error could be made.

[+]Keller, I; Yu and Rudduck.

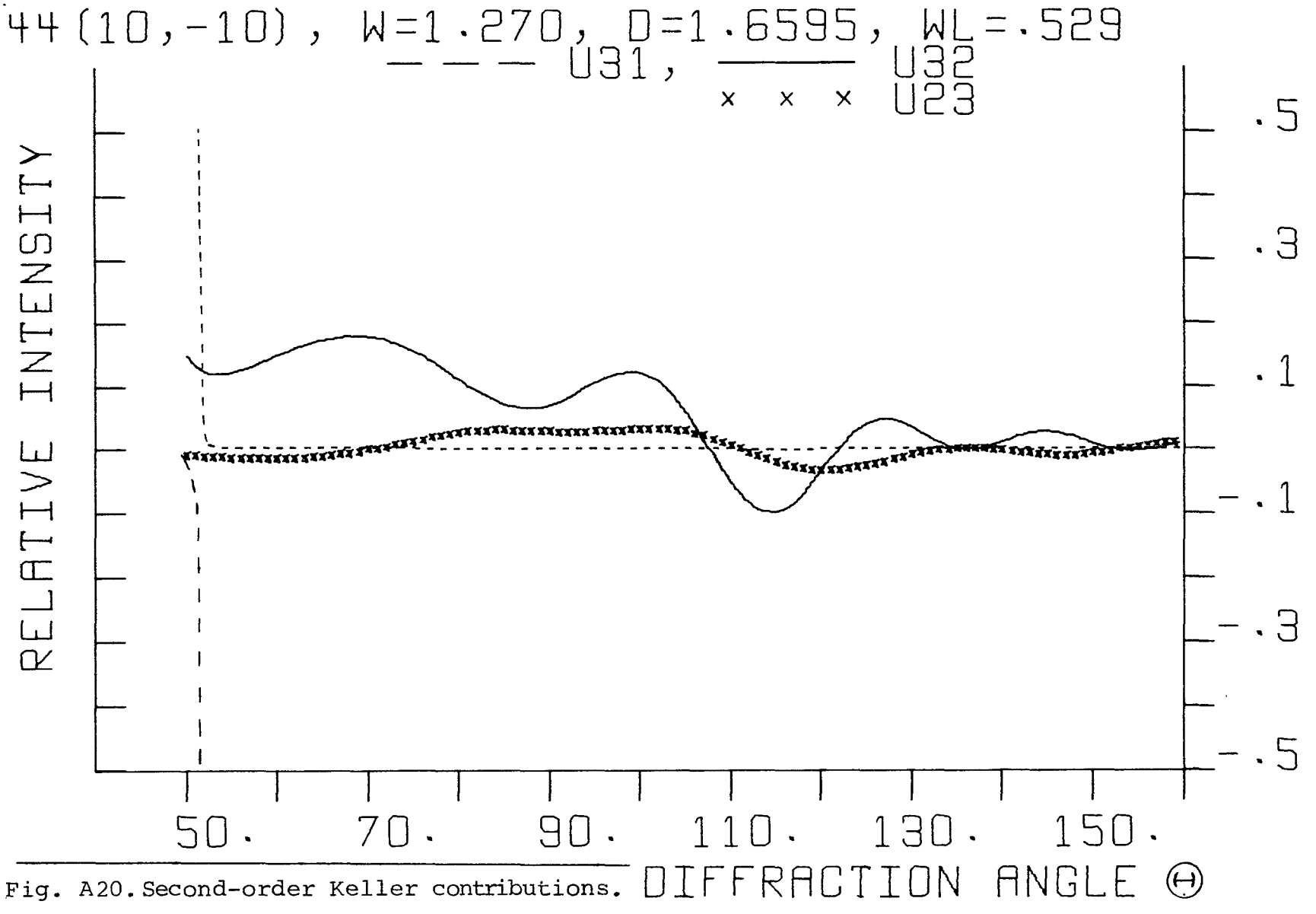

Fig. A20. Second-order Keller contributions.

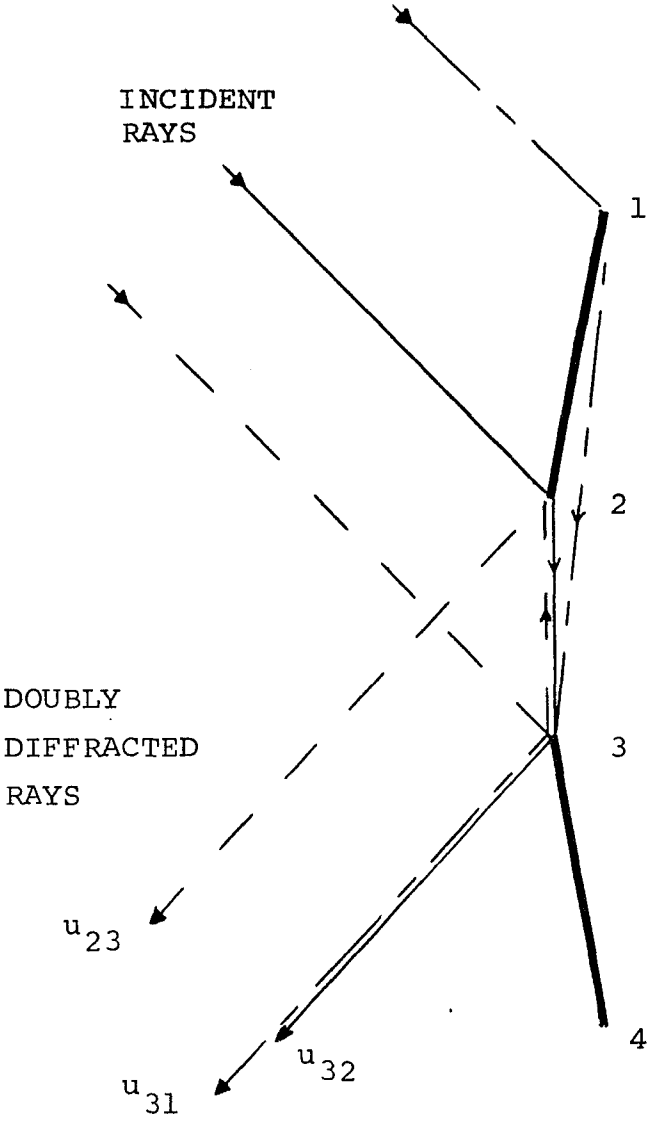

Fig. A21. Second-order effects in Keller's geometrical theory applied to the case of diffraction by two long, thin, parallel strips. Three of the eight possible doubly diffracted rays are shown.

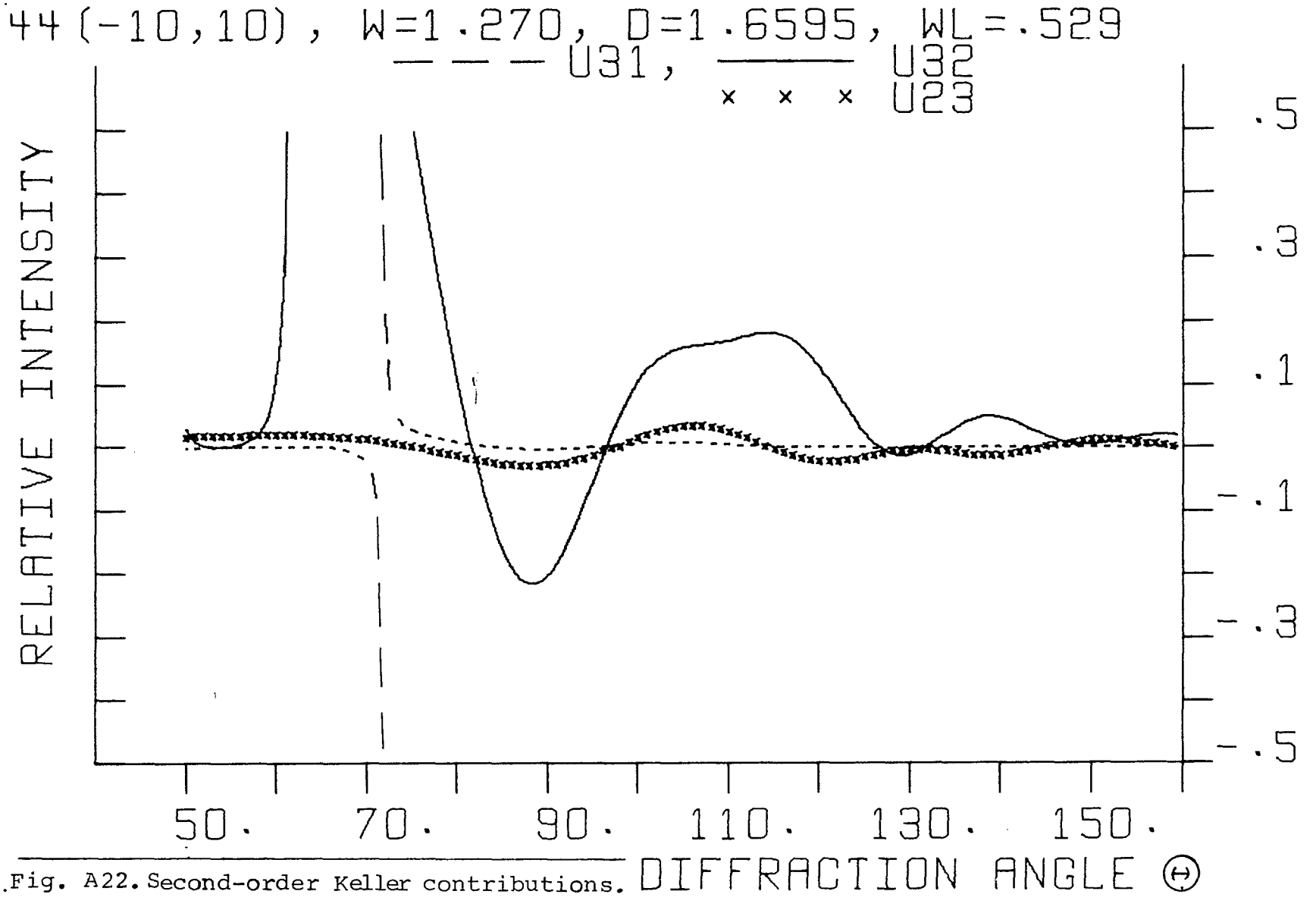

Fig. A22. Second-order Keller contributions.

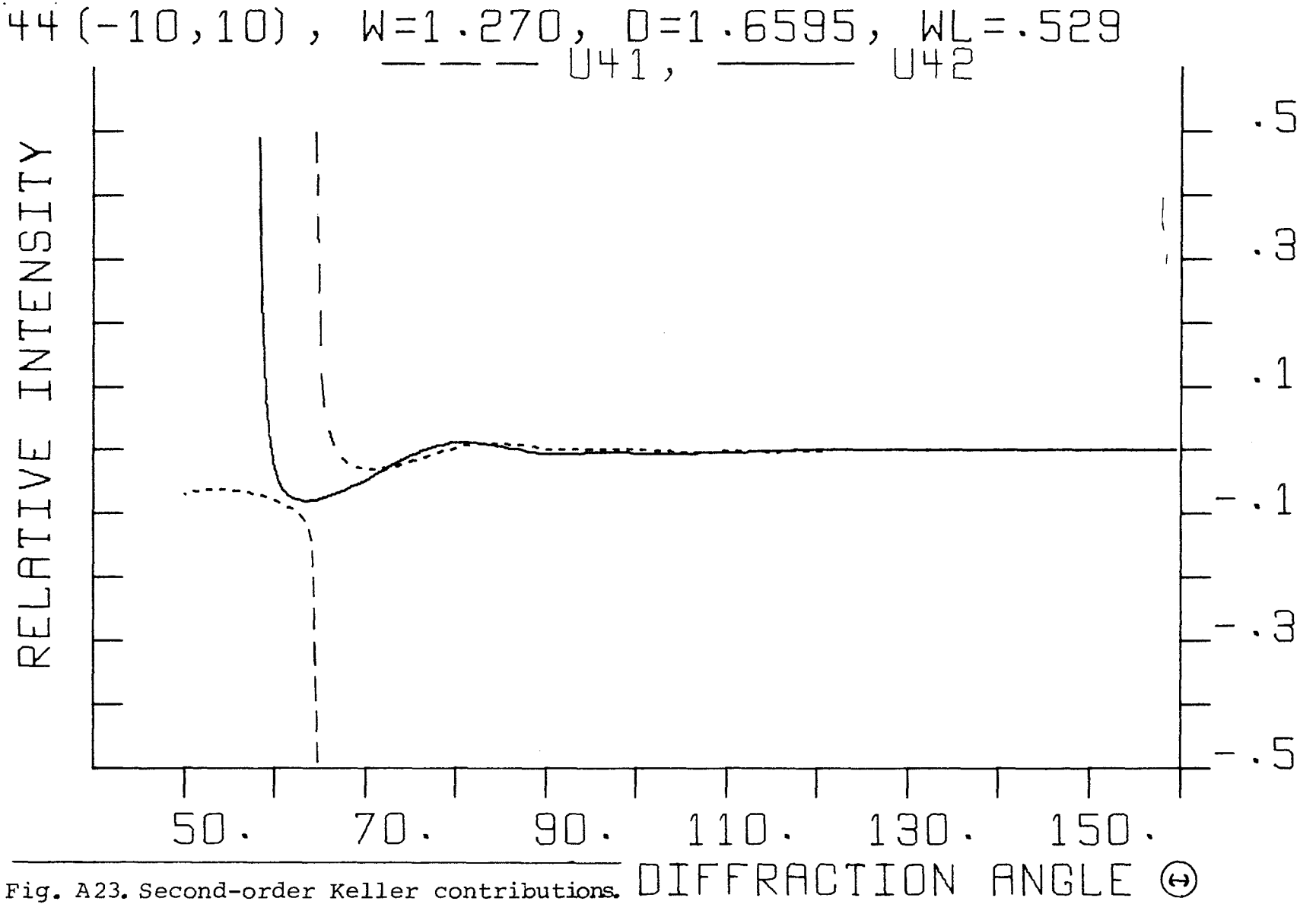

Fig. A23. Second-order Keller contributions.

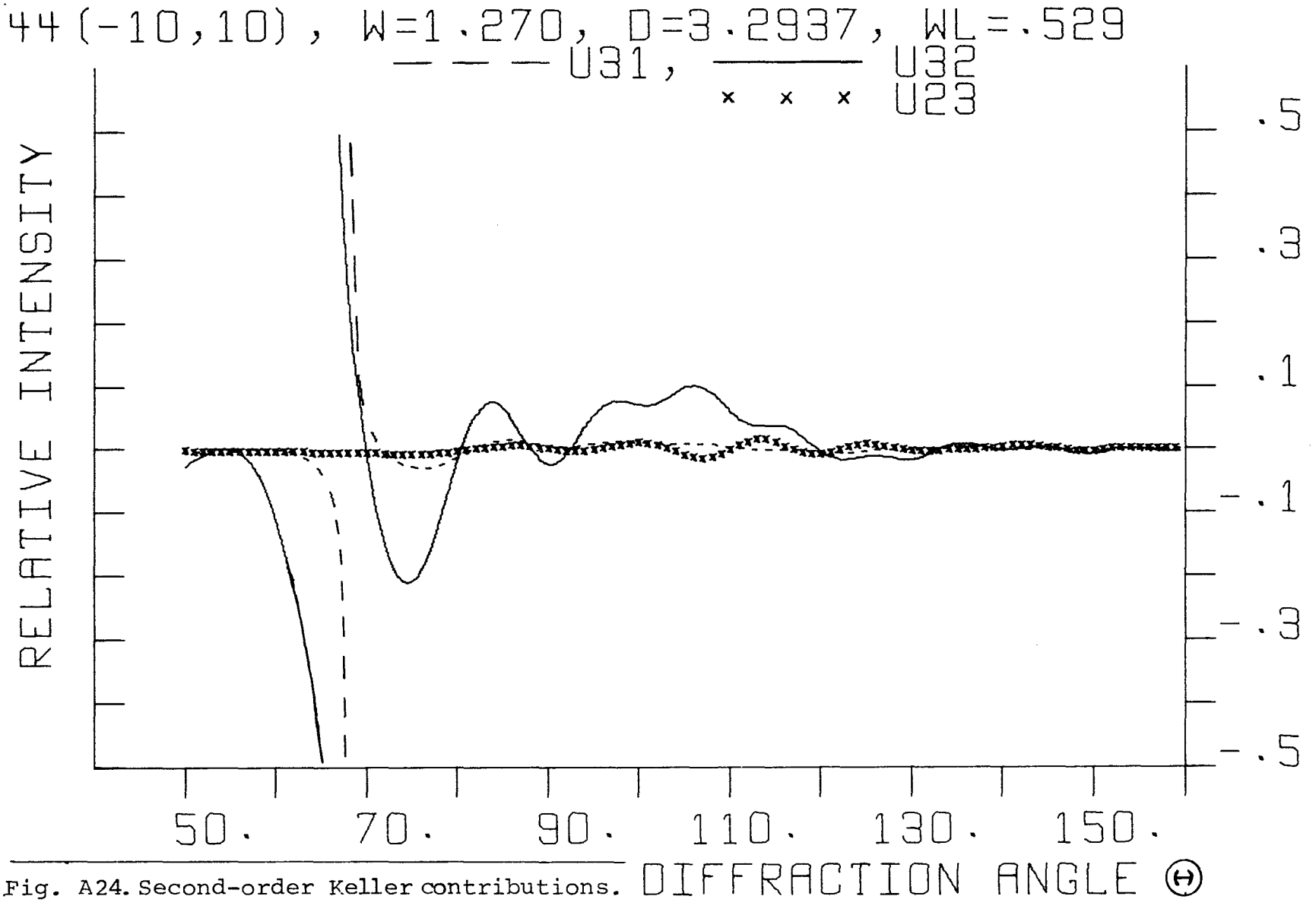

Fig. A24. Second-order Keller contributions.

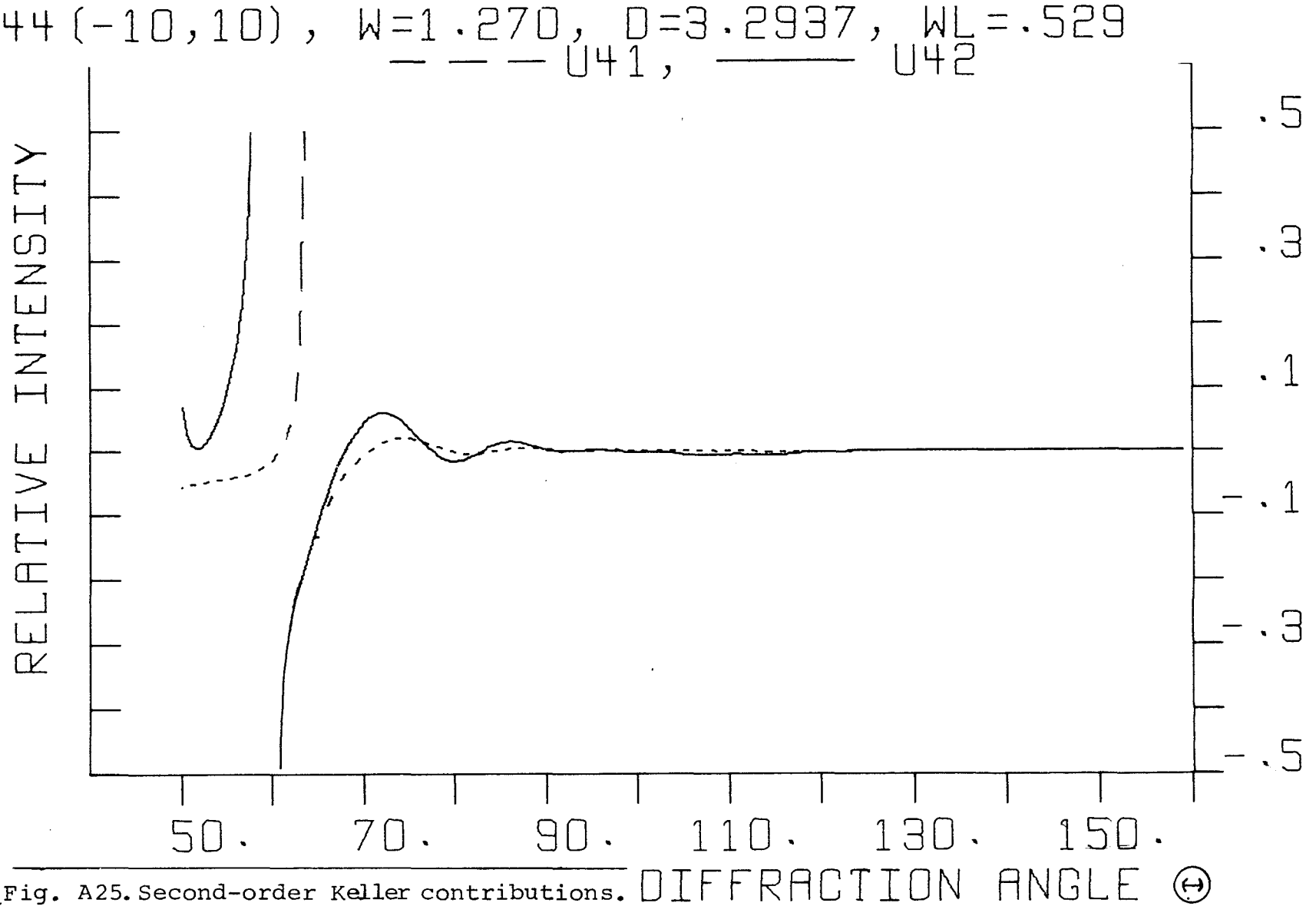

Fig. A25. Second-order Keller contributions.

Separation $\frac{D}{\lambda}$	Maximum % error in the singly diffracted ray incident upon an edge			Range around singularity at $\Theta = \Theta_s$ where the maximum error* in the doubly diffracted ray is more than 24% (20% for u_{42})			Largest % error* in u_{23} in region $50^\circ < \Theta < 160^\circ$	
Case	44(±10,∓10)			44(10,-10)	44(-10,10)		44(10,-10)	44(-10,10)
Ray	u_{23}	u_{32}	u_{42}	u_{32}	u_{32}	u_{42}	u_{23}	
				$\Theta_s=44^\circ$	$\Theta_s=64^\circ$	$\Theta_s=62^\circ$		
3	2%	24%	2%	44°	44°	21°	8%	24%
4	<1%	6%	1%	26°	26°	18°	2%	6%
5	"	3%	1%	22°	22°	16°	1%	3%
6	"	2%	<1%	18°	18°	14°	<1%	2%
7	"	1%	"	16°	16°	14°	"	1%
8	"	1%	"	14°	14°	12°	"	1%

*Not including error in incident singly diffracted ray.

Table A6. Second-order Keller theory estimates of the maximum errors in some of the singly diffracted fields which are incident upon an edge, and of the range of influence of some of the singularities which arise.

BIBLIOGRAPHY

Adey, A. W., "Diffraction of Microwaves by Long Metal Cylinders," Can. J. Phys. 33, 407-419 (1955).

Adonina, A. I., and V. P. Shestopalov, "Diffraction of Electromagnetic Waves Obliquely Incident on a Plane Metallic Grating With a Dielectric Layer," Soviet Phys-Tech Phys. 8, 479-486 (1963).

Andrews, C. L., "Diffraction Pattern of Microwaves Near Rods," J. Appl. Phys. 22, 465-468 (1951).

Baker, B. B., and E. T. Copson, The Mathematical Theory of Huygens' Principle, Oxford University Press, London, 1939.

Beard, C. I., T. H. Kays and V. Twersky, "Scattered Intensities for Random Distributions - Microwave Data and Optical Applications," Appl. Opt. 4, 1299-1315 (1965).

Bousquet, P., "Diffraction of Electromagnetic Waves by a Grating with Triangular Section Rulings," Compt. Rend. 257, 80-83 (1963).

DeAcetis, L. A.,"Wavefronts from a Parabolic Reflector for an Off-Focal Source and Comment on the Off-Axis Caustic," Am. J. Phys. 36, 909 (1968).

DeAcetis, L. A., and I. Lazar, I, "Obliquity Factors of Huygens and Kirchhoff Theories Applied to Experimental Diffraction by Two, Long, Coplanar, Parallel Strips," Am. J. Phys. 36, 830-833 (1968).

II, "Kirchhoff and Keller Theories Applied to Experimental Diffraction by Two Long, Thin, Conducting Strips," paper presented at 1968 Fall Meeting, Optical Society of America, J. Opt. Soc. Am. 58, 1567 (1968).

III, "Approximate Solutions to Single Strip Diffraction in the Limit of Small Glancing Angle and Small Strip Width," paper presented at 1969 Spring Meeting, Optical Society of America, J. Opt. Soc. Am. 59 (1969).

Erma, V. A., "An Exact Solution for the Scattering of Electromagnetic Waves from Conductors of Arbitrary Shape. I. Case of Cylindrical Symmetry," Phys. Rev. 173, 1243-1257 (1968).

Felson, L. B., and V. H. Weston, "Classical Diffraction and Scattering," Radio Science - Nat. Bur. Std. 68D, 490-499 (1964).

Germey, K., "The Diffraction of a Plane Electromagnetic Wave by Two Parallel, Infinitely Long, Ideal Cylinders of Elliptical Cross-section," Ann. Physik 13, 237-251 (1964).

Karczewski, B., and E. Wolf, "Comparison of Three Theories of Electromagnetic Diffraction at an Aperture. Part I: Coherent Matrices," "Comparison.... Part II: The Far Field," J. Opt. Soc. Am. 56, 1214-1219 (1966).

Keller, J. B., I, "Diffraction by an Aperture," J. Appl. Phys. 28, 426-444 (1957).

II, "How Dark is the Shadow of a Round-Ended Screen?" J. Appl. Phys. 30, 1452-1454 (1959).

III, "Geometrical Theory of Diffraction," J. Opt. Soc. 52, 116-130 (1962).

King, D., Measurements At Centimeter Wavelength, Boston Technical Publishers, Cambridge, 1965.

Kodis, R. D., "Diffraction Measurements at 1.25 Centimeters," J. Appl. Phys. 23, 249-255 (1952).

Labrum, N. R., "Some Experiments on Centimeter-Wavelength Scattering by Small Obstacles," J. Appl. Phys. 23, 1320-1323 (1952).

Lazar, I., "Experimental Determination of the Diffraction of 4 mm Waves From a Set of Echelette Gratings," Ph. D. Thesis, New York University, New York (1962).

Lazar, I., and L. A. DeAcetis, I, "Rays from a Parabolic Reflector for an Off Focal-Point Source," Am. J. Phys. 36, 139-141 (1968).

II, "Experimental Diffraction of 6-mm Waves from Two Very Long, Thin, Conducting Strips in a Plane," paper presented at 1968 Spring Meeting, Optical Society of America, J. Opt. Soc. Am. 58, 721 (1968).

III, "Experimental Diffraction by Two Long, Parallel Strips in a Plane. I: Vertical Polarization," Appl. Opt. 7, 1609-1612 (1968).

Lazar, I., and R. D. Hatcher, "Exact Solution and Numerical and Graphical Presentation for Diffraction of Electromagnetic waves by a Single Strip," unpublished.

Macrakis, M. S., "Theoretical and Experimental Study of the Backscattering Cross-Section of an Infinite Ribbon," J. Appl. Phys. 31, 2261-2266 (1960).

Mathur, N. C., and K. C. Yeh, "Multiple Scattering of Electromagnetic Waves by Random Scatterers of Finite Size," J. Math. Phys. 5, 1619-1628 (1964).

Meecham, W. C., "Variational Method for the Calculation of the Distribution of Energy Reflected From a Periodic Surface. I," J. Appl. Phys. 27, 361-376 (1956).

Meecham, W. C., and C. W. Peters, "Reflection of Plane-Polarized Electromagnetic Radiation from an Echelette Grating," J. Appl. Phys. 28, 216-217 (1957).

Morse, B. J., "Diffraction by Polygonal Cylinders," J. Math. Phys. 5, 199-214 (1964).

Moseley, S. T., "On-Axis Defocus Characteristics of the Paraboloidal Reflector," Final Report AF 30 (602) - 925, Syracuse Univ. 1954.

Palmer, C. H., and F. W. Phelps, Jr., "Grating Anomalies as a Local Phenomenon," J. Opt. Soc. Am. 58, 1184-1188 (1968).

Provalov, A. V., O. A. Tret'yakov, and V. P. Shestopalov, "Experimental Investigation of the Diffraction of Electromagnetic Waves on Double Metallic Gratings," Sov. Phys.-Tech. Phys. 9, 148-150 (1964).

Row, R. V., "Theoretical and Experimental Study of Electromagnetic Scattering by Two Identical Conducting Cylinders," J. Appl. Phys. 26, 666-675 (1955).

Siegel, K. M., J. W. Crispin, and C. E. Schensted, "Electromagnetic and Acoustical Scattering From a Semi-Infinite Cone," J. Appl. Phys. 26, 309-313 (1955).

Sommerfeld, A., Optics, Academic Press Inc., New York, 1954.

Stratton, J. A., Electromagnetic Theory, McGraw-Hill Book Co., New York, 1941.

Stratton, J. A., and L. J. Chu, "Diffraction Theory of Electromagnetic Waves," Phys. Rev. 56, 99-107 (1939).

Tang, C. H., "Backscattering from Dielectric-Coated Infinite Cylindrical Obstacles," J. Appl. Phys. 28, 628-633 (1957).

Tremblay, R., and A. Boivin, "Concepts and Techniques of Microwave Optics," Appl. Opt. 5, 249-278 (1966).

Twersky, V., I, "Multiple Scattering of Radiation by an Arbitrary Configuration of Parallel Cylinders," J. Acoust. Soc. Am. 24, 42-46 (1952).

II, "Multiple Scattering of Radiation by an Arbitrary Planar Configuration of Parallel Cylinders and by Two Parallel Cylinders," J. Appl. Phys. 23, 407-414 (1952).

Watson, R. B., and C. W. Horton, "On the Diffraction of a Radar Wave by a Conducting Wedge," J. Appl. Phys. 21, 802-804 (1950).

Wiles, S. T., and A. B. McLay, "Diffraction of 3.2 cm Electromagnetic Waves by Cylindrical Objects," Can. J. Phys. 32, 372-380 (1954).

Yeh, C., "Perturbation Approach to the Diffraction of Electromagnetic Waves by Arbitrarily Shaped Dielectric Obstacles," Phys. Rev. 135, A1193-A1201 (1964).

Yu, J., and R. C. Rudduck, "On Higher-Order Diffraction Concepts Applied to a Conducting Strip," IEEE Trans. on Ant. and Prop. AP-15, 662-668 (1967).

Zitron, N., and S. N. Karp, "Higher Order Approximations in Multiple Scattering. I. Two-Dimensional Scalar Case," J. Math. Phys. 2, 394-403 (1961).